The Thesis Committee for Mitchell Lee Dornak
Certifies that this is the approved version of the following thesis:

Mechanical Properties, Early Age Volume Change, and Heat Generation of Rapid, Cement-based Repair Materials

APPROVED BY
SUPERVISING COMMITTEE:

Supervisor: _____
Kevin J. Folliard

Co-Supervisor: _____
Thanos Drimalas

Mechanical Properties, Early Age Volume Change, and Heat Generation of Rapid, Cement-based Repair Materials

by

Mitchell Lee Dornak, B.S.C.E.

Thesis

Presented to the Faculty of the Graduate School of

The University of Texas at Austin

in Partial Fulfillment

of the Requirements

for the Degree of

Master of Science in Engineering

The University of Texas at Austin

May 2014

Dedication

I would like to dedicate this to my parents, Darrell and Mona Dornak, without your love and support this would not be possible.

Acknowledgements

First, I would like to thank my family. Mom and Dad, thank you for your guidance and assistance throughout my adolescence and young adult years. You have supported me every step of the way and I really appreciate everything you have done. Luke and Lee Ann, thank you for being there for me and pretending to be interested in some of my concrete materials research.

I would like to thank my supervisor and co-supervisor, Dr. Kevin Folliard and Dr. Thanos Drimalas, for all of the assistance and teaching during my 5 years at the research center. Dr. Folliard, I really appreciate the wonderful opportunities you have allowed me in the field of research. Thano, you have helped me through many mixes, analysis, and overall knowledge of the materials I have researched, without your help I would still be lost.

Michael Rung, your knowledge of any equipment, testing procedure, and material I have dealt with at the lab is insurmountable. Thank you for the constant assistance, debugging equipment, and walking me through many problems that came up during my years at the lab. Sherian, thank you for taking care of any of the orders, tuition, and any financial issues, without you I would still be here trying to receive materials.

As for all of the friends I have made at the lab, thank you for making my graduate school experience a wonderful one. First of all, Phillip, thank you for introducing me to the CMRG because I would not have known about this lab without you. Chris, I appreciate the countless hours you spent helping me use instruments around the lab that needed work, preparing outdoor site, and for dealing with my "nagging" questions about everything.

Now for my two research partners, Jose and Anthony, thank you for dealing with my panic attacks, constant reminders, and questions. Jose, I feel like you lead the way on the beginning of this project and I just tried to keep up. Thanks for getting me to work early for those 7:30 a.m. mixes which always involved the commons breakfast tacos. Anthony, you came in really eager to work during this last year of the project and you certainly put the work in. I was really surprised how quickly you picked up the nuances with our project and you really helped bring things to a close in this last year, bum arm and all.

As the rest of the graduate students, thank you for great break room discussions, help on my "fast" mixes, many coffee runs, and always being willing to pause what you were doing to answer any of my questions. I really could not have asked for a better work environment. Thank you Fred, Racheal, Trevor, Lisa, Saamiya, Sarwar, Donald, Aasiyah, Simon, Nicolas, Beth Anne, Sarah, and Adrian for making this possible. Fred, I don't know how you were able to deal with me during and after work but I really appreciate you always being willing to stop what you were doing to help. Trevor, your after work barbeques and shenanigans kept me sane and I was able to steal a few of your grilling tips. Racheal, you got to join Anthony and I researching rapid repair materials and the many struggles that come with it. Thanks for always pausing your own work to help us out.

This project could not have been completed without the help of many undergraduates such as, Stephen, J.C., Mike, J.P., and Max. Stephen, you were always willing to stay late to help us out with any mixes or measurements. J.C., when Anthony had to get surgery, you helped us finish the project and we really appreciate it. Thanks to all those I have left out because you have had a helping hand in completing this project.

Abstract

Mechanical Properties, Early Age Volume Change, and Heat Generation of Rapid, Cement-based Repair Materials

Mitchell Lee Dornak, M.S.E.

The University of Texas at Austin, 2014

Supervisors: Kevin J. Folliard and Thanos Drimalas

Currently, in Texas, there is a need for different repairs on pavements and bridge decks; rapid repair materials designed for these repairs are available but the service life and durability of these products are often inadequate. Thus, the goal for the Texas Department of Transportation (TxDOT) is to implement repairs with an extended service life in a timely manner, in order to cause minimal disruption. Research performed under TxDOT Project 6723 (Development of Rapid, Cement-based Repair Materials for Transportation Structures) evaluated a wide range of rapid repair materials, including calcium aluminate cement (CAC), calcium sulfoaluminate cement (CSA), fly ash alkali activated blends, and ordinary portland cement. Some of the properties which contribute to a long-term service life are: mechanical properties, early-age volume change, and the heat evolution; often, the early-age development of these repair materials can cause later durability issues. These properties were examined through a variety of experiments and test in the laboratory, as well as, in the field.

Table of Contents

List of Tables

List of Figures

Chapter 1: Introduction

1.1 BACKGROUND

The durability and service life of infrastructure have been a longtime focus for Texas Department of Transportation (TxDOT), as well as, any state transportation departments across the United States. Their focus is to provide safe, reliable, and economical transportation structures across the state that will last for decades. Unfortunately, various factors such as increased traffic loads, aggressive environments, poor placement, and improper design may cause premature failures within different transportation structures.

Currently, in Texas, there is a need for different repairs on pavements and bridge decks because of high volume of traffic. Some of the different repairs necessary are partial, half, and full depth repairs which require repair materials with various characteristics. These repair materials must have accelerated setting times, enhanced workability, and similar mechanical properties with the existing concrete. Not only do the repairs need to satisfy the short-term goals listed above, but the long term goals such as, durability and service life.

The different repair materials available are composed of many different binder systems. Some of the proprietary repair mixtures are portland cement-based and are combined with different fly ashes or silica fume. These blends can provide faster strength gain than normal portland cement concrete because there is an addition of supplementary cementing materials, along with accelerating admixtures. Other binder systems currently implemented are calcium aluminate cements, calcium sulfoaluminate cements, and some all fly ash alkali activated blends. Although rapid repair mixtures may meet the requirement for rapid strength gain and early opening to traffic, future repairs are often required due to cracking or failure of the repair section. The focus of this

research is to better quantify the fresh, hardened, and durability properties of rapid repair materials used to repair concrete pavements and bridge decks in order to improve the long-term performance of such repairs in Texas.

This thesis focuses on a portion of a 3-year research project funded by TxDOT, which concentrates on the characterization of different rapid, cement-based repair materials used on transportation structures. The project has been segmented into three different publications as follows: Jose R. Zuniga's thesis focused on a literary review of the different binder systems and Phase I of the project (Zuniga, 2013); Anthony M. Garcia's thesis deals with freeze-thaw deterioration , alkali-silica reaction, corrosion, and external sulfate attack for rapid repair materials (Garcia, 2014); and this thesis which focuses on the early age volume change, calorimetry, and engineering properties of the repair materials. Phase I of the project involved a screening program where the research team obtained a reasonable test matrix which satisfied sufficient working time, workability, and a compressive strength of 3000 psi (20.7 MPa) at 3 hours (Zuniga, 2013).

1.2 SCOPE AND OBJECTIVES

Some of the issues that have plagued bridge deck repairs have been directly related to the three areas of interest this report will focus on. These areas of focus are engineering properties, early-age volume change, and rapid heat generation for different rapid repair materials.

Concrete repair materials focus on generating early strength gain which notoriously leads to brittle concrete with high modulus of elasticity. Issues with restraint and cracking can occur when the existing concrete and repair are deforming at different rates. Another important engineering property of the repair material is the coefficient of

thermal expansion (CTE). It is important that the CTE of the repair material and the existing concrete is similar, so the repair and base have similar deformation with changes in the climate.

The research team performed testing on early-age volume change because some of the binder systems witness unusual deformation soon after hydration begins. Some of this testing included drying shrinkage testing, as well as, monitoring autogenous shrinkage and expansion with a smaller rigid cracking frame and free shrinkage frame. Understanding how these materials behave initially will help some of the shrinkage and expansion issues witnessed in the field.

During cement hydration there is an exothermic reaction where heat is generated as the concrete gains strength. Understanding that these repair materials have rapid strength gain, thus producing rapid and extreme heat generation is another area that the research team is investigating. The high heat created by some of these repair materials combined with the high temperature from Texas climate can cause issues with thermal cracking, evaporation of bleed water, and expansion problems. The team has monitored the heat generation of the mixture matrix with a variety of testing including: isothermal calorimetry, semi-adiabatic calorimetry, temperature gradient test slabs, and temperature gradient analysis in the field.

1.3 NOTATIONS

As the repair materials were tested and characterized, they were categorized into groups with these labels: Phase I, Phase II, and Phase III Mixtures. Phase I Mixtures included many mixtures involving the different binders and mixture proportions used in the screening process. Of the Phase I Mixtures, 13 were chosen to form the Phase II

Mixtures. These 13 mixtures were involved with all of the engineering properties, durability, and air entrainment studies. Finally, a subset (6) of these mixtures, known as Phase II Mixtures, was chosen for a field trial, corrosion and early age volume study. This subset of mixtures is the group associated as the Phase III Mixtures.

Jose Zuniga's thesis includes a description of all of the mixture identifications and binder systems with the exception of CAC-3. The CAC-3 mixture is a combination of 70% Type I O.P.C. by mass with 30% CAC-based product that also includes calcium sulfate. This formulation was added to evaluate an ettringite based system for rapid, early strength gain until the OPC has time to hydrate and eliminate some of the durability issues related to ettringite systems.

Located below are the 13 mixtures that passed Phase I noted by checked symbols:

Table 1: Mixture Classification

Mix ID	Phase III Mixture
P-1	
P-2	✓
P-3	
P-AAFA	✓
CSA-1	✓
CSA-2	
CSA-3	
CSA-Latex	
CAC-1	
CAC-2	✓
CAC-3	✓
CAC-Latex	
PC Type III	✓

1.4 CONTENT

This thesis is divided into 6 chapters. Chapter 2 describes the different engineering properties of the Phase II Mixtures. Some of these properties are studied under standard temperature considered to be 73 °F (23 °C), as well as higher and lower temperatures, 100 °F (38 °C) and 50 °F (10 °C), respectively.

Chapter 3 describes the effect of early-age shrinkage and cracking. This includes an ASTM C 157 test on all of the Phase II Mixtures and an early-age deformation study with a rigid cracking frame.

Chapter 4 is dedicated to the calorimetry testing completed during the project. The team examined the heat generation of the selective materials with isothermal and semi-adiabatic calorimetry, and the temperature gradients with varying depth slabs.

Chapter 5 is the field testing section which includes an existing field trial that the research team monitored and a simulated bridge deck pour at the research campus. This simulated bridge deck placement gave the team valuable insight on how a subset of the mixtures performed in a larger field trial setting.

Chapter 6 will summarize any key findings and will recommend any future testing.

Chapter 2: Engineering Properties

2.1 Introduction and Background

When examining engineering properties for rapid repair materials, one objective is to select repair materials with similar properties as the existing concrete. This will allow for the repair and base concrete to act homogenously which will extend the service life of the repair. The high early-age compressive strengths of rapid repair materials are one of the hallmarks of the technology, but these high early strengths often generate even higher long-term strengths and can cause appreciable mismatch with the base concrete pavement or deck.

Two of the more important engineering properties are the coefficient of thermal expansion (CTE) and modulus of elasticity (MOE). If a repair material has a high CTE, then the expansion and shrinkage of the material due to changes in temperature can cause cracking and break the bond between the base material and repair. The MOE relates to the stiffness of a material and issues can exist when repair materials have higher MOE. The higher the MOE, the more brittle a material becomes, which can lead to problems when transportation structures begin to deflect due to large loads. If the repair material has a higher MOE then there is a possibility that it will not deflect with the member, which can lead to the bond breaking or spalling of the repair material.

Normally, when following the American Society for Testing and Materials (ASTM) standards, these properties are determined at standard temperature 73 °F (23 °C). The team followed these standards but also wanted to simulate climates across Texas to determine how these materials responded to different mixing and curing temperatures. A temperature robustness study was implemented to determine the compressive strength of cylindrical specimens at two different temperatures, 50 °F (10 °C) and 100 °F (38 °C). The team can approximate other engineering properties from

these compressive strength values, in order to understand the materials performance under different conditions.

TxDOT has different criteria for concrete repairs which is located in their online database. The research team is using TxDOT's Departmental Materials Specification for concrete repair materials, specifically known as DMS-4655, as a guide for classifying the performance of the materials in our testing matrix. This document states minimum and maximum values for most of the engineering properties the team measured, thus, using these criteria to categorize repair materials as non-rapid, rapid, and ultra-rapid repairs. The team selected the criteria for Type A-Rapid Repairs, which are specified for horizontal repairs up to 4 inches in depth.

2.2 MATERIALS AND MIXTURE PROPORTIONS

This chapter will include a variety of materials that are included in the 13 mixtures that passed Phase I. These mixtures include materials composed of calcium aluminate cements (CAC), calcium sulfoaluminate cements (CSA), all fly ash blends, ordinary portland cement (OPC), and proprietary binder blends. All mixtures and proportions, except for the CAC-3 Mixture, are located in Table 12 of Jose Zuniga's Thesis (Zuniga, 2013).

The CAC-3 Mixture is composed of the following: a binder content of 752 lb/yd^3 including Type I OPC and a CAC-3 proprietary binder; a .40 w/cm ratio; a dolomitic limestone coarse aggregate (CA1) with a 3/8" (9.5 mm) max size aggregate; a siliceous natural river sand (FA1); a superplasticizer dosed at .85% of the amount of CAC-3 binder; and a retarder dosed at 0.35% of the amount of CAC-3 binder. The notations of CA1 and FA1 are described in Zuniga's Thesis as well (2013).

All of the concrete used to evaluate engineering properties, excluding the temperature robustness study, were obtained from the same batch in order to reduce any variability during mixing. A 2 ft^3 (.06 m^3) concrete mixture was needed to cast enough cylinders, prisms, unit weight, and slump for each mixture. These mixtures were cast in a 4 ft^3 (.11 m^3) steel drum concrete mixer which can be seen in Figure 1 below. The mixing procedure is described in Zuniga's Thesis for the non-proprietary blends and the research team followed mixing instructions from the producers of the proprietary blends (2013).

Figure 1: 4 ft^3 (.11 m^3) Steel Drum Concrete Mixer

Table 2: Fresh State Properties for Mechanical Properties Mixtures

Mix ID	Slump (inch)	Unit Weight (lb/ft3)	Air Content (%)
P-1	9	142.0	1.5
P-2	10.5	146.0	3.9
P-3	10	144.0	3.0
P-AAFA	8.5	150.6	3.0
CSA-1	4	147.2	2.8
CSA-2	9	137.6	10.0
CSA-3	11	144.8	3.4
CSA-Latex	9	142.4	6.5
CAC-1	9.5	138.5	8.0
CAC-2	10	143.7	7.5
CAC-3	6.5	148.0	5.0
CAC-Latex	10	144.4	4.5
PC Type III	0.5	153.6	5.0

Table 2 and were measured from the 2 ft^3 (.06 m^3) concrete mix mentioned previously. The research team followed these standards for slump, unit weight, and air content, respectively:

- ASTM C 143 (2012)
- ASTM C 138 (2013)
- ASTM C 231 (2010)

2.3 MECHANICAL PROPERTIES AT STANDARD TEMPERATURE

Table 3 provides the information on the mixtures cast at standard temperature which is considered 73 °F (23 °C). The compressive strength was measured at 3 hours because TxDOT wants to allow traffic onto the repaired section as soon as possible. Two of the mixtures, CAC-1 and CAC-Latex, have two values under the 3 hour compressive strengths designation. The second value, 4 hour compressive strength, was presented due

to the lower compressive strength at 3 hours. The other properties on Table 3 are all measured following their respective standards at 28 days after casting.

Table 3: Mechanical Properties for all Mixtures

Mix ID	3 Hour Compressive Strength (psi)	28 Day Compressive Strength (psi)	Flexural Strength (psi)	Modulus of Elasticity (ksi)	Tensile Strength (psi)
P-1	3560	7190	560	4410	520
P-2	4720	10540	1530	5140	790
P-3	--	8220	1410	5510	720
P-AAFA	3040	8910	870	5000	670
CSA-1	5040	8440	770	5290	620
CSA-2	4000	6170	700	4650	550
CSA-3	4680	7900	870	5850	660
CSA-Latex	3500	5800	790	4500	490
CAC-1	570 (4210)	6520	1190	6140	580
CAC-2	3080	7860	880	5900	690
CAC-3	3010	6760	1110	5410	640
CAC-Latex	480 (2970)	6280	1190	4680	600
PC Type III	--	11740	1230	7670	870

2.3.1 Compressive Strength

Compressive strength is an important property to report for repair materials because the repair must be as strong, if not stronger than the existing material to carry the designated load. Since the research team is focusing on repairs for bridge decks, there is not a need for high compressive strengths in the repair material because typical strengths for the concrete in bridge decks at 28 days are in the 4000 to 6000 psi (27.6 to 41.4 MPa) range (NCHRP, 2004). The focus of these repairs is on rapid strength gain to reduce the amount of time needed to block traffic.

2.3.1.1 Experimental Procedures

For this section, the research team followed ASTM C 39 Standard Test for Compressive Strength of Cylindrical Concrete Specimen. Compressive strength values were measured at 2 hours, 3 hours, 4 hours, 6 hours, 12 hours, 1 day, 3 days, and 28 days

after mixing. This provided a strength gain curve for each of the materials, which can be found in Zuniga's Thesis (2014). The team also followed ASTM C 1231 when unbonded neoprene end caps were used on the cylinders during testing (2013).

Due to the rapid setting time, the team decided to reduce the mixture size by casting 3 x 6" (76.2 mm x 152.4 mm) cylindrical specimen for determination of compressive strength. Previous research states that below a compressive strength 7250 psi (50 MPa) there is a statistical equivalence between 6 x 12" (152.4 mm x 304.8 mm) cylinders and 3 x 6" (76.2 mm x 152.4 mm) cylinders (Day & Haque, 1993). As previously mentioned, typical bridge decks do not require high compressive strengths, therefore, when the 3 x 6" (76.2 mm x 152.4 mm) and 6 x 12" (152.4 mm x 304.8 mm) cylinders can have discrepancies beyond 7250 psi (50 MPa), there is adequate strength for these applications.

2.3.1.2 Results and Discussion

The results of compressive strength tests for 12 of the mixtures were previously presented by Zuniga (2013); the strength curve for Mixture CAC-3, which was added into the testing matrix after Zuniga's thesis, is shown in Figure 2 out to an age of 28 days.

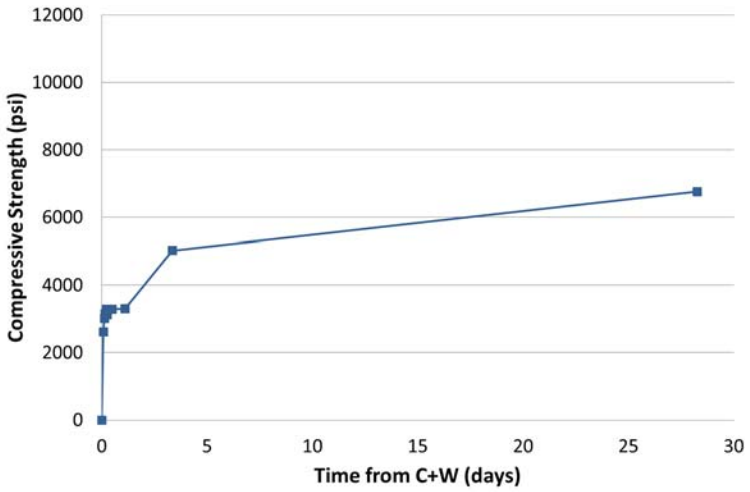

Figure 2: Compressive Strength for CAC-3 Mixture

Referring back to Table 3, it is evident that the P-3 and PC Type III mixtures have a slower strength gain compared to the other mixtures because there is a negligible compressive strength at 3 hours. This is due to the composition of these mixtures. Both P-3 and PC Type III are mainly composed of portland cement which does not gain strength as quickly as the other binder systems. CAC-1 and CAC-Latex mixtures also gained strength slower than most of the other rapid repair mixtures; however, the 4 hour compressive strength of each mixture was 4210 and 2970 psi (29 and 20.5 MPa), respectively. These CAC mixtures were slightly "sluggish" at 3 hours after mixing but once calcium aluminate mixtures start to hydrate, the strength gain is very rapid.

The 28-day compressive strengths range from 5800 to 11742 psi (40 to 81 MPa). Ironically, the PC Type III mixture had the slowest strength gain, as well as the highest 28-day compressive strength. This mixture contained a very high cement content, accelerator, and low w/cm ratio, thus contributing to a high compressive strength. It can be seen that the CSA mixtures have rapid strength gain but their 28-day strength is

weaker than the rest as a whole. Overall, the P-2 Mixture performed the best for both early (3 hour) and later (28 day) compressive strengths.

2.3.2 Flexural Strength

The flexural strength, also known as modulus of rupture, is the bending strength of unreinforced concrete beams. This bending strength is important for repairs that are larger in size on roadways and bridge decks because the force from the swelling of soils or heavy traffic loads can cause flexure in either direction. TxDOT has a current minimum specification of 620 psi (4.3 MPa) for the 28-day modulus of rupture of concrete pavements.

The 28-day flexural strength of normal-weight portland cement concrete can be approximated as 10-15% of the 28-day compressive strength according to the ACI 318 Building Code (2011). The flexural strength of rapid repair materials, which generally have higher compressive strengths, is typically higher than normal-weight portland cement concrete.

2.3.2.1 Experimental Procedures

The flexural strength of each mixture was measured following ASTM C 78 Standard Test Method for Flexural Strength of Concrete. The test specimens were wet-cured for 28 days before testing began. The flexural strength for this test is calculated using the simple beam third-point loading which ensures a constant bending moment without any shear force being applied in the middle third section (Mamlouk & Zaniewski, 2006).

2.3.2.2 Results and Discussion

The results from Table 3 range from 562 psi (3.9 MPa) for the P-1 Mixture to 1531 psi (10.6 MPa) for the P-2 Mixture. All of the mixtures, except for P-1, passed the

minimum criteria for 28-day flexural strength in concrete pavements. When examining each binder system as a group, their flexural strengths were very similar.

The mixtures containing mostly portland cement have high modulus of rupture, while the CSA binders portrayed significantly lower flexural strengths. The tensile strength for the CSA mixtures averaged 11% of their respective compressive strengths, while the CAC mixtures averaged above the range suggested by the ACI Building Code at 16% of their respective compressive strengths. All of the calcium aluminate mixtures, except for the CAC-2 Mixture, have relatively high flexural strengths.

2.3.3 Modulus of Elasticity

The modulus of elasticity of concrete is an important property in the design of concrete structures and is commonly referred to as the stiffness of the desired material. Mamlouk and Zaniewski define the modulus of elasticity or Young's modulus (E) as the proportional constant between normal stress and normal strain of a homogenous and linear elastic axially loaded member (2006). Concrete is not homogenous materials due to its composition of aggregate and cement paste, thus, negating the use of the classic relationship of Young's modulus.

One objective when making a decision on a certain repair material is to try to match the modulus of elasticity to the existing concrete. If the repair has a significantly higher or lower modulus there could compatibility issues with the existing structure. It is evident that the modulus of elasticity for concrete repairs is an area of concern for TxDOT because of the specified maximum modulus value in their Departmental Materials Specification (TxDOT, 2011). The maximum modulus of elasticity value is 5000 ksi (34.5 GPa) for rapid repair materials. While the ACI 318 Building Code suggests that the modulus of elasticity for normal-weight can be assumed to be

$Wc^{1.5}$*33*sqrt(f'c). For this equation, the Wc value refers to the unit weight of the concrete in lb/ft^3 and the f'c is the compressive strength value in psi (2011). The modulus value of concrete is highly dependent on the coarse aggregate in the mixture, such that siliceous aggregates tend to significantly increase modulus of elasticity values compared to limestone aggregates.

2.3.3.1 Experimental Procedures

The research team followed ASTM C 469 Standard Test Method for Static Modulus of Elasticity and Poisson's Ratio of Concrete in Compression (2010). This standard measures the chord modulus of the concrete specimen in the working stress range of 0 to 40% of the ultimate concrete strength. Neoprene pads were used following the unbonded end caps standard mentioned previously in the compressive strength section. Figure 3 below is an image of the setup used to determine the modulus.

Figure 3: Modulus of Elasticity Setup

2.3.3.2 Results and Discussion

Because the modulus of elasticity is typically related to compressive strength, the mixtures researched portrayed relatively higher modulus values due to their higher compressive strengths. In the previous section, Table 3 shows that out of the 13 mixtures only 7 mixtures passed TxDOT's criteria. Of the four proprietary mixtures, which are composed of different aggregates, only two were below the 5000 ksi (34.5 GPa) specified modulus. The non-proprietary mixtures were composed of dolomitic limestone for coarse aggregate and siliceous river gravel for fine aggregate. The P-1 Mixture presented the lowest modulus value at 4410 ksi (30.4 GPa), while the PC Type III Mixture had the highest at 7670 ksi (52.9 GPa). When the ACI 318 equation was used to approximate the modulus of elasticity from the compressive strength, the approximation underestimated the modulus measured. Thus, this equation should not be used to approximate the modulus of elasticity of rapid repair materials because it was 5% lower than the measured modulus.

2.3.4 Splitting Tensile Strength

The splitting tensile strength of concrete is another important property of concrete repair materials. Again, TxDOT has a designated minimum splitting tensile strength of 400 psi (2.8 MPa) for rapid repair materials following a 28 day curing period (TxDOT, 2011). According to Neville, splitting (indirect) tensile strength values for portland cement concrete vary from 2.5 MPa to 3.1 MPa (360 psi to 450 psi) (1981). This splitting tensile strength is typically lower than the direct tensile strength of the specimen, which is about 10% of the specimen's compressive strength.

2.3.4.1 Experimental Procedures

To evaluate the splitting tensile strength, the research team followed ASTM C 496 Standard Test Method for Splitting Tensile Strength of Cylindrical Concrete Specimens (2011).

2.3.4.2 Results and Discussion

Each of the 13 mixtures tested passed the minimum criteria set by TxDOT. The CSA-Latex Mixture had the lowest splitting tensile strength at 490 psi (3.4 MPa), while the PC Type III Mixture had the largest splitting tensile strength at 870 psi (6 MPa). When comparing the value of 10% of each mixture's 28 day compressive strength to its respective splitting tensile strength, it is evident that the 10% value is greater for every mixture. The CAC mixtures tensile strength values averaged 9% of the 28-day compressive strength values; the CSA mixtures, on the other hand, averaged about 8% of the 28-day strength values. This is possibly from the fact, that the compressive strengths were calculated with 3 x 6" (76.2 mm x 152.4 mm) cylinders while 4 x 8" (101.6 mm x 203.2 mm) cylinders were used to measure tensile strength. According to Mehta and Monterio, when the compressive strength of concrete increases, the 10% assumption of the tensile strength decreases; tensile values of 7 or 8% of the compressive strength have been seen for high strength concrete (1993). Thus, as the compressive strength increases, the concrete becomes more brittle which impacts the tensile strength of the specimen more than the compressive strength. This could be applicable to rapid repair materials since higher compressive strengths were observed at 28 days.

2.4 TEMPERATURE ROBUSTNESS

The temperature robustness study was implemented to examine the sensitivity of temperature for each binder. Some binders, such as calcium sulfoaluminate, have been

known to be more sensitive to temperature than other binder systems. The research team elected to test all 13 mixtures at temperatures of 50 °F (10 °C) and 100 °F (38 °C). Previous literature suggests that due to the rapid hardening ability of calcium aluminate cement can be placed at low temperatures with little reduction in strength gain (Bentivegna, 2012), but there are scarce data for many of these rapid repair mixtures for testing at varying temperature extremes.

2.4.1 Experimental Procedures

For this experiment, all of mixing materials were measured and stored in an environmental chamber at the specified temperature for 24 hours before mixing time. This ensures that all of the materials are at the specified temperature before mixing and casting. The specimens were mixed and cast in the mixing room, which is kept at standard temperature of 73 °F (23 °C), and immediately following were placed back into the environmental chamber for 24 hours after the time of mixing. The team cast a total of 18 3 x 6" (76.2 mm x 152.4 mm) cylinders, which were capped following placement, for compressive strength measurements. Each mixture's compressive strength was measured at 2, 3, 4, 6, 12, and 24 hour intervals for comparison to the compressive strengths measured at standard temperature.

The cylindrical specimens were tested in accordance of ASTM C 39, as well as, ASTM C 1231 due to the use of neoprene end caps. Figure 4 presents the environmental chamber used to heat and cool the specimen.

Figure 4: Environmental Chamber for Temperature Robustness Study

2.4.2 Results and Discussion

This section discussed the results of each mixture. For ease, the research team has grouped the following mixtures into proprietary, CSA, CAC, and portland cement mixtures. The first three proprietary blends were significantly affected by the cooler temperature, while the alkali activated fly ash blend had a higher compressive strength at 24 hours at 50 °F (10 °C) compared to 73 °F (23 °C). The P-3 Mixture is technically not a rapid repair material, according to TxDOT criteria, which is made apparent by the strength curve in Figure 7.

The straight CSA blend in Figure 9 and the CSA-Latex Mixture in Figure 12 showed a significant drop in compressive strength of 2000 psi (13.8 MPa) from the standard temperature to the cooler temperature. All four CSA mixtures do not show a significant difference when heating the material and the CSA-3 Mixture is the only mixture with a higher compressive strength at 50 °F (10 °C) when compared to 73 °F (23 °C).

As a whole, CAC mixtures do not seem to be affected by temperature change as expected. The CAC-3 Mixture is the only one to show reduced strengths at 50 °F (10 °C), where this mixture has less than 500 psi (3.4 MPa) at 24 hours. For the most part, the standard temperature mixtures had the highest compressive strengths at 24 hours.

The temperature robustness study did affect the portland cement mixture which was expected. The 100 °F (38 °C) mixture is 4000 psi (27.6 MPa) stronger than the 50 °F (10 °C) mixture at 24 hours.

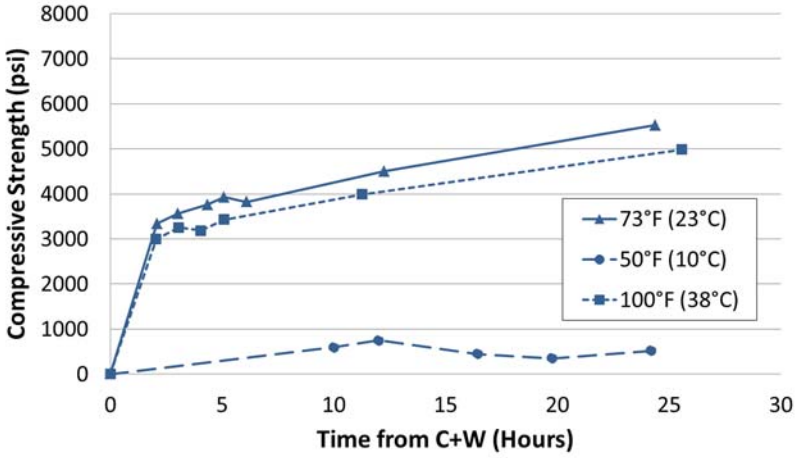

Figure 5: Compressive Strength Comparison for Mixture P-1

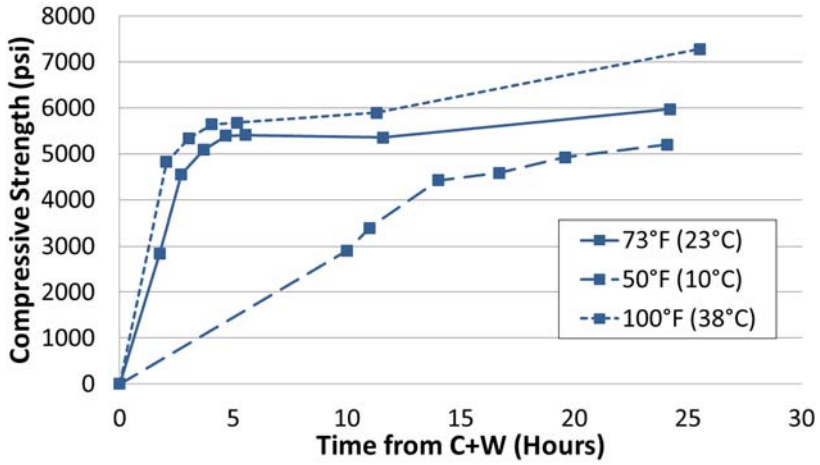

Figure 6: Compressive Strength Comparison for Mixture P-2

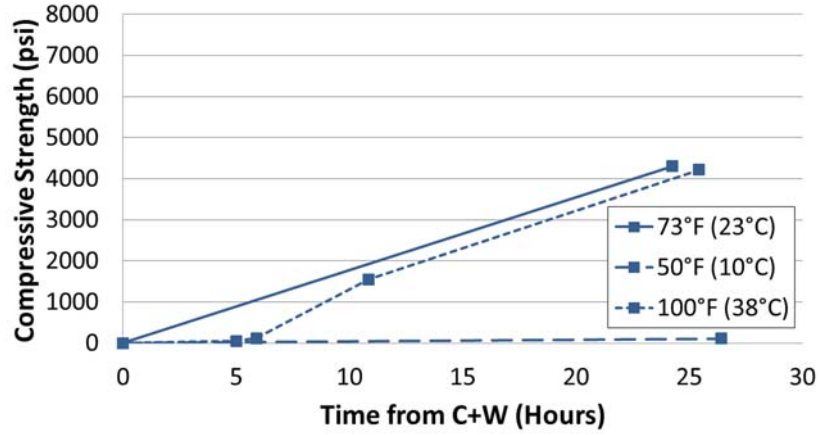

Figure 7: Compressive Strength Comparison for Mixture P-3

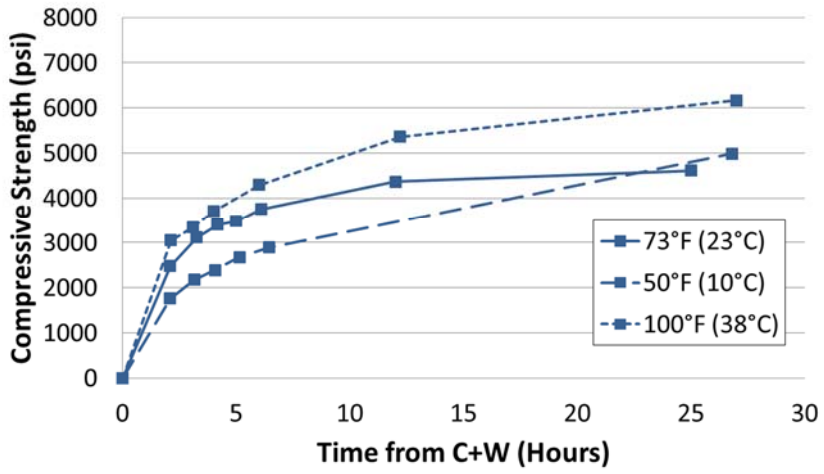

Figure 8: Compressive Strength Comparison for Mixture P-AAFA

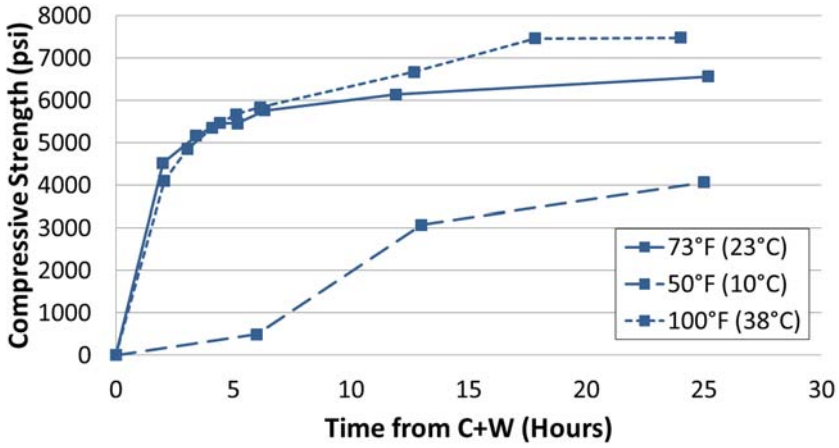

Figure 9: Compressive Strength Comparison for Mixture CSA-1

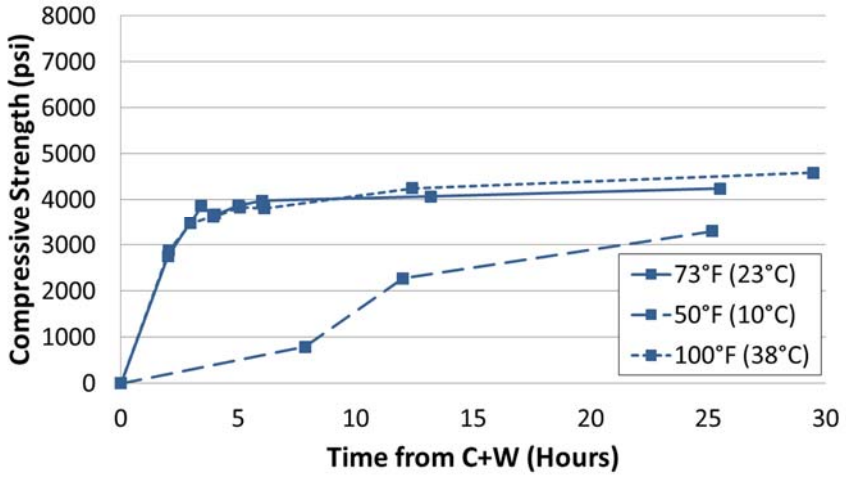

Figure 10: Compressive Strength Comparison for Mixture CSA-2

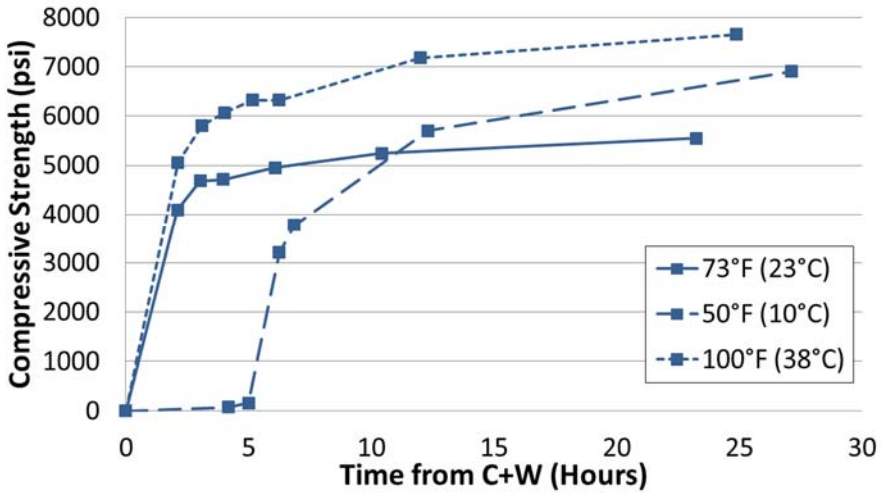

Figure 11: Compressive Strength Comparison for Mixture CSA-3

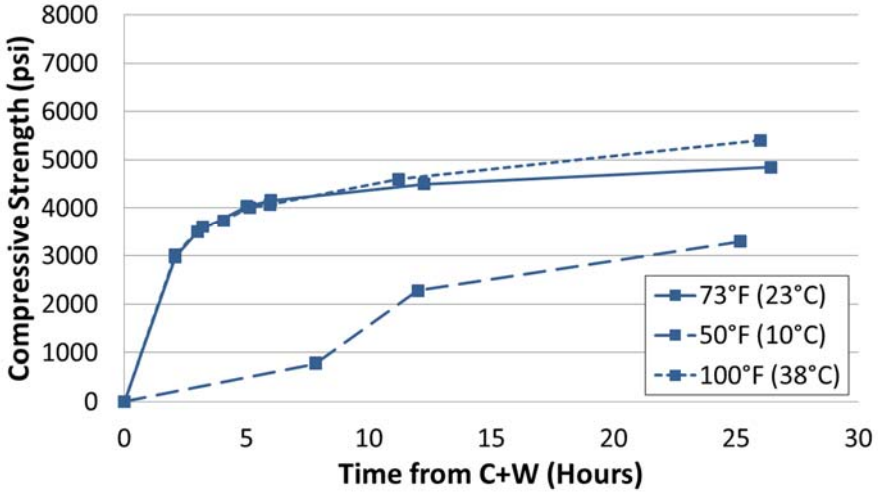

Figure 12: Compressive Strength Comparison for Mixture CSA-Latex

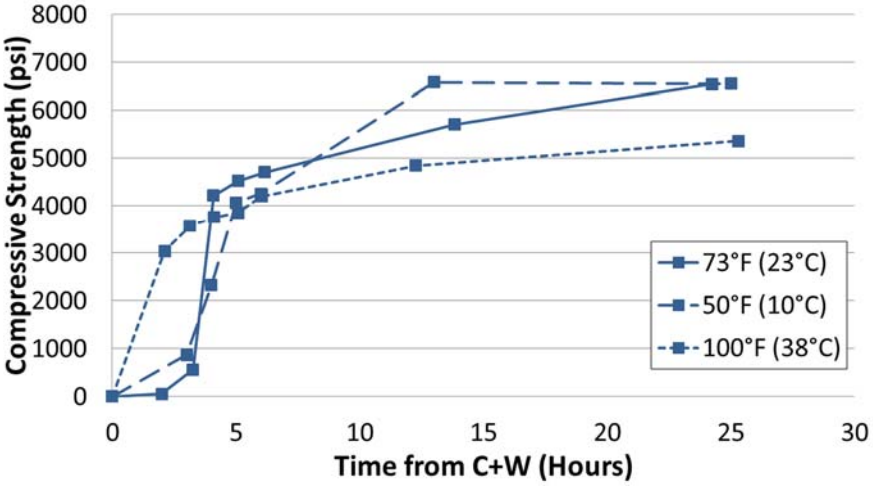

Figure 13: Compressive Strength Comparison for Mixture CAC-1

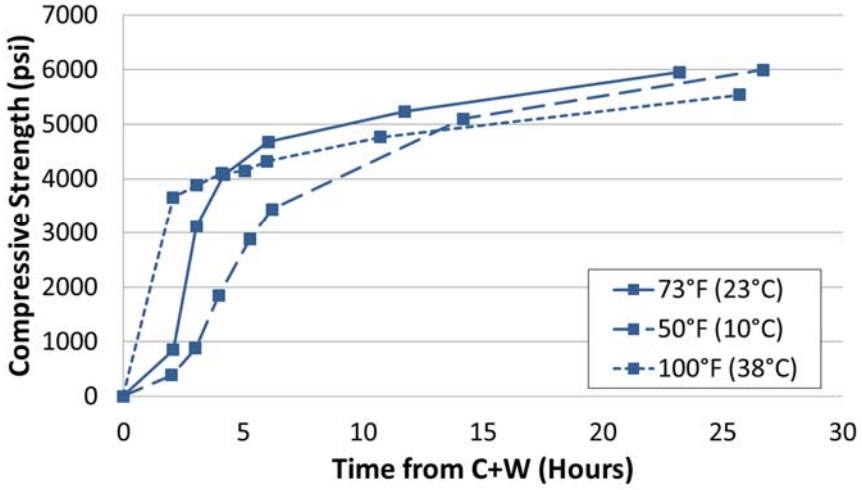

Figure 14: Compressive Strength Comparison for Mixture CAC-2

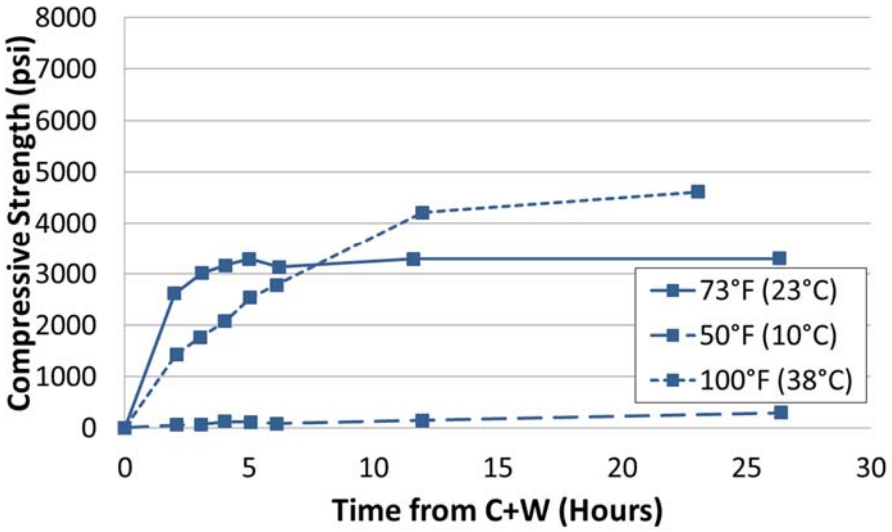

Figure 15: Compressive Strength Comparison for Mixture CAC-3

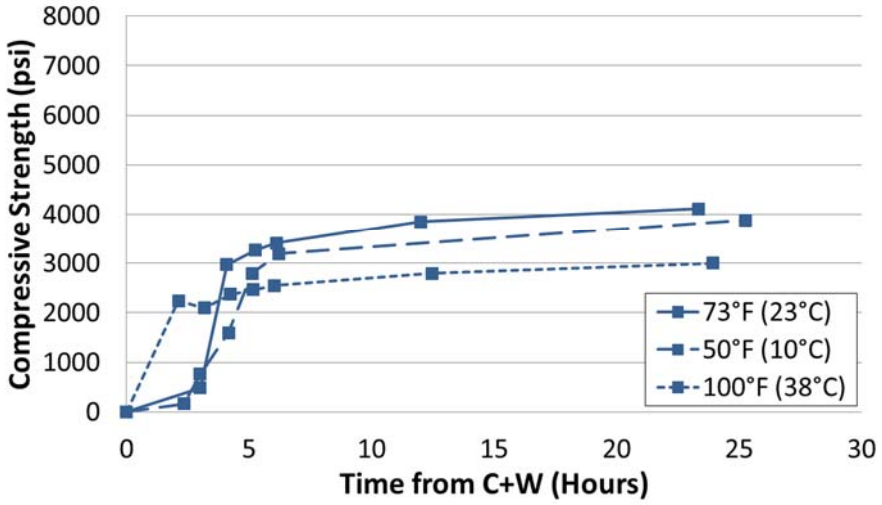

Figure 16: Compressive Strength Comparison for Mixture CAC-Latex

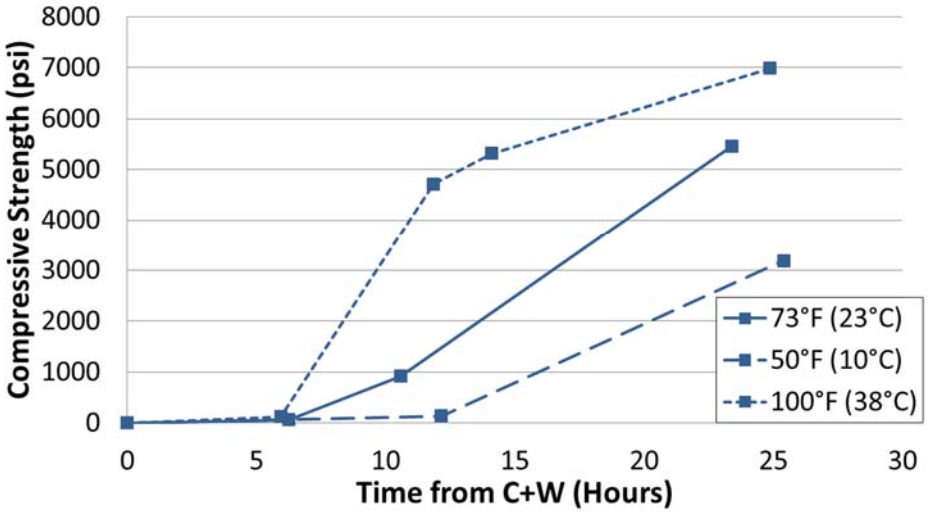

Figure 17: Compressive Strength Comparison for Mixture PC Type III

2.5 COEFFICIENT OF THERMAL EXPANSION

The coefficient of thermal expansion is the measure of a materials ability to expand and contract due to various temperatures. As previously mentioned, it is

imperative to select repair materials which have similar CTE values as the existing concrete. Ordinary portland cement concrete has CTE values ranging from 4 to 7 με/°F (8 to 12 με /°C) and TxDOT's criteria for rapid repair materials is a maximum CTE value of 6 micro strain/°F following a 28 day cure.

Typically, the type of aggregate used is the largest contributing factor towards the CTE of concrete. Limestone aggregates yield lower CTE values when compared to siliceous aggregates. Of the 13 mixtures tested, 9 of the mixtures contained a dolomitic limestone used for the coarse aggregate and siliceous river sand for the fine aggregate. Cement paste also affects the coefficient of thermal expansion but since it composes less than 30% of the volume in concrete, the paste has less influence on the CTE.

2.5.1 Experimental Procedures

The research team followed AASHTO T 336 Standard Method of Test for Coefficient of Thermal Expansion of Hydraulic Cement Concrete (2011). This method involves measuring the length deformation of a 4 x 8" (101.6 mm x 203.2 mm) cylindrical specimen submersed in water bath that ranges in temperature from 50 °F to 122 °F (10 °C to 50 °C). Figure 18 below is an image of the setup the research team used to evaluate the CTE of each mixture.

Figure 18: Coefficient of Thermal Expansion Setup

2.5.2 Results and Discussion

All 13 mixtures underwent CTE testing and the results are presented in Table 3 below. The proprietary mixtures contained various aggregates not selected by the research team which in turn, possibly contributed to higher CTE values. The only mixtures satisfying TxDOT's criteria were P-2, the three CAC mixtures, and PC Type III Mixture. The CAC mixtures values were not within tolerance of the AASHTO T 336 standard but the data are included in the table for completeness (2011). The tolerances for the CTE standard include CTE values of less than or 0.2 με/°F or 0.3 με/°C when the specimen is ramping up to 122 °F (50 °C) and down to 50 °F (10 °C). The CAC-1 and CAC-2 Mixtures would not fall within the tolerances set by AASHTO T 336 standard. Overall, the P-2 and PC Type III exhibited the lowest CTE values, attributed most likely to the aggregates used in P-2 and the PC binder used in the PC Type III. Interestingly,

latex significantly increased the CTE compared to straight CAC mixtures. This deserves more attention and additional testing in the future to confirm this behavior and if this is a repeatable trend, it is worth studying the underlying mechanisms.

Table 4: Coefficient of Thermal Expansion (CTE) for all Mixtures

	COTE	
Mix ID	(με/°F)	(με/°C)
P-1	8.23	14.81
P-2	4.78	8.61
P-3	6.63	11.94
P-AAFA	6.57	11.83
CSA-1	6.75	12.15
CSA-2	6.71	12.07
CSA-3	6.68	12.03
CSA-Latex	6.49	11.69
CAC-1	5.58	10.05
CAC-2	5.31	9.55
CAC-3	5.18	9.33
CAC-Latex	7.1	12.78
PC Type III	5.41	9.73

2.6 BOND STRENGTH

Bond strength can be described as a material's ability to adhere to its surroundings. Repair materials must have relatively high bond strengths because concrete repairs normally consist of multiple contact surfaces with the existing concrete. If the bond breaks at the contact surface, the gap formed can be a passageway for water and chlorides to reach the reinforcing steel and cause corrosion. A few ways to increase the bond strength of concrete materials are with the addition of supplementary cementing materials (SCM) or styrene butadiene rubber (SBR) latex polymer. The addition of SCM to the concrete allows for more hydration and generates more C-S-H which is considered the "glue" that binds concrete together. Latex-modified concrete is often selected with

the goal of producing a lower permeability, more flexible concrete, and as an additional effect, providing better adhesion to the base material.

2.6.1 Experimental Procedures

Multiple bond strength tests for concrete repair materials exist but two of these tests are more widely used. These two tests are the pull-off method and the slant-shear bond test. TxDOT prefers the slant-shear bond test for rapid repair materials which follows ASTM C 882 Standard Test Method for Bond Strength of Epoxy-Resin Systems Used with Concrete by Slant Shear (2012). The research team followed this standard and with the assistance of TxDOT's concrete materials lab. TxDOT provided the base specimens for these slant shear tests which contain the specifications of DMS-4655 (2011). The base specimen must be at saturated surface dry condition before casting the repair materials on top. Figure 19 can be seen below presents a substrate specimen provided by TxDOT.

Figure 19: Substrate for Slant Shear Bond Strength Study

The specimens were cast in 3 x 6" (76.2 mm x 152.4 mm) cylinders and were capped immediately after casting. The cylinders were removed from the molds at 24

hours to be cured for an additional 48 hours. TxDOT has criteria for the slant-shear bond strength of rapid repair materials of 2000 psi (13.8 MPa) at 3 days, which is when the research team elected to measure bond strength as well (TxDOT, 2011).

2.6.2 Results and Discussion

Table 5 presents the bond strength data for all 13 mixtures, along with the compressive strength data at 3 days for comparison. The CSA mixtures, as a whole, had higher bond strengths than the CAC mixtures and proprietary mixtures. The latex-modified mixtures did not seem to have higher bond strengths as literature has suggested, and in fact, bond strengths were reduced when using latex with either CSA or CAC. There was not as strong of a correlation between compressive strength and bond strength measured at the same time. Lastly, only 5 of the 13 mixtures would have been deemed acceptable by TxDOT's standards for rapid repairs at 2000 psi (13.8 MPa).

Table 5: 3-Day Compressive and Bond Strengths for all Mixtures

Mix ID	Compresssive Strength (psi)	Bond Strength (psi)
P-1	6190	1820
P-2	7220	2290
P-3	6820	1050
P-AAFA	5660	1540
CSA-1	6870	2050
CSA-2	4940	2020
CSA-3	5720	2800
CSA-Latex	4810	1700
CAC-1	6550	2010
CAC-2	6360	1710
CAC-3	5020	1810
CAC-Latex	4510	1710
PC Type III	7590	1790

2.7 SUMMARY AND CONCLUSIONS

The following table summarizes the performance of the Phase II Mixtures compared to the limits set by TxDOT for the engineering properties of rapid repair materials. The boxes with check symbols suggest that the designated mixture passed the requirements set by TxDOT, while unmarked boxes suggest that the designated material did not meet the requirements.

Table 6: TxDOT's Criteria for Rapid Repair Materials (TxDOT, 2011)

Mix ID	Compressive Strength	Modulus of Elasticity	Splitting Tensile Strength	Coefficient of Thermal Expansion	Bond Strength
P-1	✓		✓		
P-2	✓	✓	✓	✓	✓
P-3		✓	✓		
P-AAFA	✓	✓	✓		
CSA-1	✓	✓	✓		✓
CSA-2	✓		✓		✓
CSA-3	✓	✓	✓		✓
CSA-Latex	✓		✓		
CAC-1		✓	✓	✓	✓
CAC-2	✓	✓	✓	✓	
CAC-3	✓	✓	✓	✓	
CAC-Latex	✓		✓		
PC Type III		✓	✓	✓	

The following conclusions can be made from the information provided in the chapter:

- The selection of the repair materials should not be focused on the material with the strongest or highest values for the engineering properties but rather, selecting a repair material with similar properties to those of the existing substrate. Selecting repair materials in this manner will increase the service life on any repair.
- The P-2 Mixture satisfied the most criteria when considering all of the properties measured at standard temperatures.

- The CAC mixtures presented the best behavior during the temperature robustness study but did not fall within the tolerances set by the AASHTO T 336 standard (2011).
- Combining latex with either CSA or CAC had significant impact on the engineering properties, reducing compressive strength, modulus of elasticity, tensile strength (for CSA mixture only), and bond strength and increasing the flexural strength. According to Bentivegna's field study, the latex modified CAC overlays showed worse signs of deterioration when compared to plain CAC mixtures (2011).

Chapter 3: Early-Age Volume Change

3.1 Introduction and Background

Early-age volume change is an important topic for rapid repair materials due to the restrained nature of a repair. When a partial, half depth, or full depth repair is placed on a bridge deck there is restraint from all directions excluding the surface. This restraint can cause cracking when there is a significant volume change, thus leading to a shortened service life of the repair and existing structure. This can be exacerbated when the mechanical and thermal properties of the repair material are significantly different than the base concrete.

The research team evaluate multiple forms of volume change, including drying shrinkage, autogenous deformation, and thermal volume changes. Drying shrinkage is caused when concrete is placed in a dry or unsaturated environment which allows for the water from the surface of the concrete to evaporate. This causes the surface pores to shrink due to the surface tension created by capillary action.

Autogenous shrinkage occurs in concrete with low water-to-cement ratios due to the lack of water during cement hydration. This causes some of the pores to be filled with a water-vapor mix that creates surface tension. The surface tension places tensile forces on the concrete matrix, which in turn forces the paste to shrink around the aggregate (Riding, 2007). Autogenous shrinkage, known as "external" volume reduction, is only a factor up until setting time, where the concrete develops enough tensile strength to restrain the shrinkage. Although, chemical shrinkage and autogenous shrinkage are similar, differences exist within each of their mechanisms. The volume of cement and water when separate is greater than when they are combined, and this reduction in volume is referred to as chemical shrinkage. Chemical shrinkage occurs as a result of

hydration throughout the life of the concrete and is considered "internal" volume reduction (Ideker, 2008).

A miniature rigid cracking frame (RCF) and free shrinkage frame (FSF) are two instruments that were used to monitor autogenous deformation and thermal volume changes. The devices typically used by researchers at UT for portland cement concrete are much larger than those used in this study; miniature frames were developed at UT for evaluating rapid repair materials in order to maintain temperature control during rapid heat generation. The miniature frames are roughly 1/3 the size of the larger frames and the dimensions of each frame are noted in each section below. The rigid cracking frame restricts movement in the concrete and measures the stress generated from thermal effects, autogenous deformation, and strength development. The free shrinkage frame allows for unrestrained (free) movement under controlled temperature which gives us the autogenous deformation of a concrete or mortar mixture.

3.2 MATERIALS AND MIXTURE PROPORTIONS

This drying shrinkage portion of this chapter includes all 13 mixtures passing Phase I. All of these mixture proportions and mixing procedures for these different binders are located in Table 12 of Zuniga (2013), excluding the CAC-3 Mixture which was mentioned previously in Section 2.2. Because calcium aluminate and calcium sulfoaluminate binders (CSA-1 and CAC-2) were evaluated using the miniature RCF and FSF, these mixtures were also evaluated for drying shrinkage.

3.3 DRYING SHRINKAGE

The underlying mechanism for drying shrinkage is related the movement of water out of the pore structure of the concrete matrix (Ideker, 2008). Drying shrinkage occurs when the concrete is stored in unsaturated air which causes the water at the surface to

evaporate. The rate of water loss on concrete surfaces is highly dependent upon environmental factors such as wind, relative humidity, and ambient temperature (Whigham, 2005). Normally, drying shrinkage is not an issue for ordinary portland cement concrete as long as the proper curing procedures are followed. This is not always the case for rapid repair materials which tend to have high thermal effects that can drive water to the surface more frequently. TxDOT has drying shrinkage criteria for rapid repair materials which requires the concrete to have less than 0.07% expansion at 28 days from mixing (TxDOT, 2011).

3.3.1 Experimental Procedures

The research team followed the ASTM C 157 Standard Test Method for Length Change of Hardened Hydraulic-Cement Mortar and Concrete. This standard was modified due to the interest in early age properties. Instead of curing the specimens to 28 days, the team removed the specimens from molds when a compressive strength of 3000 psi (20.7 MPa) was obtained, and initial drying shrinkage measurements were recorded. These specimens were measured according to ASTM C 157, along with additional measurements at 3, 6, 12, 24, 48, and 72 hours if 3000 psi (20.7 MPa) was reached at 3 hours. Figure 20 below presents the specimens in a room kept at 73 °F (23 °C) and 50% relative humidity.

Figure 20: Drying Shrinkage Prisms

3.3.2 Results and Discussion

The drying shrinkage values for all 13 mixtures are presented in

Table 7 below. When comparing the drying shrinkage values of the 13 mixtures to the criteria set by TxDOT, only 4 of the 13 mixtures have greater than 0.07% expansion. The CAC mixtures exhibited the higher shrinkage values at 28 days, as 3 of the 4 mixtures did not pass TxDOT's criteria. The mixtures containing fly ash performed worse than mixtures without fly ash. The CSA-1 Mixture had the lowest percent expansion at 28 days, while the CAC-Latex mixture had the highest at .094% expansion.

Table 7: Drying Shrinkage Values for All 13 Mixtures

Mix ID	28-Day Drying Shrinkage (με)	28-Day Drying Shrinkage (%)	64-Week Drying Shrinkage (με)	64-Week Drying Shrinkage (%)
P-1	57	0.006	133	0.013
P-2	410	0.041	633	0.063
P-3	550	0.055	733	0.073
P-AAFA	867	0.087	813	0.081
CSA-1	33	0.003	140	0.014
CSA-2	263	0.026	433	0.043
CSA-3	237	0.024	323	0.032
CSA-Latex	193	0.019	177	0.018
CAC-1	297	0.030	543	0.054
CAC-2	880	0.088	1153	0.115
CAC-3	840	0.084	1303	0.130
CAC-Latex	943	0.094	1070	0.107
PC Type III	290	0.029	427	0.043

3.4 RESTRAINED STRESS DEVELOPMENT

The rigid cracking frame was invented in Munich, Germany when portland cement concrete began to crack on the autobahn in Austria. This frame was designed to incorporate testing of autogenous deformation, thermal effects, creep, relaxation, and strength development (Ideker, 2008). The rigid cracking frame is composed of copper tubing and insulation to control the internal temperature of the concrete. Stress measured by the frame occurs so in a passive manner; thus, when the concrete tries to expand,

compressive stresses are formed within the mixture which causes tensile stresses in the two Invar steel bars shown below in Figure 21. Strain gauges are mounted on the Invar side bars to measure the strain, convert it to stress with the properties of the Invar, and then reverse the stress due to the passive nature of the system.

Figure 21 shows a top view of the rigid cracking frame. The Invar side bars run along the sides of the concrete, while the frame resembles "dog-boned" shape for restraint of the system. The crossheads provide restraint with metal "teeth" to ensure there is no slipping of the concrete. The miniature rigid cracking frame is a third the size of the original frame and has dimensions of 2 in x 2 in x 21.5 in (50.8 mm x 50.8 mm x 546 mm).

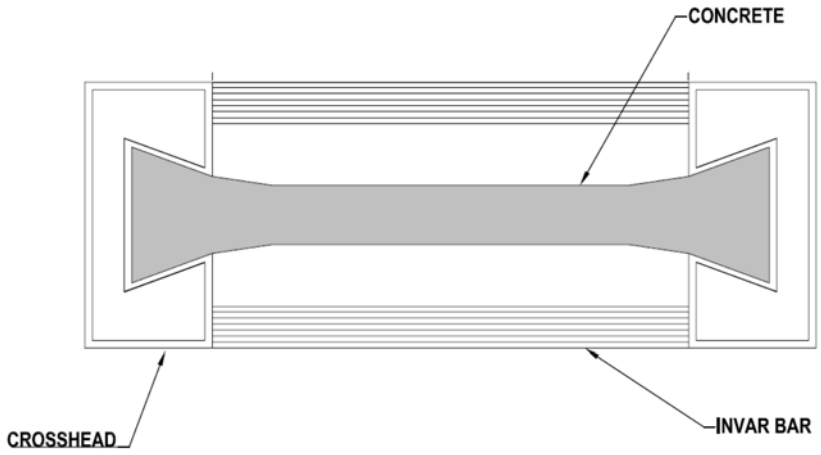

Figure 21: Top View Schematic of RCF (Ideker, 2008)

Thermal effects, autogenous deformation, and strength development can be measured by the stresses in the concrete when the frame follows a time temperature history; however, rapid repair materials have high early heat generation which causes difficulties when trying to control the temperature of the concrete within certain tolerances. For this reason, the research team decided to test the rigid cracking frame

isothermally at 73 °F (23 °C), thus, eliminating the thermal effects of the mixture. The stresses measured in the frame will provide the team with valuable information on the autogenous behavior of the binder.

3.4.1 Experimental Procedures

As mentioned in the section 3.2 Materials and Mixture Proportions, the CAC-2 and CSA-1 Mixtures were selected for this study. These two mixtures were mixed in a 1.75 ft^3 (.05 m^3) drum mixer described in Zuniga (2013). The research team needed 0.35 ft^3 (.01 m^3) of concrete to cast specimen in the RCF, FSF, and time of set specimen. The setting time was measured by penetration resistance in accordance with ASTM C 403 for the free shrinkage frame (2008).

Before mixing could begin, the rigid cracking frame was cleaned and sealed to prevent drying, thus ensuring autogenous shrinkage only when testing is done at a fixed temperature. Plastic sheeting was placed in the center section of the frame and was taped down with waterproof HVAC aluminum foil tape. The plastic sheeting was not used in the crossheads because the team wanted to ensure sufficient bonding for restraint. Then, silicone was applied to seal and smooth the gaps between the bottom crossbars, crossheads, and center section of the frame.

One water bath was used to control the temperature of the rigid cracking frame, free shrinkage frame, and time of set can. A T-valve was connected to the output of the water bath, such that both frames would receive equal amounts of water simultaneously. The team placed one thermocouple in crosshead section of the frame and another in the center of the specimen to record the temperature throughout the frame and drive the water bath temperature.

The mixture was cast into the rigid cracking frame in two layers where consolidation was achieved with plastic tamping rods. After the excess concrete was removed, the two thermocouples were placed in the specimen and a piece of plastic sheeting cut to the "dog-bone" shape was taped down with the foil tape. The top section of the frame was then attached, thus, creating an autogenous system where no water was permitted to enter or leave the specimen. The water bath was connected to begin the isothermal temperature control of the frame and the setting time was measured immediately. The research team selected to run the isothermal conditions to 72 hours after mixing since a cracking temperature was not the objective of the experiment.

3.4.2 Results and Discussion

The two figures presented below contain the results of the isothermal stress development for both, a CSA and CAC mixture. These binder systems were chosen due to their vastly different early-age characteristics which are depicted on the stress development figures.

The CSA binder system generates early-age strength development with an ettringite based system, which is typically, but not always, expansive. It is for this reason that CSA concrete has been known as shrinkage compensating or shrinkage reducing concrete. This is evident in Figure 22 above where the CSA-2 Mixture witnesses compressive stresses up to 190 psi (1.3 MPa). This mixture also has tensile stresses at 2.5 hours from mixing which is due to a temperature drop of 3 °C while the research team monitored the specimen. This drop was caused when ice was added to the water bath to cool the bath as the specimen was generating heat during the final setting of the concrete.

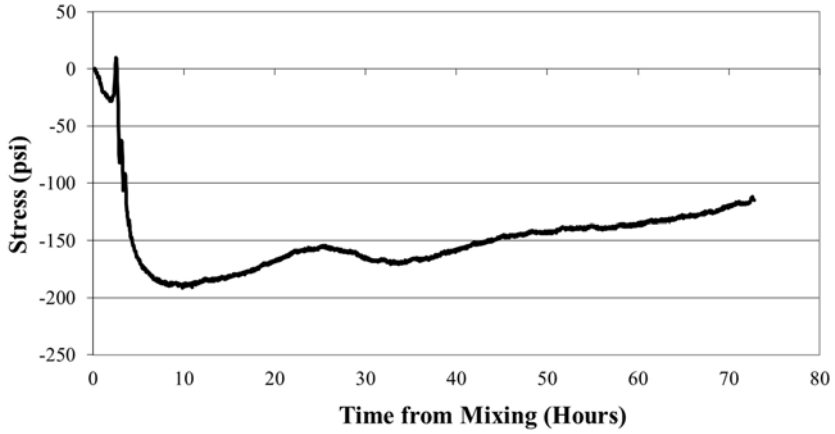

Figure 22: Restrained Stress Development for CSA-1 Mixture

Figure 23 presents the stress development for the CAC-2 Mixture above. This mixture tries to expand while the repair material is still plastic but once final setting occurs the mixture attempts to shrink causing tensile stresses. These tensile stresses increase over the 72 hours up to 270 psi (1.9 MPa) and seem to still increase after the research team had completed their testing. The CAC-2 Mixture generates tensile stresses similar to a typical portland cement concrete mixture would under a 73 °F (23 °C) environment.

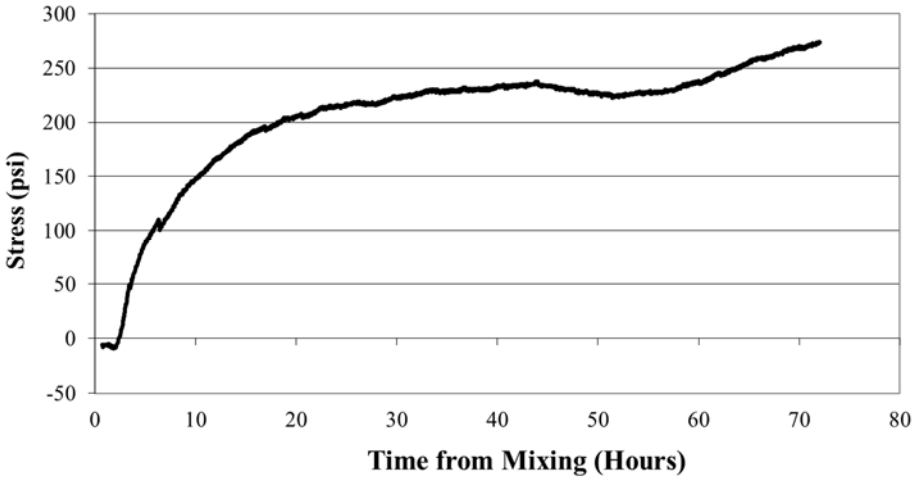

Figure 23: Restrained Stress Development for CAC-2 Mixture

3.5 UNRESTRAINED (FREE) DEFORMATION

The unrestrained deformation of a concrete mixture can be measured with an instrument known as a free shrinkage frame. This frame measures the linear movement of a concrete specimen in a sealed, temperature controlled environment; this linear movement is used to calculate autogenous shrinkage. As with the rigid cracking frame, a smaller version of the free shrinkage frame is necessary to control the temperature for rapid repair materials. Figure 24 presents a side view of the free shrinkage frame.

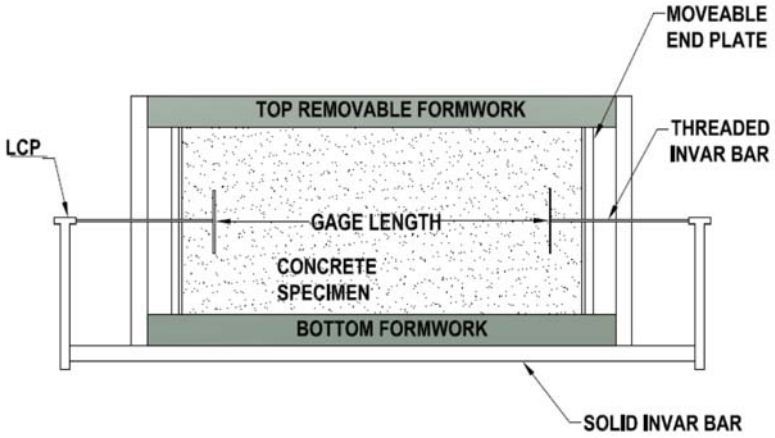

Figure 24: Side View Schematic of FSF (Ideker, 2008)

The cross-section of the free shrinkage frame and the rigid cracking frame are the same at 2 x 2" (50.8 mm x 50.8 mm), but the total length of the free shrinkage frame is 6.9" (175 mm) with a 5.3" (135 mm) gage length between Invar bars. The solid Invar bars below the frame and the threaded Invar bars were selected due to their resistance to thermal deformations. Each of the threaded Invar bars are screwed onto a linear control potentiometer (LCP) at both ends which measure changes in voltage resulting in length change. Aluminum end squares were constructed in order to reduce slippage between the concrete and the small threaded Invar rods. These end squares are 0.5 x 0.5" (13 mm x 13 mm) and have been tapped in the center to allow for the threaded Invar rod to screw into them.

As mentioned earlier, both the rigid cracking frame and the free shrinkage frame run off of the same water bath. The free shrinkage frame is composed of copper pipes within the formwork, as well as with insulation to keep the specimen controlled at a specific temperature. At both ends of the frame are two moveable steel plates bolted to sides the frame. These end plates are in contact with the concrete specimen until the final

setting of the concrete, when the end plates are released, thus allowing for unrestrained deformation.

3.5.1 Experimental Procedures

Before mixing began, the free shrinkage frame was cleaned and prepped. First, the steel end plates needed to be bolted to the frame and extended to allow for a smooth release at final setting of the concrete. The frame was oiled and plastic sheeting was then taped carefully inside the frame to make certain that the cross-section of the frame was not being reduced. A second layer of plastic and oil was added to the body of the frame, while the steel end plates were coated in thick grease to prevent friction during release. After the aluminum end squares were screwed onto the threaded Invar rods, the LCPs were adjusted until they were at mid-stroke so that the specimen would not deform out of the range of the equipment.

The same mixing procedure and batch were used for both the RCF and FSF specimens. The concrete was mechanically vibrated into the frame with plastic tamping rods until the mixture was consolidated. Once the excess concrete was removed, two thermocouples were placed at third points of the specimen to get a uniform temperature profile. Finally, the top piece of plastic sheeting was placed down using aluminum foil tape before the top of the frame was set on the specimen. The water bath tubes were connected to the frame to begin temperature control while the setting time was monitored with the penetration resistance test following ASTM C 403 (2008). Both of the steel plates were released once final setting had occurred to allow for free deformation.

3.5.2 Results and Discussion

The two figures below present the unrestrained deformation of the CSA-1 and CAC-2 Mixtures from initial setting to 72 hours from the setting time. The CSA-1

Mixture in Figure 25 presents atypical results when compared to portland cement concrete. Portland cement concrete at low w/cm ratios usually witness autogenous shrinkage, while the CSA-1 Mixture exhibits autogenous expansion due to the expansive products formed during hydration. This autogenous expansion confirms the compressive stresses generated in the RCF with expansive strains up to 700 με. The CAC-2 Mixture presents typical trends of a portland cement concrete mixture where an initial expansion occurred, followed by a steady shrinkage out to 72 hours. This also confirms the behavior witnessed in the RCF where the mixture generated tensile stresses under the isothermal conditions.

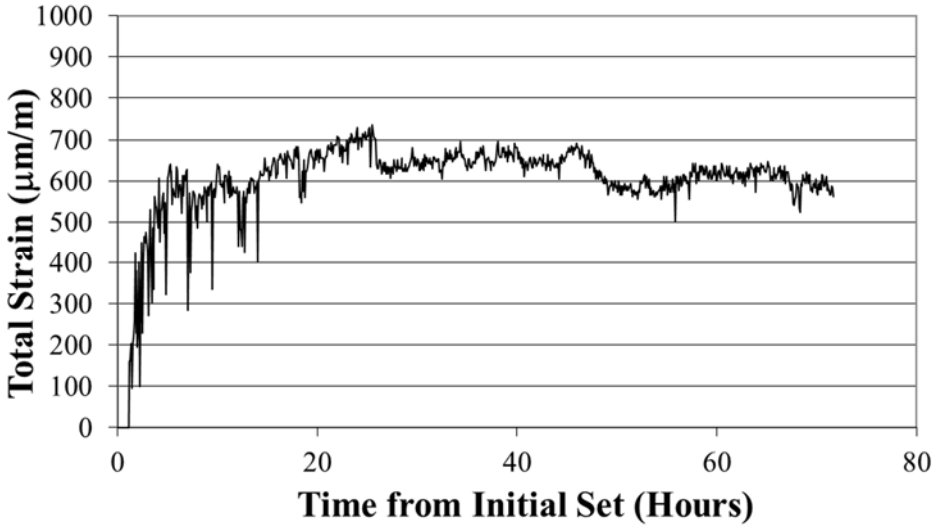

Figure 25: Unrestrained (Free) Deformation for CSA-1 Mixture

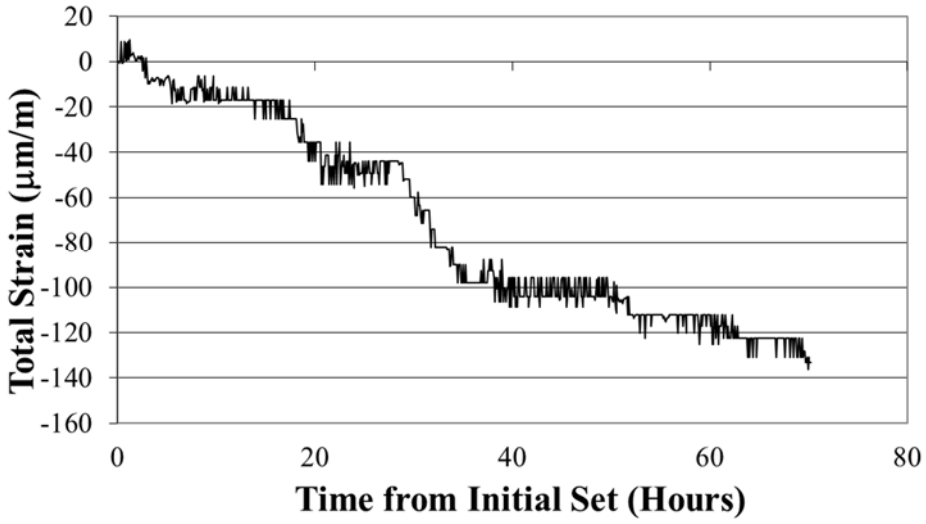

Figure 26: Unrestrained (Free) Deformation for CAC-2 Mixture

3.6 SUMMARY AND CONCLUSIONS

The following conclusions have been made with the information provided from this chapter:

- The CSA binder system had less drying shrinkage than the CAC binder system at both 28 days and 64 weeks. CAC mixtures amassed 3 of the 4 mixtures which did not meet TxDOT criteria at 28 days from mixing.
- Mixtures containing fly ash contained more drying shrinkage than mixtures not containing fly ash.
- The CSA-1 Mixture presented autogenous expansion and compressive stresses for both the FSF and RCF confirming the shrinkage compensating property for this binder.
- The CAC-2 Mixture presented autogenous shrinkage and tensile stresses for both, the FSF and RCF, which is similar behavior of a typical portland cement concrete with low w/cm ratio.

Chapter 4: Calorimetry

4.1 Introduction and Background

Calorimetry or heat evolution is an important property to obtain for both portland cement, as well as rapid repair materials. Heat evolution and heat flow are measured with different methods such as, isothermal calorimetry, semi-adiabatic calorimetry, and gradient calorimetry; these methods of temperature evaluations can assist in the understanding of early-age performance issues for rapid repair materials. For portland cement-based systems, investigating material combinations at different isothermal temperatures allows one to calculate an apparent activation energy which can be combined with data/information from semi-adiabatic calorimetry to predict thermal distributions in mass concrete applications (Poole, 2007) and (Riding, 2007). Unfortunately, a similar analysis of activation energy is not possible for rapid repair materials, such as CAC, due to the different hydration products that form at different temperatures.

Isothermal calorimetry is obtained by controlling the designated material's temperature to desired conditions with thermostats, heating fans, and cooling fans, while measuring the heat generated from the material with heat flow sensors. For portland cement the heat evolution generally continues for several days or even weeks, depending if SCMs are added to the mixture, while most rapid repair material's heat evolution is complete by 24 hours. Rapid repair materials exhibit an initial peak due to the dissolution of materials which is neglected in the calculation of heat of hydration properties. The methods used in the comparison of different mixtures were a relationship involving heat flow and time, the amount of time to the peak heat flow, the peak heat flow for a mixture, and a cumulative heat flow for a mixture.

The semi-adiabatic calorimeter, or Q-drum, was created to measure the heat generated from a cylindrical concrete specimen to determine different hydration parameters. Generally, these hydration parameters are combined with the apparent activation energy calculated from isothermal calorimetry, along with other properties from the cementitious material used in the mixtures to develop an adiabatic temperature curve. This temperature curve was used to model different mass concrete elements commonly used in the field and was combined with different climates from across the state. This information was implemented into a program called ConcreteWorks which can provide heat generation and transfer for different mass concrete elements if the properties of the concrete and specifics of construction are known.

Thermal gradients exist in every concrete structure but are a larger issue in mass concrete members for portland cement, as well as in any rapid repair materials member where there is high heat generation. Many jobs in Texas are now requiring contractors to measure and monitor these temperature gradients in mass concrete elements; thus, formwork insulation may be used to control the temperature gradients in concrete (Riding, 2007). The issue with thermal gradients in mass concrete elements is that the exothermic reaction generated by cement hydration is still occurring in the center of these structures, while the concrete at the surface is dissipating heat into the environment. This difference in temperature causes different expansion and shrinkage, which lead to stresses developing between the interior and exterior of the element. For rapid repair materials, the issue is related to how quickly their heat evolution occurs since the elements are still gaining strength as high amount of heat are generated. The smaller repair elements can dissipate heat more easily at the surface which causes the same thermal stresses at an earlier age.

4.2 MATERIALS AND MIXTURE PROPORTIONS

The 13 mixtures passing Phase I of the project were studied using isothermal, semi-adiabatic, and cylindrical calorimetry. Only the Phase III Mixtures were implemented into the temperature gradient slabs study. All of the concrete mixture proportions and mixing procedures are described in Zuniga (2013). The team tested each of the 13 mixtures as concrete, mortar, and paste for isothermal calorimetry, where only the paste materials were preheated and precooled for the samples tested at 50 °F (10 °C) and 100 °F (38 °C). For the remaining test, each material was stored at 73 °F (23 °C) 24 hours before mixing. The 3 x 6" (76.2 mm x 152.4 mm) calorimetry cylinders were cast from the large mechanical properties at standard temperature study because the team desired to see the peak temperature generated for each mixture at this time. The remaining mixtures were cast in standalone mixtures due to the different applications of each study.

4.3 ISOTHERMAL CALORIMETRY

Isothermal calorimetry measures the heat flow from cement hydration reactions by differential heat flow sensors that allow for comparison of different mixtures and provide time-lapsed understanding of the hydration mechanisms. The timing and shape of heat flow curves can provide an understanding of the performance of different cementitious systems (Bentivegna, 2012). The excess heat release of rapid repair materials initiated the research group at the University of Texas at Austin to design and construct a new isothermal calorimeter. This task was assumed by Anthony Bentivegna in 2012 and he was able to construct and calibrate a new calorimeter tailored the heat generation of calcium aluminate. Because the rapid repair materials used in this project have similar behavior to calcium aluminate cement, the calorimeter Bentivegna constructed was used. More information on the design, construction, calibration, and

properties of the calorimeters can be found in Bentivegna's Dissertation (2012). Figure 27 presents the insulated chamber for the Bentivegna's calorimeter.

Figure 27: Stainless Steel Calorimeter Chamber

The isothermal calorimetry study was performed on concrete, mortar, and paste at 50 °F, 73 °F, and 100 °F (10 °C, 23 °C, and 38 °C); due to constructability issues only the paste mixtures materials were cooled or preheated. This allows for less "noise" in the beginning of the data acquisition while the sample holder and the material itself are acclimating to the calorimeter temperature. It is for this reason that the results section will focus on the paste samples but the concrete and mortar data can be found in Appendix A: Isothermal Calorimetry Mixture Tables and Appendix B: Isothermal Calorimetry Plots.

Heat flow (mW/g), which is one of the methods mentioned earlier for comparing different mixtures, is measured by heat flow sensors within each channel which measure voltage changes. The differences in voltage can produce a power output when the proper calibration factors are applied. The power is then normalized per gram of cementitious material and plotted against time of mixing to generate the relationships presented in the results and discussion section. Table 8 also presents the time to peak heat flow, as well

as the peak heat for each mixture. The time to peak heat flow provides the research team with a comparison method for the hydration rates of different mixtures, while the peak heat value can give insight to which mixtures are more likely to have internal thermal effects.

The cumulative heat release (J/g) provides a comparison method involving the amount of energy release per gram of cementitious material. The cumulative heat release can provide a comparison of the total hydration for each mixture. This value includes the area under the heat flow curve up to 48 hours but neglects the initial drop or rise in heat flow when the specimen are placed into the calorimeter. The research team used Simpson's rule for numerical integration to calculate the cumulative heat release.

4.3.1 Experimental Procedures

The cement, admixtures, and water for each mixture were weighed out prior to mixing and the total mass of each paste specimen was approximately 15 grams. The paste sample mass was selected based on Bentivegna's previous work with calcium aluminate cement based on its high early heat release. The mixing procedure for the paste specimen were as follows: add the cement to the water in the sample holder and tap the cup on the counter for thirty seconds; place on the ultrasonic mixer for thirty seconds; place the lid on the sample holder; set into appropriate calorimetry channel and start the program. An ultrasonic mixer was used to mix the paste samples and was set on the highest vibration setting to achieve sufficient hydration of all cement grains. The average time from mixing cement and water to starting the calorimeter was 1.5 minutes. Figure 28 presents images for the sample holders suggested by Grace Construction Products and the ultrasonic mixer used for paste samples.

Figure 28: A) Grace AdiaCal TC Calorimetry Sample Holder (Bentivegna, 2012) B) Ultrasonic Mixer used for Paste Samples

After the concrete was mixed, a portion of the mixture was wet sieved through a No. 4 sieve on a vibrating table. This allowed the research team to remove some variability that occurs during mixing because both concrete and mortar would be sampled from the same mixture. The concrete samples were measured to approximately 100 grams for the 73 °F and 50 °F (23 °C and 10 °C) calorimetry mixtures, but due to the acceleration of hydration at 100 °F (38 °C) smaller sample sizes were weighed out to 50 grams. The mortar samples were measured to 30 grams for the 73 °F and 50 °F (23 °C and 10 °C) calorimetry mixtures, and 20 grams for the 100 °F (38 °C) mixtures. Again, all of these masses were selected upon Bentivegna's results in 2012. The average time from mixing until the sample was placed into the calorimeter was 6 minutes; this time was taken into account for the time to peak heat value.

4.3.2 Results and Discussion

As mention previously, the analysis of calorimetry will focus on the paste specimen but the concrete and mortar data are located in Appendix A and Appendix B. Appendix A contains tables displaying the time to peak heat, peak heat, and cumulative heat for each mixture, while Appendix B includes graphs of concrete, mortar, and paste behaviors at different temperatures. Figure 68 in Appendix B presents the graphs for P-AAFA where the 50 °F (10 °C) graph does not appear to have a hydration peak. The calorimeter was cooling the specimen down to 50 °F (10 °C) as it was generating heat; therefore, the hydration peak was overlapped with the cooling curve. This is the only mixture to have this issue because of P-AAFA Mixture's rapid heat evolution.

Table 8 presents all of properties of the isothermal calorimetry curves for the paste specimen. The proprietary mixtures are excluded from this table because the research team could not construct adequate paste samples from "all-in-one" package. When focusing on time to peak heat, the CSA mixtures seem to retard more at 50 °F (10 °C) than the CAC mixtures. Another trend to highlight is the time to peak heat for the CAC-1 and CAC-Latex Mixtures are slower at 73 °F (23 °C) than 50 °F (10 °C). Overall, the PC Type III Mixture, as to be expected, has the longest time to peak heat. The table also indicates that for the peak heat flow the CAC-1 and CAC-Latex Mixtures have the largest variability between 73 °F (23 °C) and 100 °F (38 °C) and, as well as the highest peak heat of 97 and 100 mW/g, respectively. The CAC-3 Mixture had the lowest peak heat flow value for the 50 °F (10 °C) mixtures. The CAC and CSA mixtures with and without latex have higher cumulative heat at 50 °F (10 °C) than at 73 °F (23 °C), which is the opposite of the other mixtures' behavior. The CSA-1 Mixture has the highest cumulative heat; however, the CAC mixtures have a higher cumulative heat as a binder system.

Table 8: Paste Summary Table for Isothermal Calorimetry

Mix ID	Temperature °F (°C)	Time to Peak Heat (Hours)	Peak Heat Flow (mW/g cement)	Cumulative Heat (J/g)
CSA-1	50 (10)	7.65	21	225
	73 (23)	1.62	29	132
	100 (38)	1.02	60	346
CSA-2	50 (10)	9.22	15	165
	73 (23)	2.12	30	180
	100 (38)	0.77	62	214
CSA-3	50 (10)	8.75	20	153
	73 (23)	2.43	26	167
	100 (38)	1.25	57	207
CSA-Latex	50 (10)	7.98	29	221
	73 (23)	1.92	54	211
	100 (38)	0.63	84	202
CAC-1	50 (10)	1.48	23	242
	73 (23)	2.53	23	196
	100 (38)	0.27	97	249
CAC-2	50 (10)	7.95	7	189
	73 (23)	3.70	15	235
	100 (38)	0.38	59	242
CAC-3	50 (10)	1.82	2	138
	73 (23)	1.12	8	215
	100 (38)	0.90	26	223
CAC-Latex	50 (10)	1.45	22	261
	73 (23)	3.53	30	302
	100 (38)	0.28	100	267
PC Type III	50 (10)	16.82	2	179
	73 (23)	10.35	4	206
	100 (38)	5.92	8	237

The CSA mixtures were influenced the most when varying the temperature, specifically the mixture at 50 °F (10 °C). There is a delay of 6 to 8 hours when the materials were cooled prior to mixing and placed in a 50 °F (10 °C) calorimeter. Of the CSA mixtures, the CSA-Latex Mixture had the largest peak heat flow values at each temperature.

The CAC-1 and CAC-Latex Mixtures performed similarly under all three temperatures which was expected because both mixtures contain the same components except latex. This suggests that latex does not affect the heat evolution of calcium aluminate cements, although results shown earlier in this thesis exhibited a lower rate of strength gain when latex was combined with CAC. These two mixtures also had faster

heat evolution at 50 °F (10 °C) than 73 °F (23 °C), which is different than all other mixtures and suggests temperature has a more significant effect on CAC mixtures than previously thought. The CAC-2 Mixture performed about how one would expect with the descending and slower heat flows as the temperature decreased. The CAC-3 Mixture performed poorly at 50 °F (10 °C) where there was virtually no peak heat flow. This mixture did show a second peak beginning at 24 hours after mixing for the other two temperatures which suggests that the portland cement in the mixture begins to hydrate and generate heat later.

The last figure presents the heat evolution of the PC Type III Mixture which exhibits the type of heat generation expected with portland cement mixtures. The higher the temperature, the faster the heat generation and higher the peak heat flow.

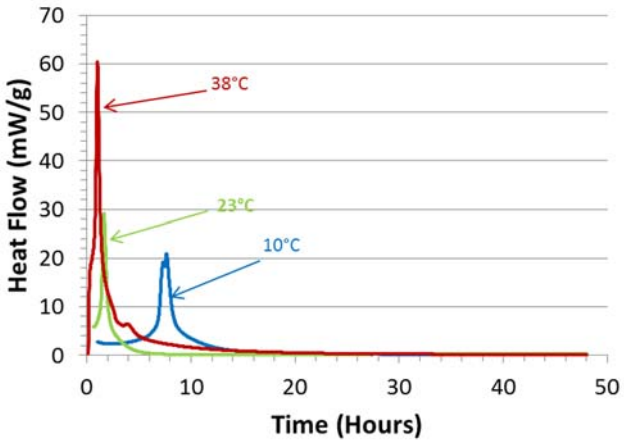

Figure 29: Isothermal Calorimetry for CSA-1 Paste Mixture

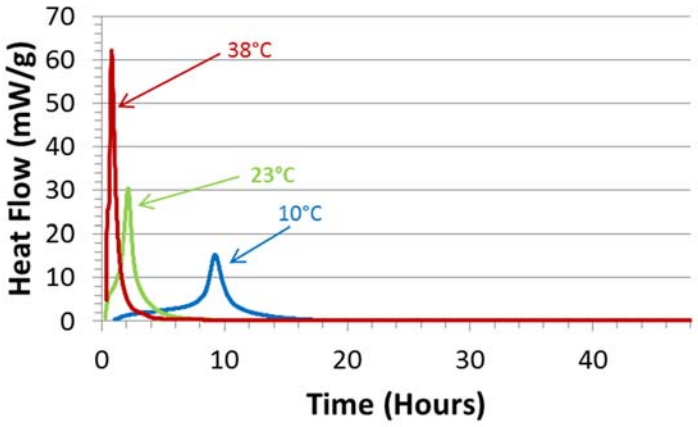

Figure 30: Isothermal Calorimetry for CSA-2 Paste Mixture

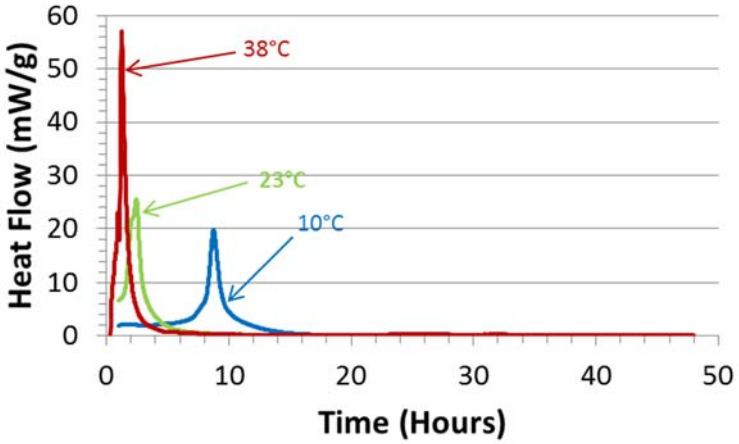

Figure 31: Isothermal Calorimetry for CSA-3 Paste Mixture

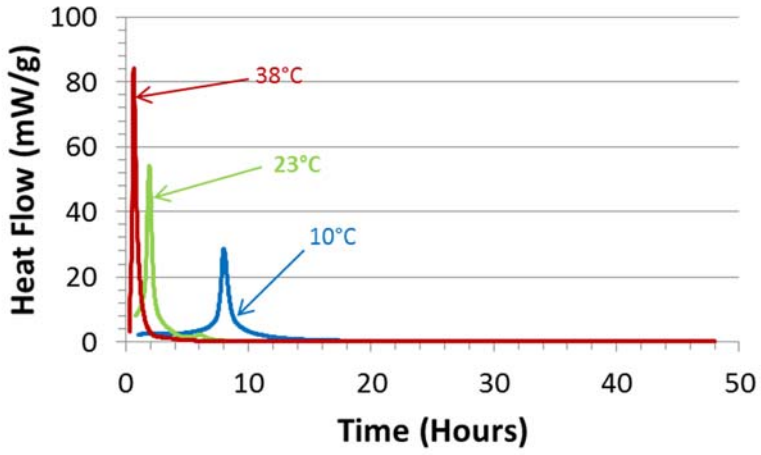

Figure 32: Isothermal Calorimetry for CSA-Latex Paste Mixture

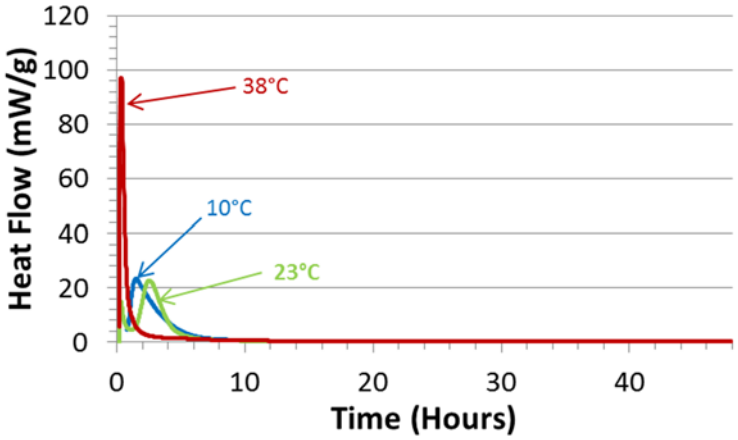

Figure 33: Isothermal Calorimetry for CAC-1 Paste Mixture

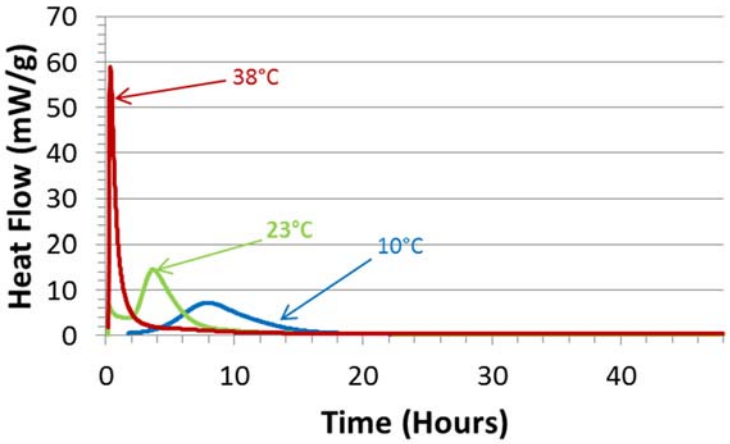

Figure 34: Isothermal Calorimetry for CAC-2 Paste Mixture

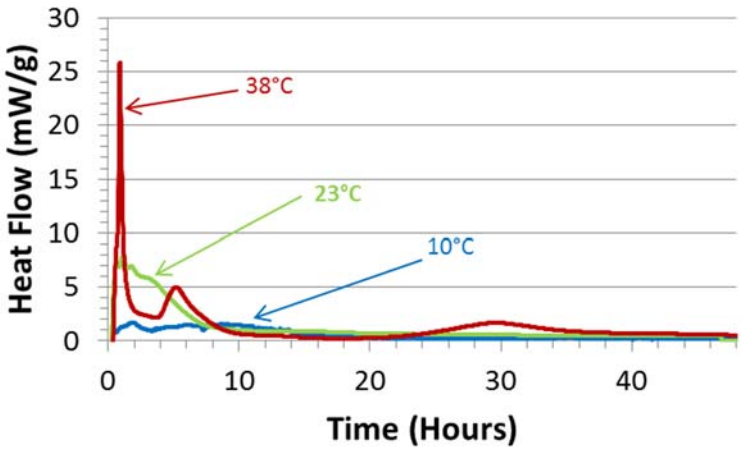

Figure 35: Isothermal Calorimetry for CAC-3 Paste Mixture

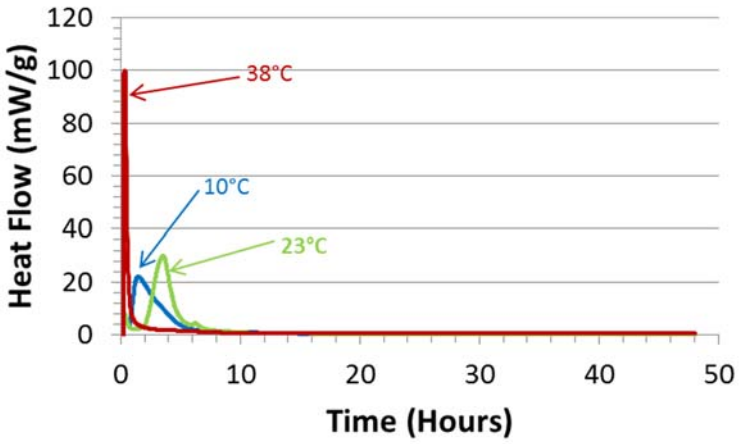

Figure 36: Isothermal Calorimetry for CAC-Latex Paste Mixture

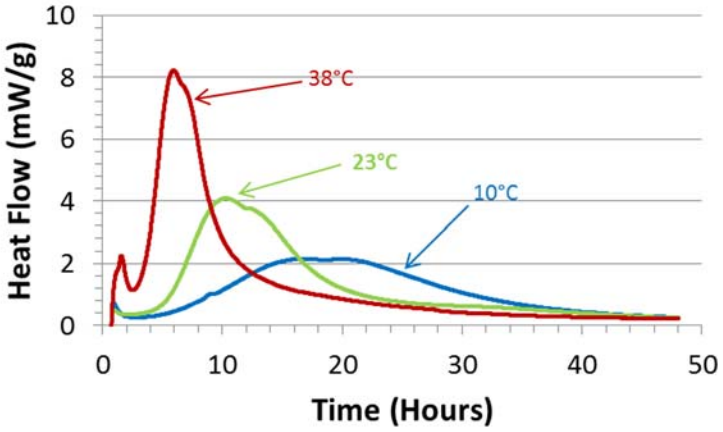

Figure 37: Isothermal Calorimetry for PC Type III Paste Mixture

4.4 Semi-Adiabatic Calorimetry and Calorimetry Cylinders

When semi-adiabatic calorimetry is tested on portland cement concrete, hydration parameters such as, α_u, β, and τ can be computed from different sections of the temperature curve. These hydration parameters can be combined with the apparent activation energy from isothermal calorimetry to model the thermal distributions in a hydrating concrete element. This, however, cannot be computed for the rapid repair

materials at hand because these materials contain different hydration products than portland cement, which prevents the calculation of hydration parameters.

The semi-adiabatic calorimeter can still generate a temperature evolution and key temperature related properties for rapid repair materials. Some of the same properties from isothermal calorimetry can be computed for semi-adiabatic, such as the time to peak heat, the peak heat, and the cumulative heat. Another property added to this section is related to the T_{off} value for calcium aluminate cement. Bentivegna describes T_{off} as the time at which calcium aluminate cement increases in temperature by 1 °C from the initial temperature (2012). The research team wanted to use the same concept but for an increase of 3 °C from initial temperature due to the variability in temperature in the semi-adiabatic calorimeters. The notation for this temperature property is $T_{\Delta 3°C}$.

The semi-adiabatic calorimeter or Q-drum measures the temperature of a mixture with a thermocouple placed in the center of a 6 x 12" (152.4 mm x 304.8 mm) concrete cylinder. The heat flux escaping the drum is also measured, in order to capture all of the heat generated by this concrete specimen. Another method the research team used to monitor the heat generation of a mixture was by placing a thermocouple in a 3 x 6" (76.2 mm x 152.4 mm) cylinder. This cylinder was cast as a part of the mechanical properties mixture at standard temperature to correlate the temporary heat profile with the mechanical properties of a mixture. The same temperature properties applied to the Q-drum specimen are applied to 3 x 6" (76.2 mm x 152.4 mm) specimen as well.

4.4.1 Experimental Procedures

The 6 x 12" (152.4 mm x 304.8 mm) cylinder for the Q-drum was mixed in the 1.75ft^3 (.01 m^3) mixer mentioned previously. Three lifts of concrete were placed and rodded in the Q-drum cylinder. The specimen was weighed and a Type K thermocouple

was placed in the center of the cylinder at mid-depth to record the temperature of the concrete. The heat flux was measured at the control box located on the side of the metal 30 gallon drum, which was filled with insulation to prevent heat loss. Any heat does escape the insulation was measured by the sensors picking up the heat flux. The cylinder was placed in the Q-drum where time was recorded from the time of mixing until the start of the program; on average, this time was 6 minutes and it was included in the calculation of the heat evolution properties. The heat generation was measured from 120 to 160 hours depending on how long it took for the heat to dissipate from the specimen.

The 3 x 6" (76.2 mm x 152.4 mm) calorimetry cylinder was cast in two lifts which were consolidated on a vibrating table. Then, a Type J thermocouple was placed in the center of the cylinder at mid-depth; the cylinder was capped immediately after and temperature was recorded out to 24 hours when the cylinder was removed from the mold to continue the curing process.

4.4.2 Results and Discussion

This section presents plots of the semi-adiabatic calorimetry on the left and the 3 x 6" (76.2 mm x 152.4 mm) calorimetry cylinders on the right for one mixture. Also, all of these temperature plots are in degree Celsius due to the nature of calorimetry.

Some of the trends presented for the proprietary mixtures are that the time to peak and time to 3 °C are slower for the Q-drum mixtures than for the 3 x 6" (76.2 mm x 152.4 mm) calorimetry cylinders. The P-3 Mixture took the longest to reach peak heat at almost 30 hours for the Q-drum cylinders, while the P-AAFA Mixture was the quickest to peak heat in 0.8 hours for the calorimetry cylinders. The P-AAFA and P-1 Mixtures each had very similar times to 3 °C for the Q-drum and calorimetry cylinders. P-AAFA

Mixture was the only mixture to have very similar peak temperatures for the Q-drum and the calorimetry cylinders.

The CSA mixtures had the most repeatability of any binder system for all of the properties. The time to peak heat for this binder system was very quick and the peak temperatures were high as well. The CSA-1 and CSA-Latex Mixtures performed very similar on all of the calorimetry properties just as with the isothermal calorimetry. The heat curve for CSA-2 Mixture has a second peak which does not seem to be part of the behavior for any of the other CSA mixtures.

The CAC-1 Mixture has the highest peak temperature of any mixture for the Q-drum and calorimetry cylinders, while the CAC-3 has the lowest peak temperature of any mixture for the Q-drum. Similarly to isothermal calorimetry, the CAC-1 and CAC-Latex Mixtures generated the same amount of heat which further proves that latex does not reduce the amount of heat generated in a mixture. The CAC-3 Mixture was slower to gain heat due to it being mostly composed of portland cement. The CAC-2 Mixture seemed to slow the time to peak heat, as well as reduce the peak temperature.

The PC Type III Mixture's calorimetry cylinders had the lowest peak temperature which is to be expected because it is not a rapid repair material. This mixture also has a slower time to peak than the other mixtures. When the PC Type III Mixture was tested in the Q-drum, a higher peak heat was reached than expected and the P-3 Mixture had a slower time to peak heat than this mixture.

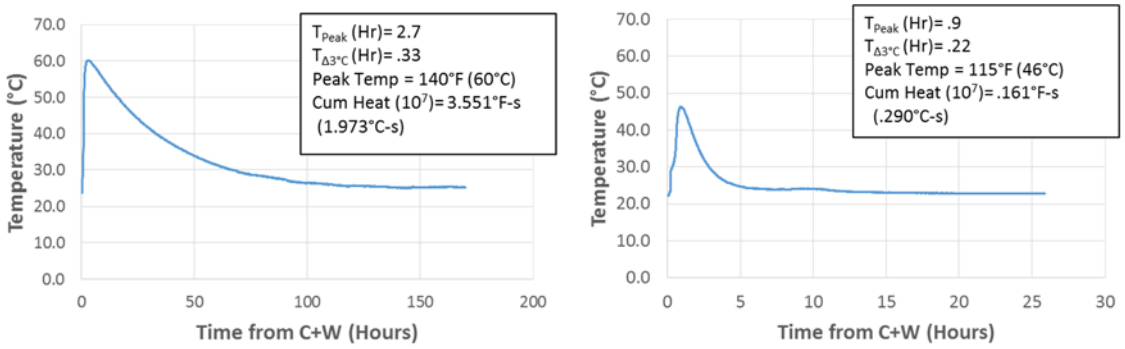

Figure 38: Mixture P-1 Q-drum and Cylinder Calorimetry

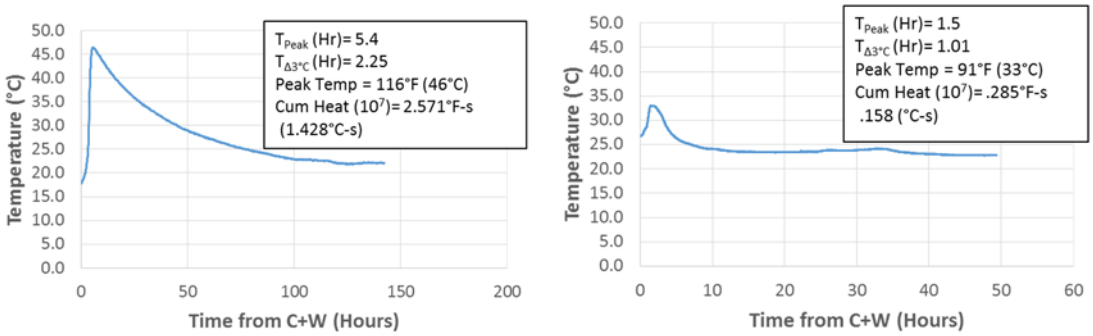

Figure 39: Mixture P-2 Q-drum and Cylinder Calorimetry

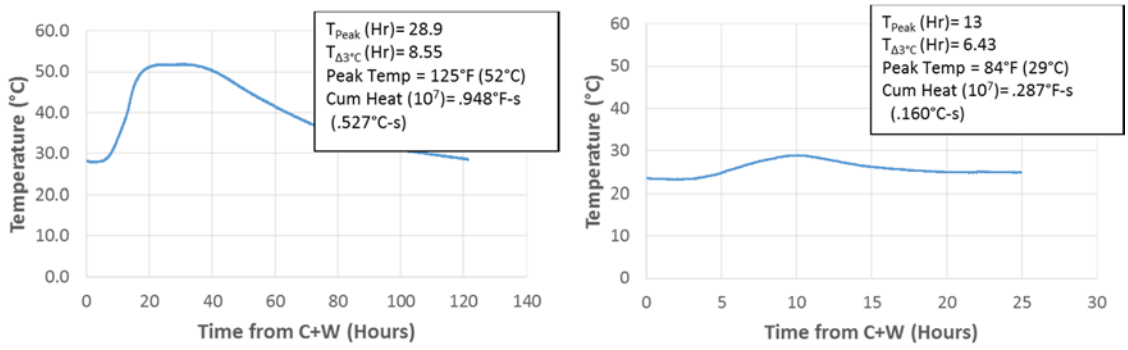

Figure 40: Mixture P-3 Mixture Q-drum and Cylinder Calorimetry

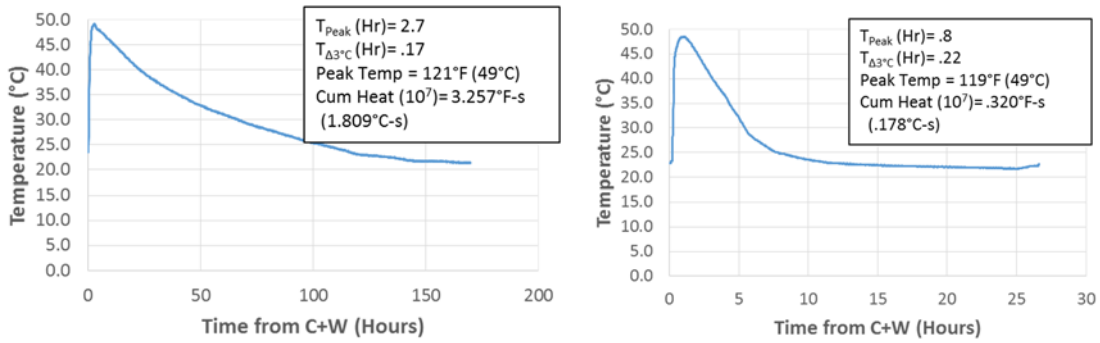

Figure 41: Mixture P-AAFA Mixture Q-drum and Cylinder Calorimetry

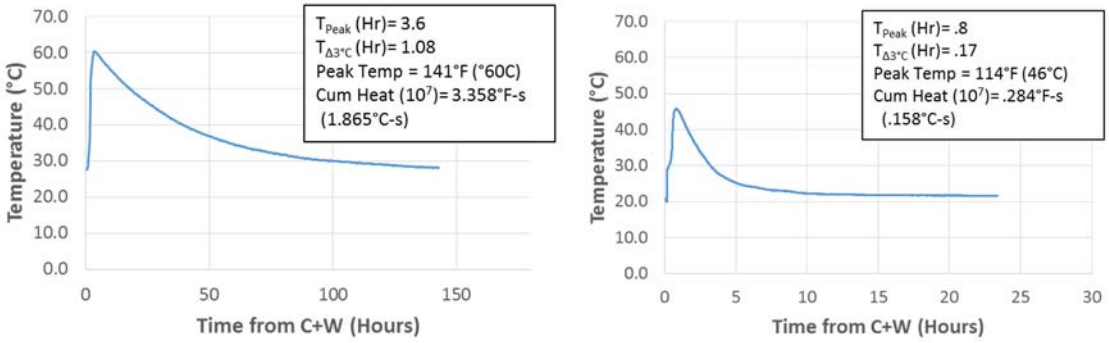

Figure 42: Mixture CSA-1 Mixture Q-drum and Cylinder Calorimetry

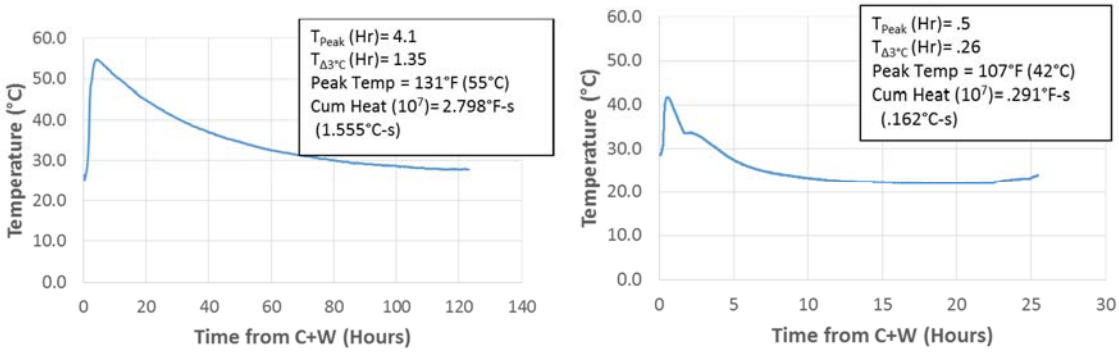

Figure 43: Mixture CSA-2 Mixture Q-drum and Cylinder Calorimetry

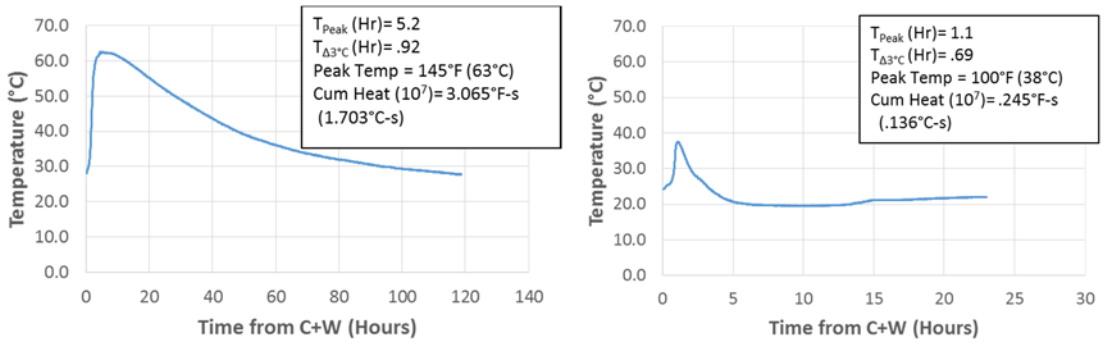

Figure 44: Mixture CSA-3 Mixture Q-drum and Cylinder Calorimetry

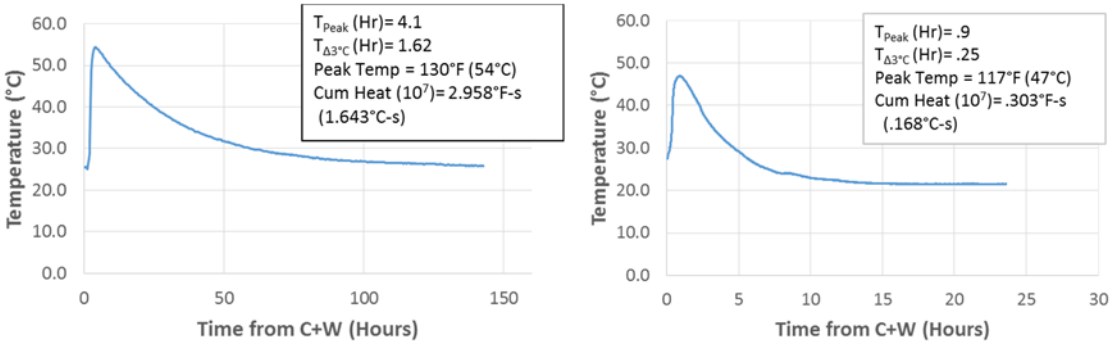

Figure 45: Mixture CSA-Latex Mixture Q-drum and Cylinder Calorimetry

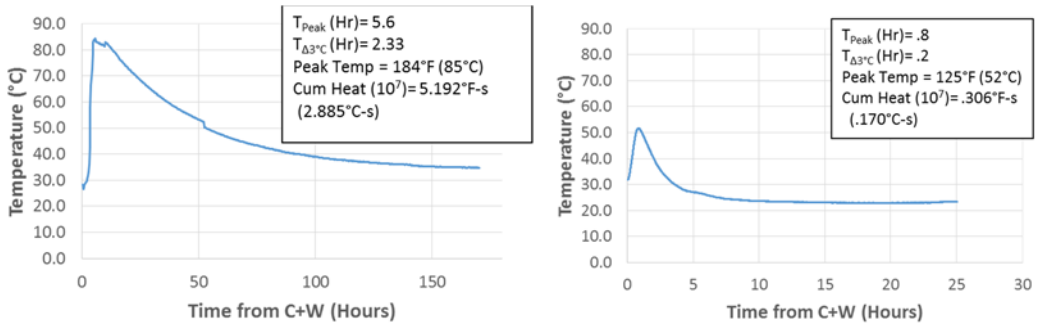

Figure 46: Mixture CAC-1 Mixture Q-drum and Cylinder Calorimetry

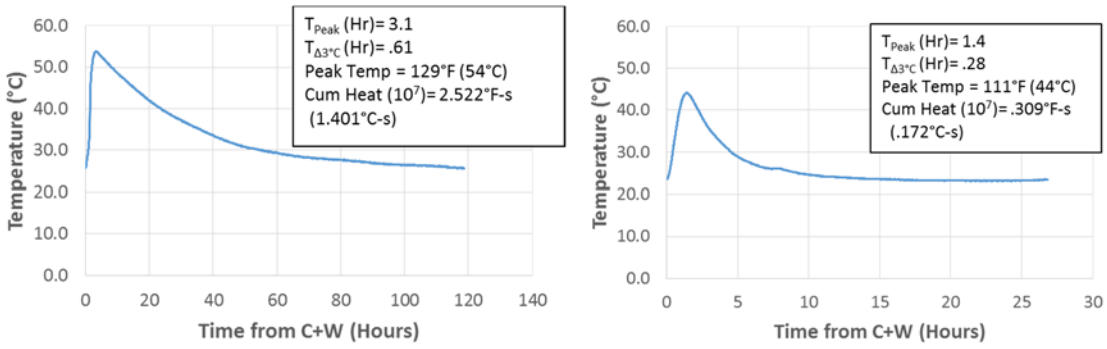

Figure 47: Mixture CAC-2 Mixture Q-drum and Cylinder Calorimetry

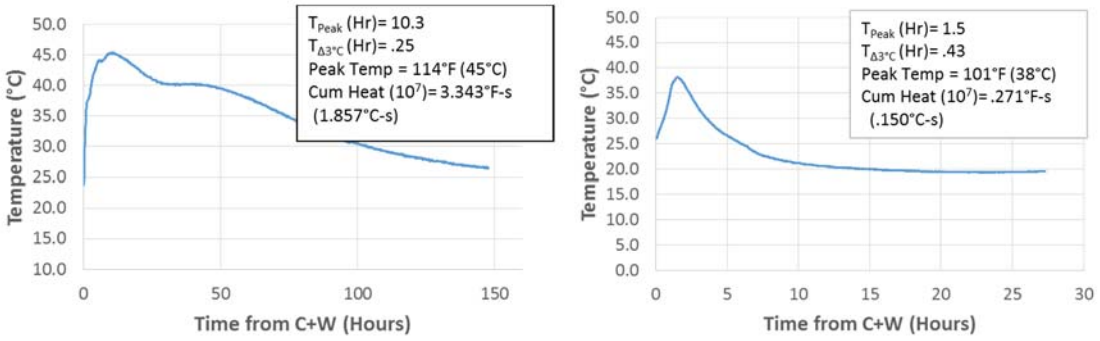

Figure 48: Mixture CAC-3 Mixture Q-drum and Cylinder Calorimetry

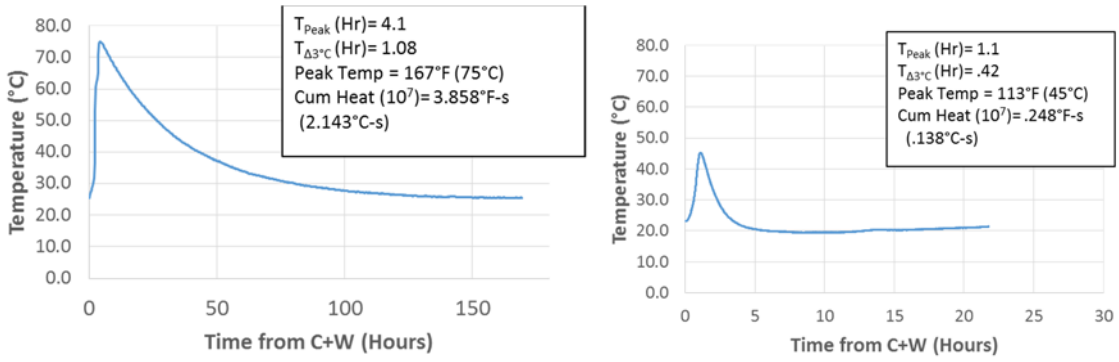

Figure 49: Mixture CAC-Latex Mixture Q-drum and Cylinder Calorimetry

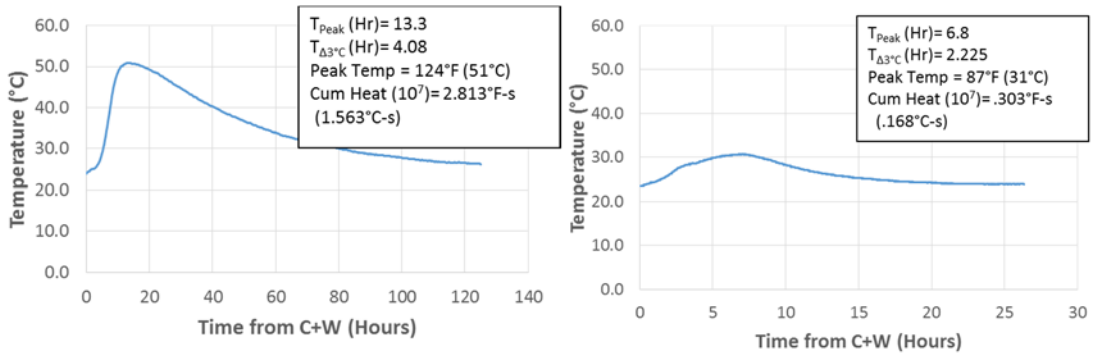

Figure 50: Mixture PC Type III Mixture Q-drum and Cylinder Calorimetry

4.5 TEMPERATURE GRADIENT SLABS

As mentioned previously, thermal gradients can be issues for rapid repair materials when the exothermic reaction, occurring during cement hydration, produces high early-age heat generation before the repair generates sufficient strength. The temperature differential between the center of the element and the surface causes thermal stresses to be formed; these stresses can cause thermal cracking if the stress exceeds the tensile strength of the concrete. This is normally an issue when there is a cooler environment and the rapid repair material generates a high early-age heat even at this lower temperature. The CAC mixtures presented this behavior during the isothermal calorimetry study at 50 °F (10 °C) where the heat evolution was more rapid and higher than at 73 °F (23 °C).

For this study the team cast 3 different temperature gradient slabs, with varied depths. The dimensions for these slabs were chosen to simulate the common depths for rapid repair materials and each temperature slab remained in their respective wooden formwork for the entire test. The goal was to measure the temperature differential from the center of a slab at 1" (25.4 mm) increments for the Phase III Mixtures. The research team wanted to examine the time to peak heat, the time to a 3 °C increase, the peak temperature, and the cumulative heat generated, as well as the temperature differential of

1” (25.4 mm) from the top surface and the mid-depth of the slab in a 73 °F (23 °C) environment. If this temperature differential is large enough and occurs early in the hydration of the repair materials then thermal cracking may be of concern.

4.5.1 Experimental Procedures

The temperature gradient slabs were mixed in a 9 ft^3 (.25 m^3) steel drum mixer per the mixing procedure laid out by Zuniga (2013). The dimensions for these slabs were a 2.5 x 2.5’ cross-section with depths of 2, 4, and 6 inches. Before mixing, the formwork was constructed of common lumber and plywood, while plastic rods were cut to 1, 3, and 5 inches and epoxied to the center of the formwork. Then, Type J thermocouples were tied to the plastic rods at 1” (25.4 mm) increments, starting from the bottom of the formwork, to record the temperature.

On the mixing day, the wooden formwork was lubricated with form oil to preserve the formwork and the data logger was initiated. The mixing time was recorded so that the time to peak heat could be calculated. The 3 temperature slabs required 4.8 ft^3 (.14 m^3) of concrete and a mechanical vibrator was carefully used to consolidate the concrete without moving the thermocouples. Each of the mixtures was measured out to 120 hours from mixing time in a 73 °F (23 °C) environment. An image of the 3 temperature gradient slab formworks is presented in Figure 51.

Figure 51: The 3 Temperature Gradient Slabs Formwork

4.5.2 Results and Discussion

Figure 52-Figure 57 below contain a maximum temperature gradient value from their respective 6" (152.4mm) depth slab. The other properties were selected from the 4" (101.6mm) depth slab because this is a typical depth repair for bridge decks. The temperatures were recorded at every inch; however, for presentation purposes the data plotted is from the thermocouple at mid-depth for each of the slabs.

The two proprietary mixtures had a temperature differential of around 4 °F (2.2 °C) through 3 inches of concrete. The P-AAFA Mixture had a faster heat generation, higher peak temperature, and more uniform temperature curves for each depth. The P-2 Mixture seems to generate much less heat for the 2" (50.8mm) depth slab and all of the slabs seemed to take longer to dissipate the heat from the center of the member, thus resulting in larger cumulative heat values.

Both of these mixtures generated the highest temperatures and temperature gradients, which could be problematic if these mixtures were cast in cooler temperatures.

The team observed no thermal cracking on any of the temperature slabs. A 10.13 °F (5.63 °C) temperature gradient through 3 inches of concrete is a significant difference. The CSA-1 Mixture reached its peak temperature faster than the CAC-2 Mixture; however, the CAC Mixture seemed to present a more uniform heat evolution when altering the depth of the member.

The PC Type III Mixture presented the slowest time to peak heat and highest cumulative heat among all of the mixtures, which was expected due to the nature of portland cement. Both of these mixtures were composted of mostly portland cement but the CAC-3 Mixture had a 30% replacement of a rapid setting blend to speed up heat evolution and strength gain triggered by ettringite formation. These two mixtures also have an interesting trend for the 2" (50.8mm) slab where the temperature curve dips below the ambient temperature immediately following the decrease of the hydration curve.

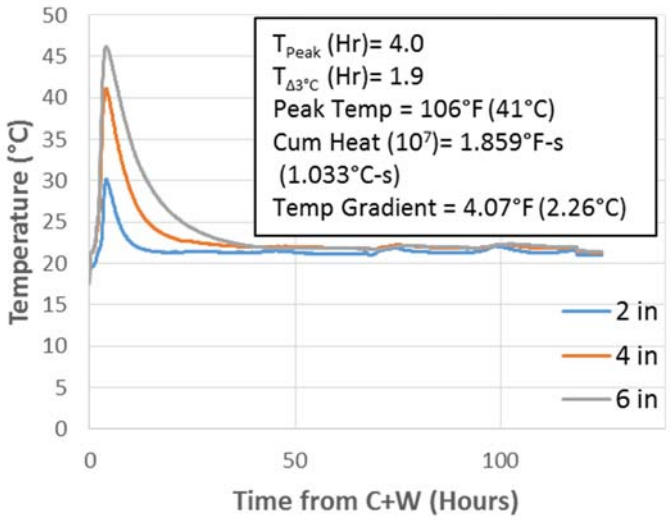

Figure 52: Mid-depth Temperature for each of Temperature Gradient Slabs for P-2 Mixture

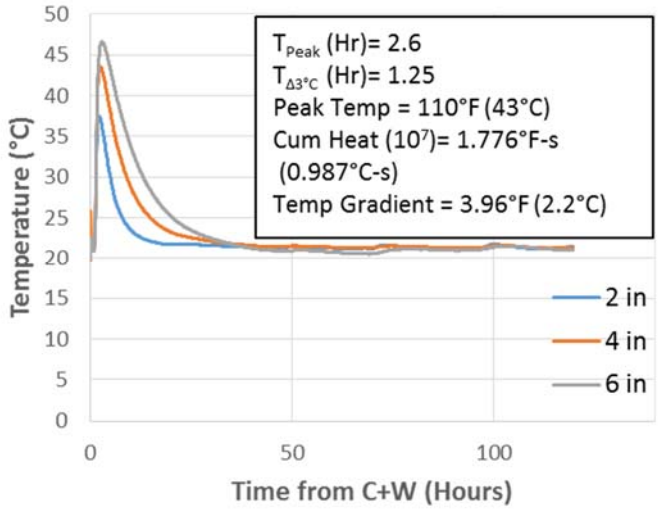

Figure 53: Mid-depth Temperature for each of Temperature Gradient Slabs for P-AAFA Mixture

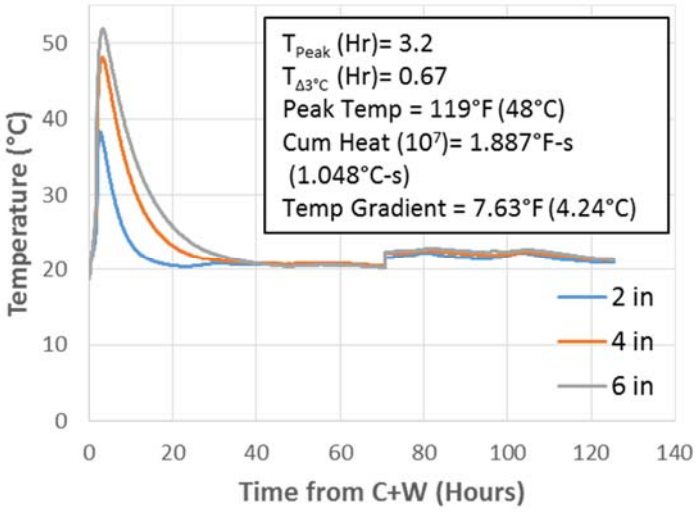

Figure 54: Mid-depth Temperature for each of Temperature Gradient Slabs for CSA-1 Mixture

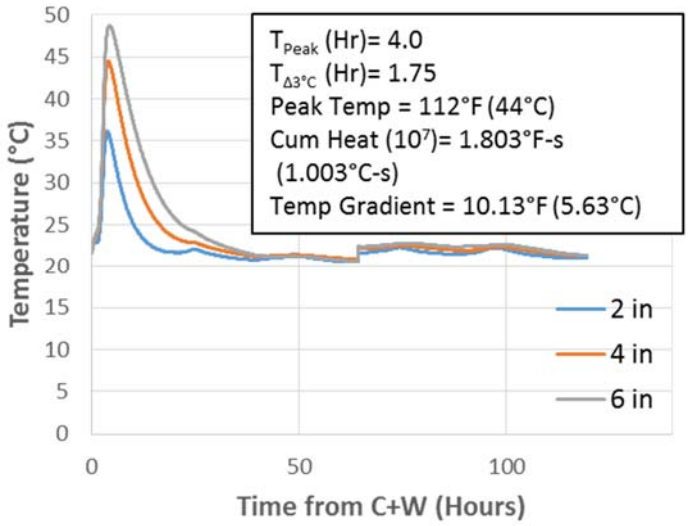

Figure 55: Mid-depth Temperature for each of Temperature Gradient Slabs for CAC-2 Mixture

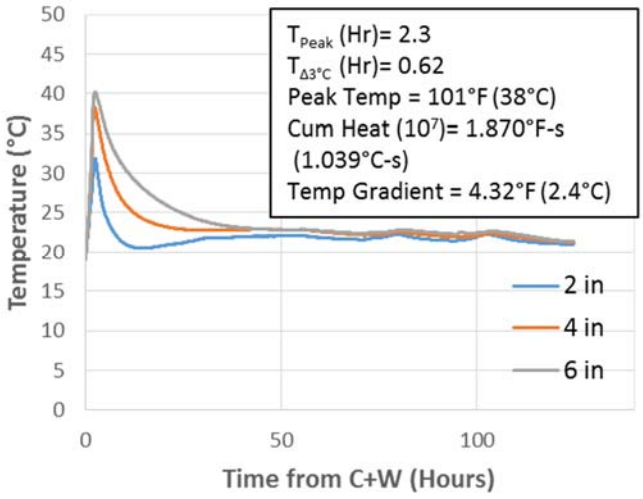

Figure 56: Mid-depth Temperature for each of Temperature Gradient Slabs for CAC-3 Mixture

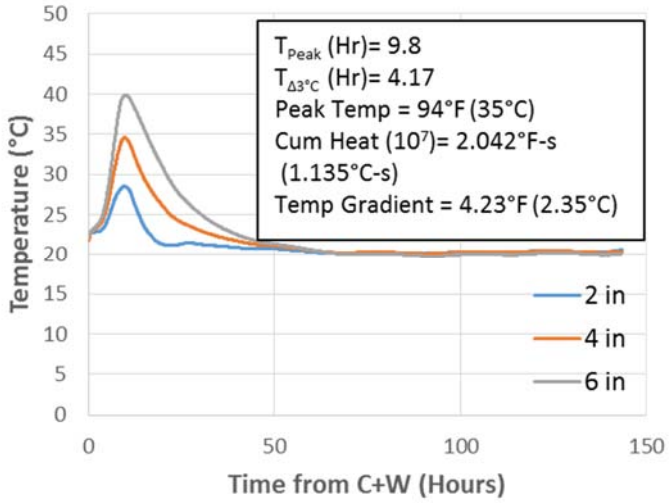

Figure 57: Mid-depth Temperature for each of Temperature Gradient Slabs for PC Type III Mixture

4.6 SUMMARY AND CONCLUSIONS

The summary of the calorimetry performances of each binder system are as follows:

- The P-AAFA-Mixture has a rapid time to peak heat and generates about the same peak temperature when studied at 50 °F, 73 °F, and 100 °F (10 °C, 23 °C, and 38 °C).
- The CAC mixtures were the most variable as a whole with the CAC-3 Mixture having very slow heat generation, lower peak temperatures, and relatively no heat generation at 50 °F (10 °C) compared to the other 3 mixtures. Contrary to the CAC-3 Mixture, the remaining CAC mixtures had very rapid heat generation, highest peak temperatures, largest temperature gradient, and the best performance at 50 °F (10 °C) of any mixture.
- The CSA mixtures were retarded by the cooler temperatures at 50 °F (10 °C) but had a high temperature gradient at 7.63 °F (4.24 °C) when cured at 73 °F (23 °C).

For semi-adiabatic calorimetry, these mixtures had around the same calorimetry properties and temperature curves.

- The mixtures containing mostly portland cement, P-3 and PC Type III, had slower heat generation and lower peak temperature values than the other rapid repair materials.

Chapter 5: Field Testing

5.1 Introduction and Background

The field performance of these rapid repair materials is a very important aspect within this project. One of the biggest challenges in research is to overcome the disconnect between laboratory results and results in the field. The most practical method of correlating the two results is to implement the mixtures tested in the laboratory to the field. It is rather difficult to simulate live traffic loads and exposure conditions on rapid repair materials due to the size and nature of repairs, thus, the best method for measuring a material's service life is with implementation in the field.

As mentioned, the research team had an opportunity to use an existing series of bridge deck sections from a previously funded TxDOT project for applying a subset of repair materials. Sections of the decks were saw-cut and removed, so that the Phase III Mixtures could be cast into six different repair sections which are 2 x 12' (0.61 m x 3.66 m) in cross-section and 4" (101.6 mm) in depth. The team measured fresh state properties, compressive strength, temperature gradients, and a complete visual inspection for cracking. These repair sections will provide the team with certain performance properties not witnessed in the laboratory.

TxDOT has an ongoing in-house research project evaluating pavement repairs using different rapid setting materials which include some of the rapid repair materials studied by the research team. One of the key objectives for the research team was to perform a visual survey of selected repair jobs performed by TxDOT prior to or during this project. This objective was made possible when the team accompanied different TxDOT employees to a previous repair site in Cotulla, Texas. This site contained twelve

highway pavement repairs cast with different repair materials; six of these materials were a part of the team's mixture matrix.

5.2 Materials and Mixture Proportions

The simulated bridge deck repair mixture proportions and procedures are explained in Zuniga's Thesis (2013). The site visit mixture identifications are listed in Table 9; however, the proportions for the non-proprietary mixtures are unknown because the cast date was completed prior to the site visit. TxDOT followed instructions listed on the proprietary mixtures' bags which are what the team followed for the P-1, P-2, and P-AAFA Mixtures.

5.3 Simulated bridge deck Repairs

The simulated bridge deck repairs implemented at the research campus allowed for a multitude of tests on these repair materials at real-world exposure conditions. The repair section dimensions were chosen at long aspect ratios to promote transverse cracking due to large volume changes in the longitudinal direction. The team did not use reinforcement in order to examine which mix would resist cracking. Visual inspections for cracking were monitored daily for the first week and then the team examined the sections weekly; however, the majority of the cracking was generated in the first week following casting. The fresh state properties and compressive strength were measured at 73 °F (23 °C) for quality control and comparisons to previous mixes. Six cylinders were cast from the outdoor mixtures, which were left on the bridge decks for a comparison of compressive strengths at ambient and standard temperature. The temperature of the repair sections was also recorded with thermocouples out to 5 days at different depths, in order to generate a temperature gradient profile for each repair section.

These bridge deck repairs were cast on three different dates grouped into two casting periods. The P-2, PC Type III, and P-AAFA Mixtures were cast on August 13, 2013. The CAC-3 Mixture was cast on the following day and Figure 58 below is an image of one of the bridge deck sections and schematic of these bridge decks.

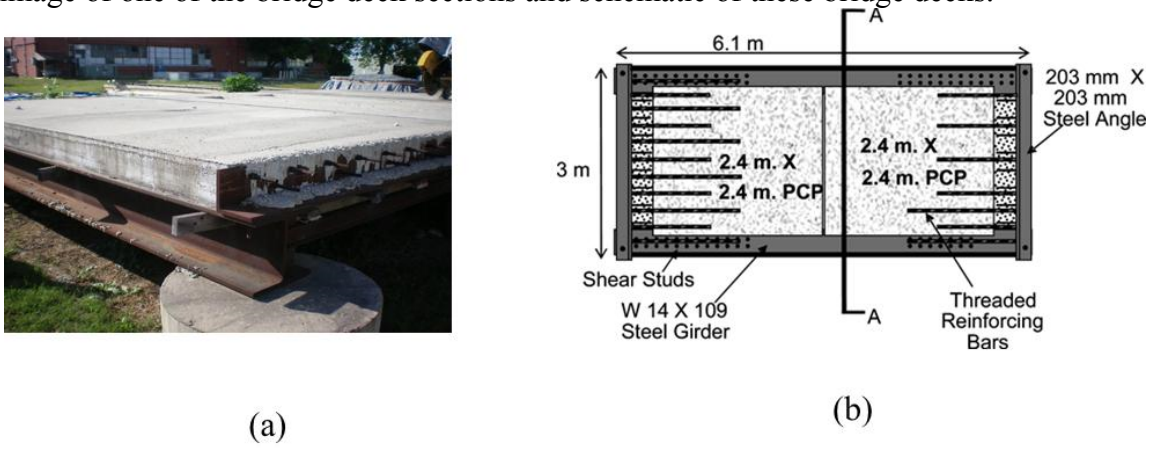

Figure 58: A) Photo of Large-scale Bridge Deck Elements B) Schematic of Large-scale Bride Deck Elements (Reference thesis this came from)

5.3.1 Experimental Procedures

Prior to mixing, the repair section needed to be construction, prepped, and instrumented. The first task was the removal of concrete by a concrete wet-saw, two 90 pound pneumatic jackhammers, and sandblasting equipment. Once the deteriorated concrete and excess blast sand had been removed, a hammer drill was used to create a hole for plastic rods cut to 4" (101.6mm). These plastic rods were epoxied into the holes and thermocouples were attached at 1, 2, and 3" (25.4mm, 50.8mm, and 76.2mm) depths with zip-ties to be monitored by a datalogger.

All of the mixture materials were placed in a 73 °F (23 °C) environment 24 hours before mixing. Each repair material was cast indoors for the fresh state properties and the majority of the compressive cylinders, as well as, outdoors for the repair section and six

compression cylinders for comparison. The indoor mixture was produced in a 4ft^3 (.11 m^3) steel drum concrete mixer where the slump, unit weight, air content, and 18 4 x 8" (101.6 mm x 203.2 mm) compression cylinders were cast. The 4 x 8" (101.6 mm x 203.2 mm) cylinders were consolidated on a vibrating table and immediately capped for a 24 hours curing period.

The outdoor mixture required 10 ft^3 (.28 m^3) of concrete to fill the repair section. This large amount of concrete needed two 9 ft^3 (.25 m^3) concrete drum mixers which were placed on top of the bridge decks to allow for a direct pour from the mixer to the repair slot. On the morning of each cast date, the repair section was lightly sprayed with water to pre-wet the concrete to prevent the existing substrate from pulling water from the repair mixture. After the concrete was poured into the repair sections, the mixture was vibrated, finished, and cured with wet burlap. The P-AAFA Mixture was the only repair section not wet-cured per the producer's instructions. Six 4 x 8" (101.6 mm x 203.2 mm) cylinders were also cast, rodded, and left on the decks for an ambient temperature cure to simulate compressive strength of the repair.

5.3.2 Results and Discussion

Images of these experimental procedures previously described, along with tables for fresh state properties and a cracking log for the Phase III Mixtures can be found in Appendix C: Field Performance. This section will include discussion on the compressive strength generation, heat evolution analysis, and crack mapping for the Phase III Mixtures.

Figure 59 presents the compressive strength data of the six Phase III Mixtures measured out to 12 hours. The compressive cylinders were tested to 28 days but the team focused on the early-age strengths. All of the mixtures excluding the PC Type III

Mixture reached 3000 psi (20.7 MPa) compressive strength by 3 hours which was one of the criteria TxDOT placed on these repair materials. The CSA-1 and P-2 Mixtures presented the most rapid strength gain of the repair materials, while the CAC-2, CAC-3, and P-AAFA Mixtures had similar strength gains up to 6 hours.

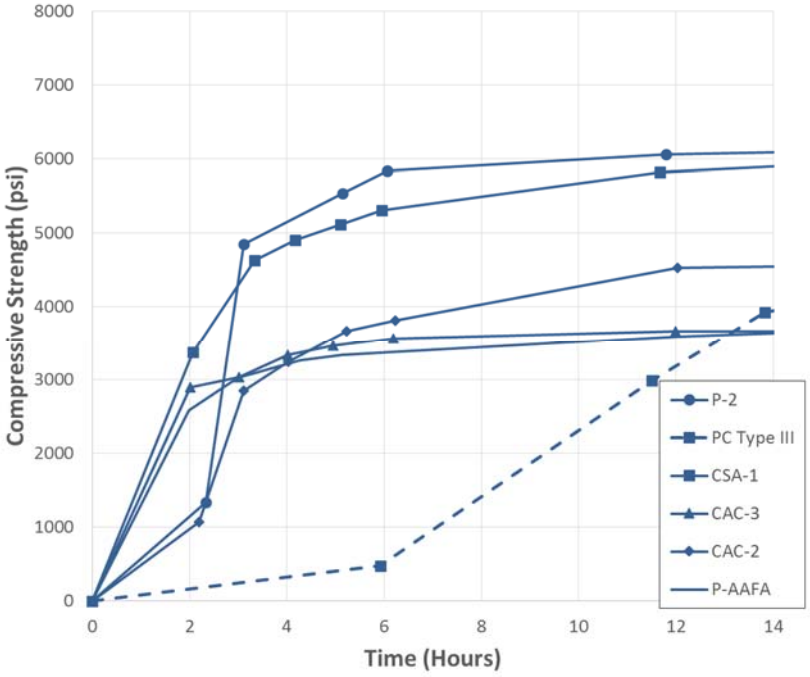

Figure 59: Compressive Strength Curves for Phase III Mixtures

The two figures below present the temperature analysis for the thermocouple placed at mid-depth for all 6 mixtures included in the simulated bridge deck study. Of the 4 mixtures a part of the 1st cast period, the CAC-3 Mixture generated the highest temperature which occurred on a day with a cooler ambient temperature. The CAC-3 Mixture also presented an early small peak which represents the ettringite system responsible for early strength gain, as well as a higher peak about 12 hours later that could represent the portland cement hydration. After the first 24 hours for each mixture, the heat generation is complete as seen in isothermal calorimetry; therefore, any

discrepancies in temperature past the first day are related to the amount of heat absorbed from direct sunlight for darker shades of concrete.

The second cast period compared the CAC-2 and P-AAFA Mixtures, which presents that the CAC mixture generates more heat than the proprietary mixture. An interesting trend for the P-AAFA Mixture is that by the 4th day the concrete is only generating as much heat as the ambient temperature. This was not seen by any of the other mixtures.

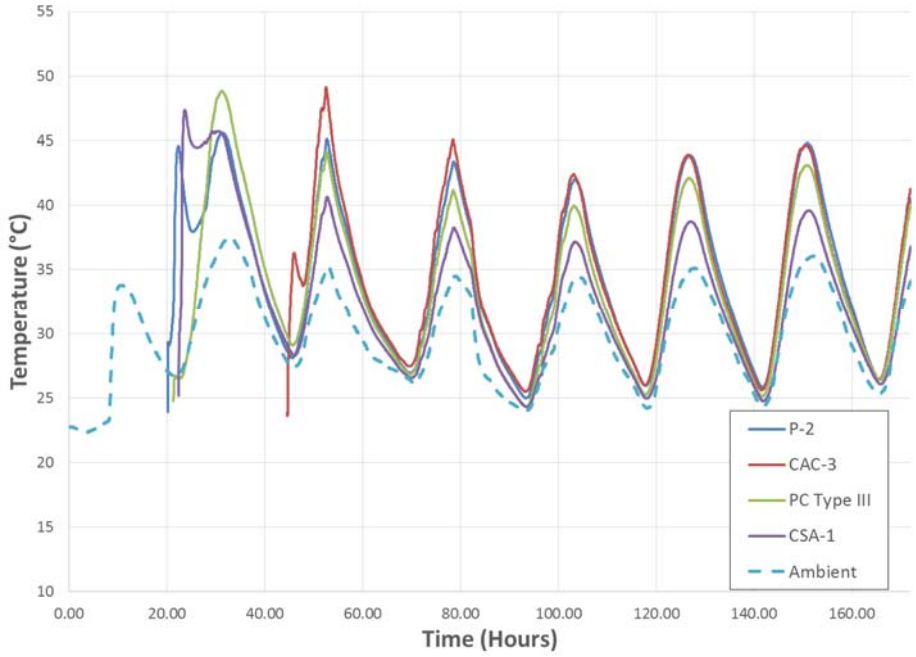

Figure 60: Temperature Analysis for 1st Cast Period

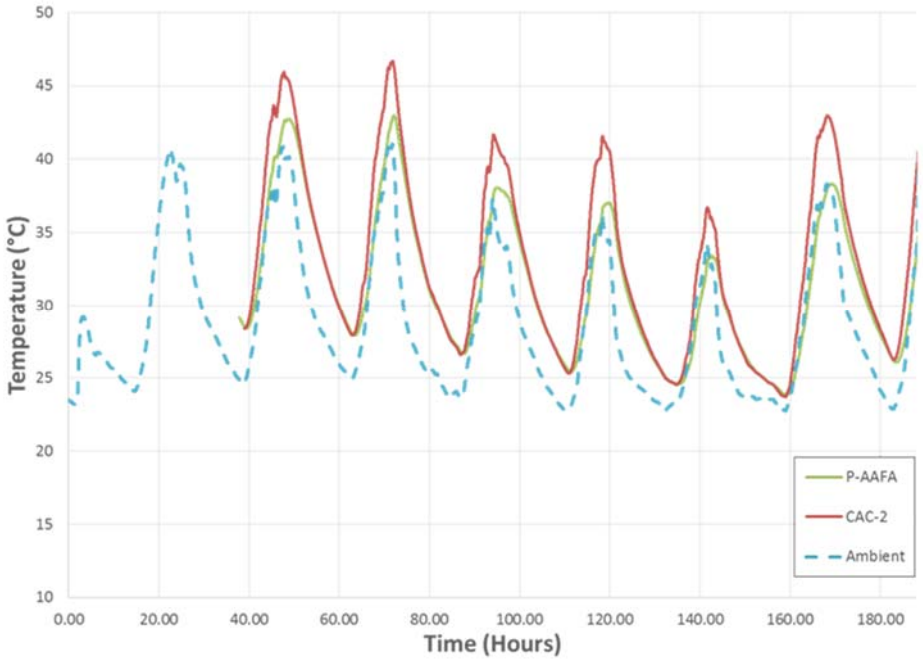

Figure 61: Temperature Analysis for 2nd Cast Period

The figures above present the temperature gradients measured for all 6 of the Phase III Mixtures. The gradients were measured from top and bottom thermocouple and the largest gradients for each mixture were within the first 24 hours. After the first 24 hours, the slab is heating and cooling with the ambient temperatures with an average peak differential of 6 °C. The CAC-3 Mixture exhibited the highest temperature differential of all the Phase III Mixtures, however, the 2nd cast period ambient temperature was lower so a fair comparison cannot be made. Just as before, after the 4th day the only difference between the temperatures measured in each mixture is based on how much heat is absorbed from the environment.

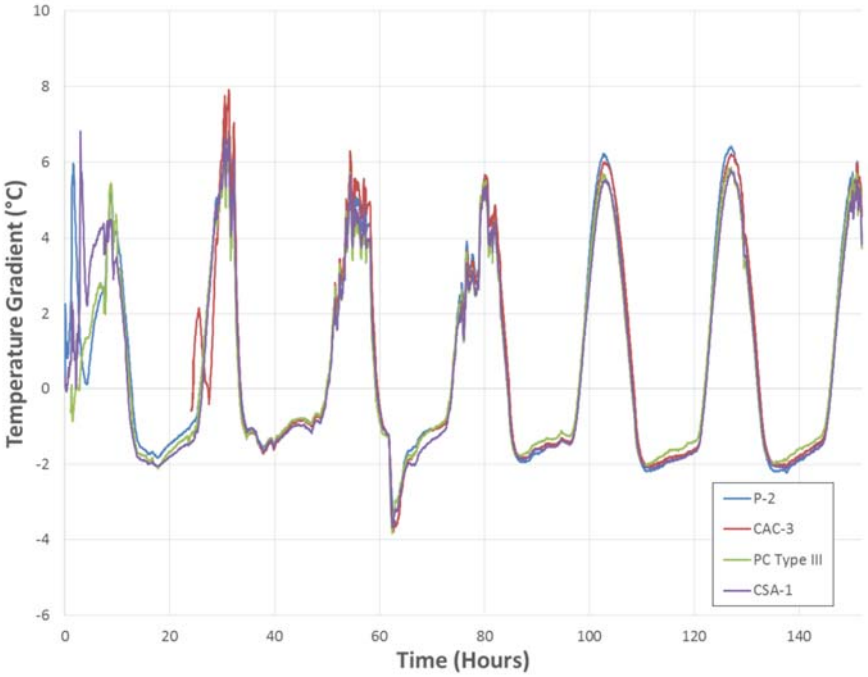

Figure 62: Temperature Gradients for 1st Cast Period

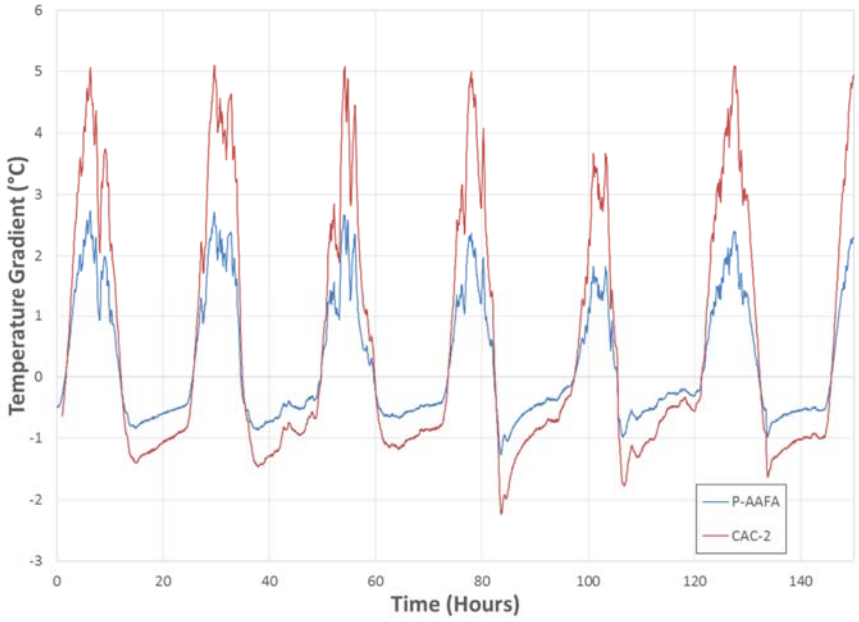

Figure 63: Temperature Gradients for 2nd Cast Period

Figure 64 presents a crack map of the all six repairs at 6 months from each cast period. It is important to note that all of the cracking occurred in the first 7 days, except for the crack in the center of the P-AAFA repair. All of the other mixtures obtained a crack in the center of the repair within 72 hours. The P-2 and CAC-3 Mixtures were cast into a bridge deck with fibers in the existing concrete which could have resisted movement during temperature changes, thus, causing stresses and cracking when the repairs were trying to expand and shrink with changes in temperature. The CAC-2 Mixture seemed to have excess water on the casting day which could have contributed to drying shrinkage cracking when the concrete was acclimating to the environment.

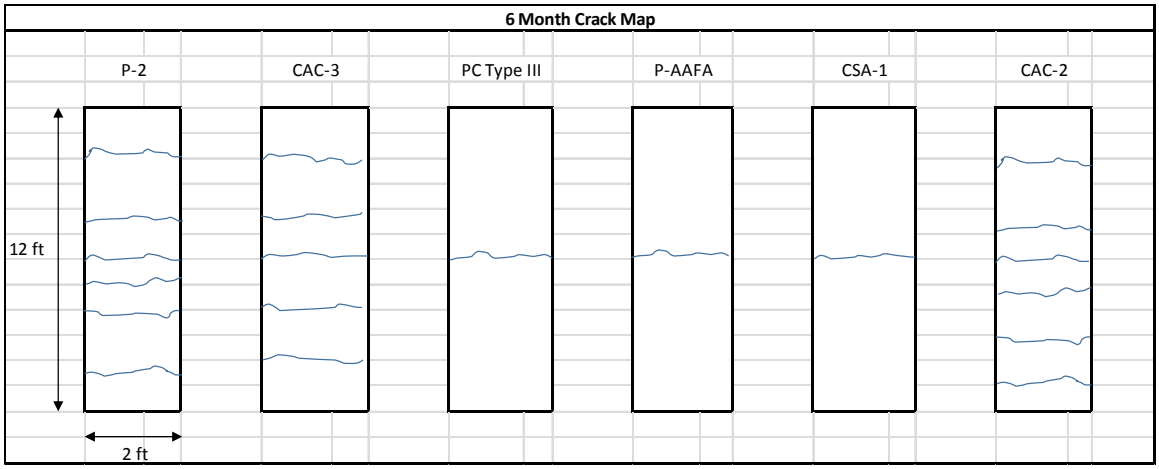

Figure 64: Crack Map of Bridge Deck Repairs

5.4 HIGHWAY REPAIR EVALUATION

The highway repair evaluation, was a part of the key objectives selected by the research team because of the importance of field performance data. Unfortunately, the casting date occurred before the team was notified about the repair site but some details were given from the mixing day. TxDOT had the producers of each repair material tested come to the site on the casting date and place their respective material. This plan was

implemented in order to have each material be placed in the correct fashion, so that the mixing variable could be removed and just the durability and service life of the repair would be tested.

The site visited was just outside of Cotulla, Texas on a divided four lane highway. The site was composed of 12 repair sections; 6 of these sections contained materials tested by the research team. The six mixtures implemented were P-1, P-2, P-AAFA, CSA-1, CSA-2, and CSA-3. All of these mixtures were cast in November of 2012 and the research team inspected the site 8 months later in July of 2013. The team focused on a visual inspection, crack mapping and measuring crack width, and soundness testing.

5.4.1 Experimental Procedures

First, the traffic control crew blocked off the highway lane containing all 12 repair sections. The research team, along with a TxDOT team began examining each of the repairs. The dimensions of each repair were reported, along with the distance between transverse cracking, any crack width, notation of longitudinal cracking if occurred, delamination, spalling, and any visual details. Pictures were taken of each repair to note any interesting characteristics and one of the TxDOT engineers checked the bond of the repair by tapping the repair with a hammer and listening for a dull sound.

After the site investigation, the research team and TxDOT engineers shared reports and resources to allow for a more detailed evaluation of the repair sites.

5.4.2 Results and Discussion

This section will discuss the results from Information Table below for each mixture implemented at the Cotulla site. Additional images from the site investigation can be found in Appendix C: Field Performance.

Table 9: Cotulla Site Visit Cracking Information

	Repair Dimensions (inches)		Cracks			Cast Date Information		
Material	Length	Width	Transverse (No or Spacing)	Longitudinal	Max (inches)	Date	Temperature (°F)	Weather Conditions
P-1	48	20	No	Yes	0.008	11/1/2012	90	Foggy Morning
P-2	60	20	No	No		11/13/2012	70	Cloudy, light wind
P-AAFA	137	21	20 to 34"	No		11/14/2012	50	Cloudy, light rain
CSA-1	57	18	(1) @ 17" from outside	No	0.03	11/14/2012	50	Cloudy, light rain
CSA-2	79	21	8 to 15"	No	0.03	11/14/2012	50	Cloudy, light rain
CSA-3	138	28	No	No		11/1/2012	90	Foggy Morning

Of the proprietary mixtures at the repair site, only the P-1 Mixture was not strong enough to resist the previous longitudinal crack and the surface was slightly worn with a brown coloration. The P-2 Mixture performed very well, and did not show any transverse or longitudinal cracking which indicates the repair material is both compatible to the existing concrete and strong enough to resist the original crack. The P-AAFA Mixture proved to have a very rapid setting time because the material formed a cold joint where one of the batches set up. This caused some delamination which was observed when tapping the hammer on the repair but the material resisted the original crack. There were transverse cracks about every 2' but the surface showed little degradation from traffic.

All of the CSA mixtures were strong enough to resist the previous longitudinal crack; however, the CSA-1 and CSA-2 Mixtures had transverse cracks. The CSA-2 Mixture had multiple cracks at about every 12" (304.8mm) which could suggest that the repair was not compatible with the existing pavement. The surface of the CSA-2 Mixture was in good condition and showed little degradation due to traffic loads and friction. Only one transverse crack appeared on the CSA-1 Mixture which was located on the wheel path; there was some plastic cracking which can be seen in Figure 90. The CSA-3 Mixture performed very well and showed no cracking or surface deterioration.

5.5 SUMMARY AND CONCLUSIONS

The summary of the field performance of selected mixtures are as follows:

- All of the Phase III Mixtures, excluding the PC Type III Mixture, reached 3000 psi (20.7 MPa) at 3 hours after mixing for the simulated bridge deck repair.
- After the first 24 hours of the temperature gradient analysis, the heat evolution for each mixture had dissipated and the fluctuation in temperatures was due to the fluctuation in the ambient temperature.
- The CAC-3 Mixture generated the highest heat and heat differential than all of the other Phase III Mixtures. It also presented a quicker ettringite induced peak followed by a larger delayed peak approximately 8 hours later which could be the portland cement hydrating.
- The P-AAFA Mixture emitted as much heat as the ambient temperature 4 days after mixing, while the other mixtures experienced slightly elevated temperatures.
- All of the cracking in the repair sections occurred within the first 7 days post casting except for the P-AAFA Mixture.
- The CAC-2 Mixture seemed to have excess water which could have contributed to drying shrinkage or plastic cracking.
- The P-2 and CSA-3 Mixtures performed the best at the Cotulla site because neither showed cracking or surface defects after 8 months of frequent and high axle loads.
- All three CSA mixtures have performed well, so far. The only issue is the transverse cracking with the CSA-2 Mixture but this could suggest that it is not compatible with the existing pavement.

Chapter 6: Conclusion

In summary, the following conclusions can be drawn from the research described in this thesis:

- The selection of the repair materials should not be focused on the material with the strongest or highest values for the engineering properties but rather, selecting a repair material with similar properties to those of the existing substrate. Selecting repair materials in this manner will increase the service life on any repair.
- The P-2 Mixture satisfied the most criteria when considering all of the properties measured at standard temperatures.
- The CAC mixtures presented the best behavior during the temperature robustness study, highlighting its potential for use in cold weather repairs.
- Combining latex with either CSA or CAC had significant impact on the engineering properties, reducing compressive strength, modulus of elasticity, tensile strength (for CSA mixture only), and bond strength and increasing the flexural strength. According to Bentivegna's field study, the latex modified CAC overlays showed worse signs of deterioration when compared to plain CAC mixtures (2011).
- The CSA binder system had less drying shrinkage than the CAC binder system at both 28 days and 64 weeks. Three of the four CAC mixtures exceeded the drying shrinkage limits specified by TxDOT.
- Mixtures containing fly ash contained more drying shrinkage than mixtures not containing fly ash.

- The CSA-1 Mixture presented autogenous expansion and compressive stresses for both the FSF and RCF confirming the shrinkage compensating property for this binder.
- The CAC-2 Mixture presented autogenous shrinkage and tensile stresses for both, the FSF and RCF, which is similar behavior of a typical portland cement concrete with low w/cm ratio.
- The P-AAFA-Mixture has a rapid time to peak heat and generates about the same peak temperature when studied at 50 °F, 73 °F, and 100 °F (10 °C, 23 °C, and 38 °C).
- The CAC mixtures were the most variable as a whole with the CAC-3 Mixture having very slow heat generation, lower peak temperatures, and relatively no heat generation at 50 °F (10 °C) compared to the other 3 mixtures. Contrary to the CAC-3 Mixture, the remaining CAC mixtures had very rapid heat generation, highest peak temperatures, largest temperature gradient, and the best performance at 50 °F (10 °C) of any mixture.
- The CSA mixtures were retarded by the cooler temperatures at 50 °F (10 °C) but had one of the highest temperature gradients at 7.63 °F (4.24 °C) when cured at 73 °F (23 °C). For semi-adiabatic calorimetry, these mixtures yielded similar calorimetry data and temperature curves.
- The mixtures containing mostly portland cement, P-3 and PC Type III, had slower heat generation and lower peak temperature values than the other rapid repair materials.
- All of the Phase III Mixtures, excluding the PC Type III Mixture, reached 3000 psi (20.7 MPa) at 3 hours after mixing for the simulated bridge deck repair.

- After the first 24 hours of the temperature gradient analysis, the heat evolution for each mixture had dissipated and the fluctuation in temperatures was due to the fluctuation in the ambient temperature.
- The CAC-3 Mixture generated the highest heat and heat differential than all of the other Phase III Mixtures. It also presented a quicker ettringite-induced peak followed by a larger delayed peak approximately 8 hours later which could be the portland cement hydrating.
- The P-AAFA Mixture emitted as much heat as the ambient temperature 4 days after mixing, while the other mixtures experienced slightly elevated temperatures.
- All of the cracking in the repair sections occurred within the first 7 days post casting except for the P-AAFA Mixture.
- The CAC-2 Mixture seemed to have excess water which could have contributed to drying shrinkage or plastic cracking.
- The P-2 and CSA-3 Mixtures performed the best at the Cotulla site because neither showed cracking or surface defects after 8 months of frequent and high axle loads.
- All three CSA mixtures have performed well, so far. The only issue is the transverse cracking with the CSA-2 Mixture but this could suggest that it is not compatible with the existing pavement.
- The findings reported in this thesis will be combined with those reported by Zuniga (2011) and Garcia (2014) to develop final project conclusions and recommendations for implementation.

Appendix A: Isothermal Calorimetry Mixture Tables

Table 10: Isothermal Calorimetry Table for P-1

	Mix Type	Time to Peak Heat (Hours)	Peak Heat Flow (mW/g cement)	Cumulative Heat (J/g)
50°F (10°C)	Concrete	2.57	8	139
	Mortar	2.72	8	161
	Paste	--	--	--
73°F (23°C)	Concrete	1.70	22	151
	Mortar	1.78	22	183
	Paste	--	--	--
100°F (38°C)	Concrete	0.48	36	120
	Mortar	0.43	40	134
	Paste	--	--	--

Table 11: Isothermal Calorimetry Table for P-2

	Mix Type	Time to Peak Heat (Hours)	Peak Heat Flow (mW/g cement)	Cumulative Heat (J/g)
50°F (10°C)	Concrete	9.93	10	187
	Mortar	10.10	9	156
	Paste	--	--	--
73°F (23°C)	Concrete	2.55	21	155
	Mortar	2.57	21	134
	Paste	--	--	--
100°F (38°C)	Concrete	1.08	31	154
	Mortar	1.05	30	164
	Paste	--	--	--

Table 12: Isothermal Calorimetry Table for P-3

	Mix Type	Time to Peak Heat (Hours)	Peak Heat Flow (mW/g cement)	Cumulative Heat (J/g)
50°F (10°C)	Concrete	29.93	1	81
	Mortar	30.72	0	24
	Paste	--	--	--
73°F (23°C)	Concrete	23.90	2	227
	Mortar	23.57	1	84
	Paste	--	--	--
100°F (38°C)	Concrete	9.72	3	166
	Mortar	9.65	4	163
	Paste	--	--	--

Table 13: Isothermal Calorimetry Table for P-AAFA

	Mix Type	Time to Peak Heat (Hours)	Peak Heat Flow (mW/g cement)	Cumulative Heat (J/g)
50°F (10°C)	Concrete	0.12	87	331
	Mortar	0.13	113	191
	Paste	--	--	--
73°F (23°C)	Concrete	0.53	23	91
	Mortar	0.50	19	74
	Paste	--	--	--
100°F (38°C)	Concrete	0.45	11	35
	Mortar	0.40	13	37
	Paste	--	--	--

Table 14: Isothermal Calorimetry Table for CSA-1

	Mix Type	Time to Peak Heat (Hours)	Peak Heat Flow (mW/g cement)	Cumulative Heat (J/g)
50°F (10°C)	Concrete	4.58	30	216
	Mortar	4.75	26	154
	Paste	7.65	21	225
73°F (23°C)	Concrete	1.65	48	171
	Mortar	1.68	36	115
	Paste	1.62	29	132
100°F (38°C)	Concrete	0.65	67	170
	Mortar	0.58	55	138
	Paste	1.02	60	346

Table 15: Isothermal Calorimetry Table for CSA-2

	Mix Type	Time to Peak Heat (Hours)	Peak Heat Flow (mW/g cement)	Cumulative Heat (J/g)
50°F (10°C)	Concrete	6.77	19	196
	Mortar	6.60	15	178
	Paste	9.22	15	165
73°F (23°C)	Concrete	1.72	35	154
	Mortar	1.70	34	137
	Paste	2.12	30	180
100°F (38°C)	Concrete	0.68	61	192
	Mortar	0.63	50	122
	Paste	0.77	62	214

Table 16: Isothermal Calorimetry Table for CSA-3

	Mix Type	Time to Peak Heat (Hours)	Peak Heat Flow (mW/g cement)	Cumulative Heat (J/g)
50°F (10°C)	Concrete	7.02	20	174
	Mortar	6.78	16	68
	Paste	8.75	20	153
73°F (23°C)	Concrete	2.13	40	185
	Mortar	2.15	36	206
	Paste	2.43	26	167
100°F (38°C)	Concrete	0.78	61	164
	Mortar	0.73	43	136
	Paste	1.25	57	207

Table 17: Isothermal Calorimetry Table for CSA-Latex

	Mix Type	Time to Peak Heat (Hours)	Peak Heat Flow (mW/g cement)	Cumulative Heat (J/g)
50°F (10°C)	Concrete	6.45	28	187
	Mortar	6.57	18	127
	Paste	7.98	29	221
73°F (23°C)	Concrete	1.83	46	178
	Mortar	1.87	39	131
	Paste	1.92	54	211
100°F (38°C)	Concrete	0.75	63	147
	Mortar	0.67	53	136
	Paste	0.63	84	202

Table 18: Isothermal Calorimetry Table for CAC-1

	Mix Type	Time to Peak Heat (Hours)	Peak Heat Flow (mW/g cement)	Cumulative Heat (J/g)
50°F (10°C)	Concrete	1.67	21	273
	Mortar	1.63	14	171
	Paste	1.48	23	242
73°F (23°C)	Concrete	2.88	39	436
	Mortar	2.83	31	376
	Paste	2.53	23	196
100°F (38°C)	Concrete	0.72	75	257
	Mortar	0.58	51	246
	Paste	0.27	97	249

Table 19: Isothermal Calorimetry Table for CAC-2

	Mix Type	Time to Peak Heat (Hours)	Peak Heat Flow (mW/g cement)	Cumulative Heat (J/g)
50°F (10°C)	Concrete	2.13	12	227
	Mortar	2.22	8	109
	Paste	7.95	7	189
73°F (23°C)	Concrete	2.53	19	303
	Mortar	2.53	10	187
	Paste	3.70	15	235
100°F (38°C)	Concrete	0.52	31	199
	Mortar	0.52	33	171
	Paste	0.38	59	242

Table 20: Isothermal Calorimetry Table for CAC-3

	Mix Type	Time to Peak Heat (Hours)	Peak Heat Flow (mW/g cement)	Cumulative Heat (J/g)
50°F (10°C)	Concrete	0.13	64	184
	Mortar	0.13	137	148
	Paste	0.12	101	138
73°F (23°C)	Concrete	1.43	12	204
	Mortar	0.68	18	334
	Paste	1.12	8	215
100°F (38°C)	Concrete	0.43	17	221
	Mortar	0.43	7	115
	Paste	0.90	26	223

Table 21: Isothermal Calorimetry Table for CAC-Latex

	Mix Type	Time to Peak Heat (Hours)	Peak Heat Flow (mW/g cement)	Cumulative Heat (J/g)
50°F (10°C)	Concrete	1.75	16	228
	Mortar	1.92	15	162
	Paste	1.45	22	261
73°F (23°C)	Concrete	3.32	19	190
	Mortar	3.33	12	137
	Paste	3.53	30	302
100°F (38°C)	Concrete	0.70	72	291
	Mortar	0.68	66	230
	Paste	0.28	100	267

Table 22: Isothermal Calorimetry Table for PC Type III

	Mix Type	Time to Peak Heat (Hours)	Peak Heat Flow (mW/g cement)	Cumulative Heat (J/g)
50°F (10°C)	Concrete	13.58	2	185
	Mortar	14.65	1	111
	Paste	16.82	2	179
73°F (23°C)	Concrete	6.98	4	193
	Mortar	7.07	2	93
	Paste	10.35	4	206
100°F (38°C)	Concrete	4.18	8	233
	Mortar	4.20	5	113
	Paste	5.92	8	237

Appendix B: Isothermal Calorimetry Plots

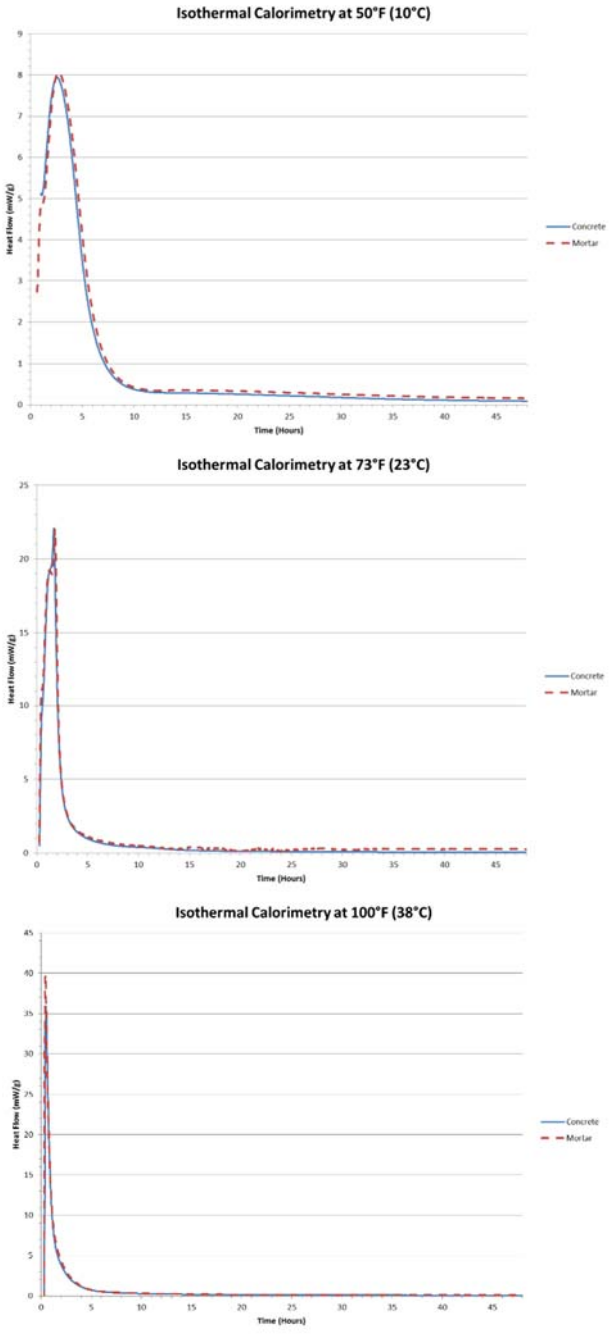

Figure 65: Isothermal Calorimetry for P-1 Mixture

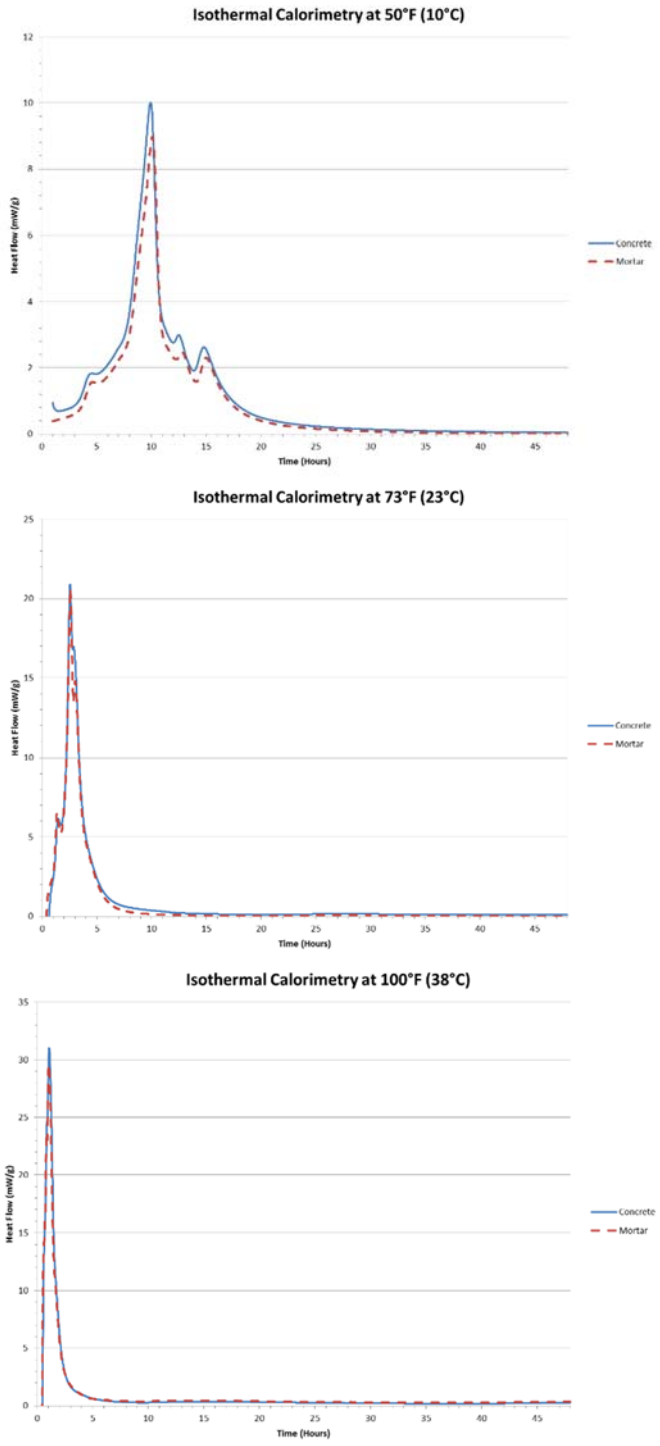

Figure 66: Isothermal Calorimetry for P-2 Mixture

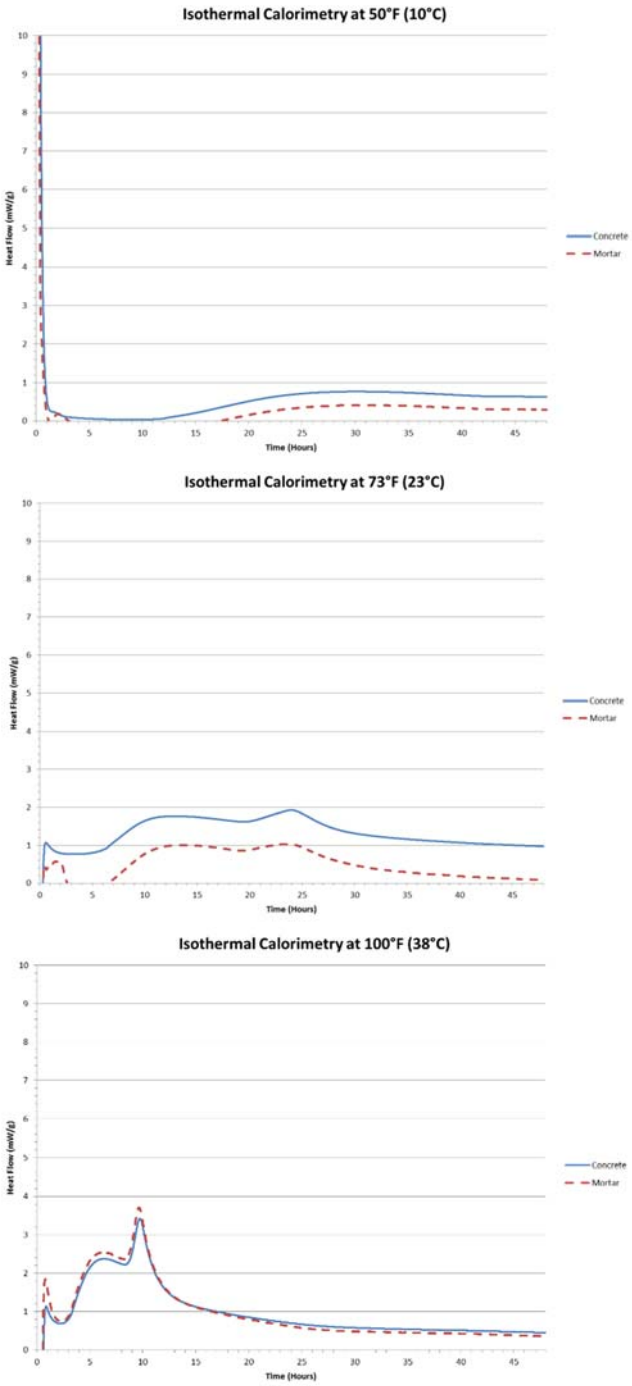

Figure 67: Isothermal Calorimetry for P-3 Mixture

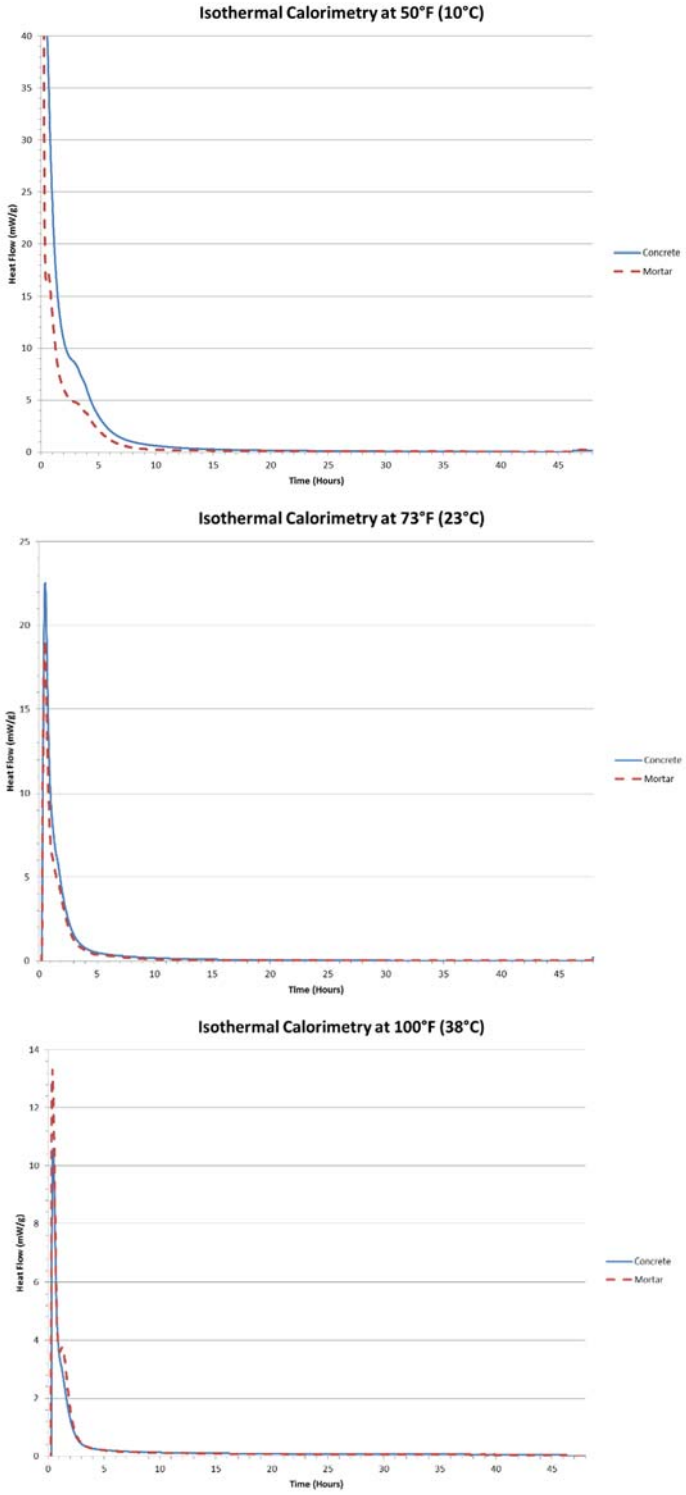

Figure 68: Isothermal Calorimetry for P-AAFA Mixture

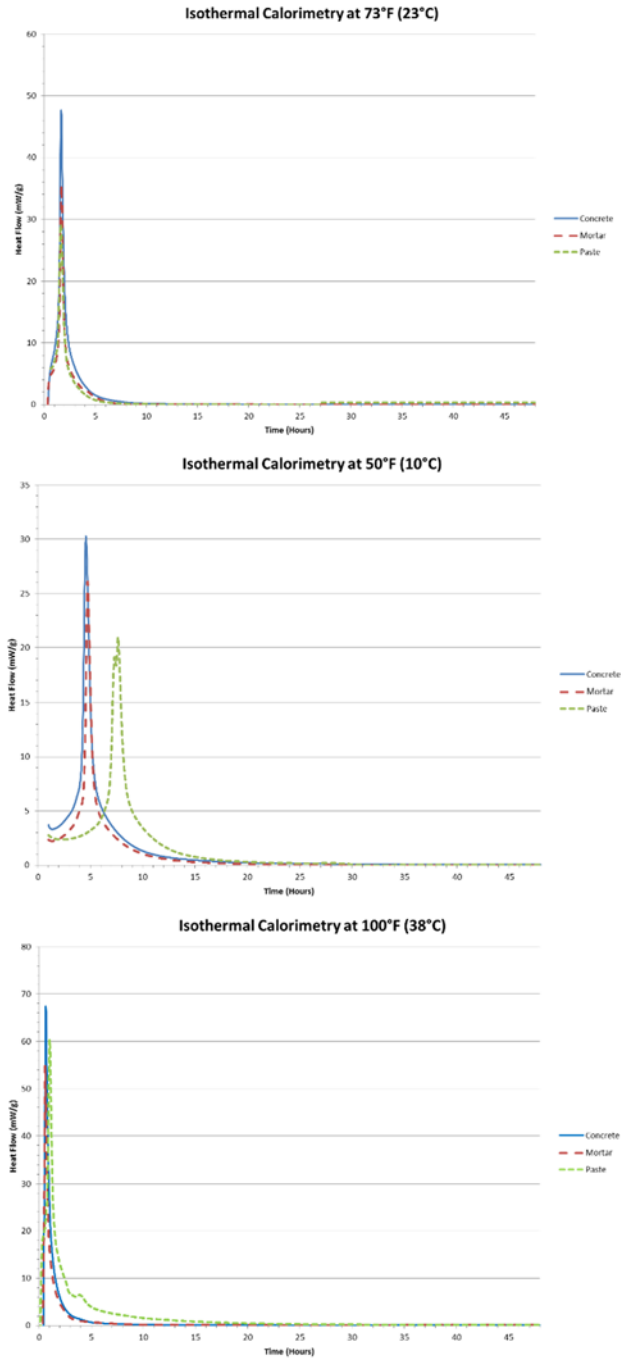

Figure 69: Isothermal Calorimetry for CSA-1 Mixture

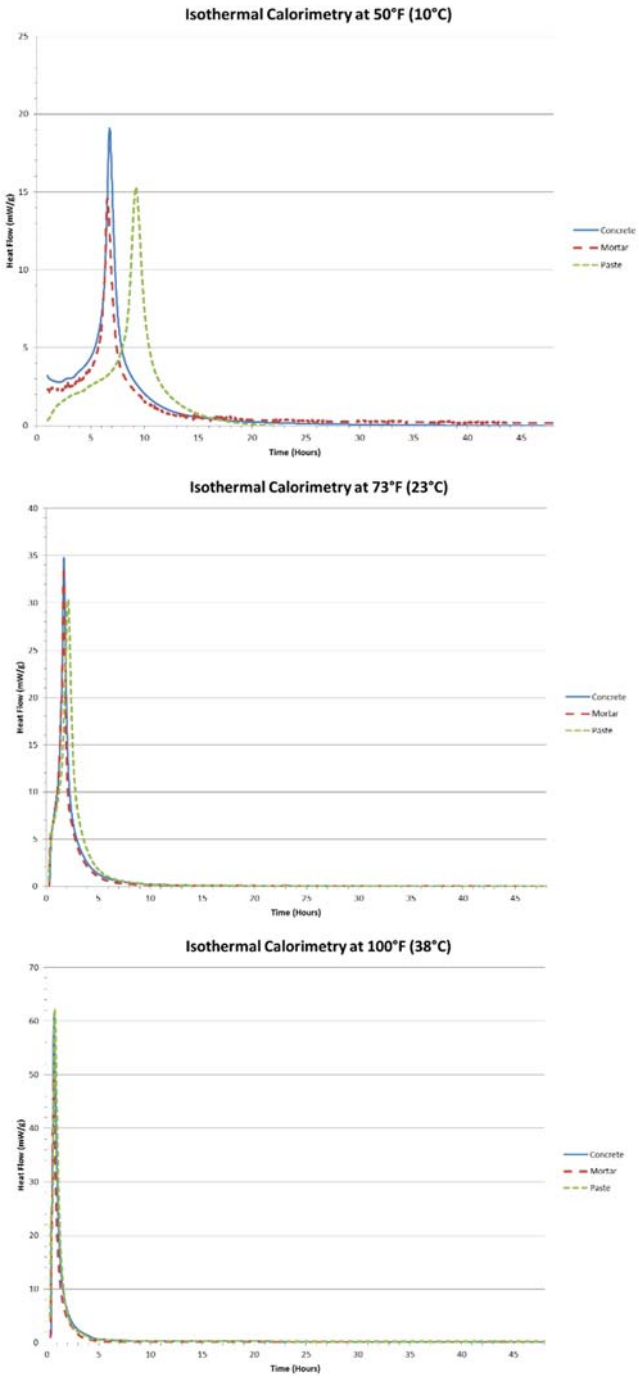

Figure 70: Isothermal Calorimetry for CSA-2 Mixture

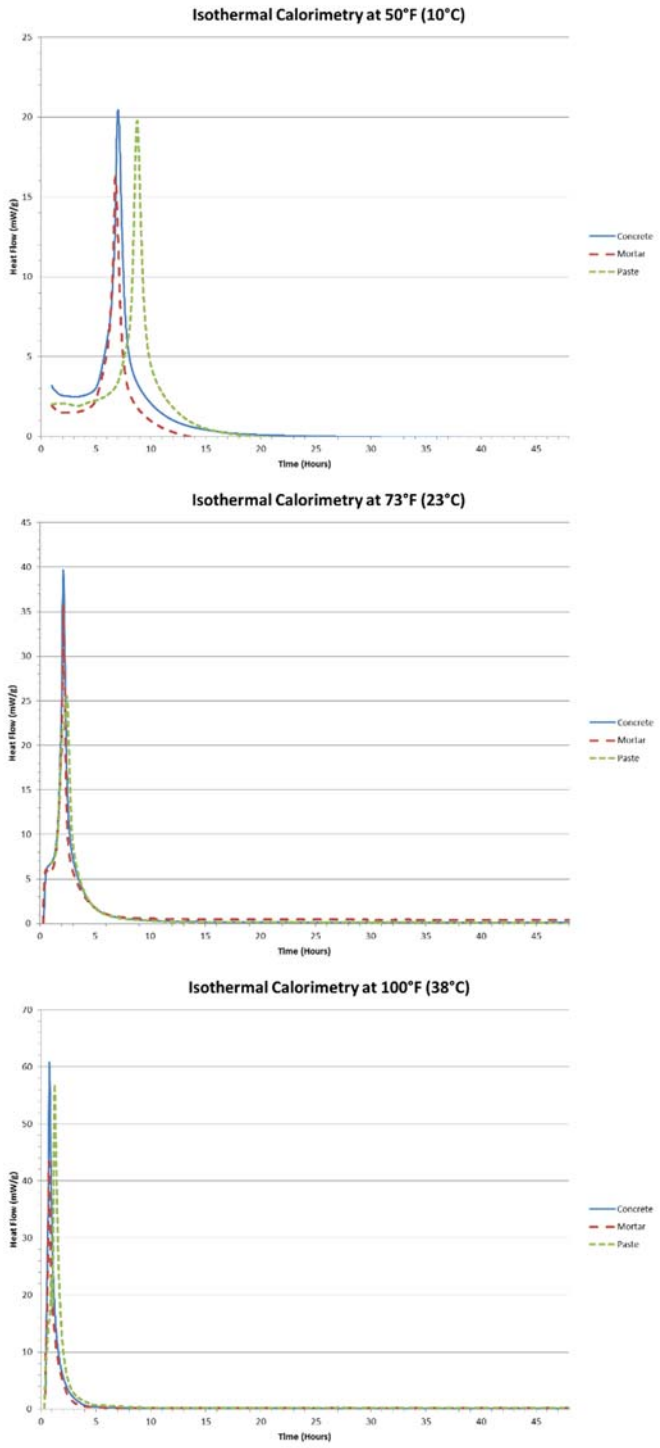

Figure 71: Isothermal Calorimetry for CSA-3 Mixture

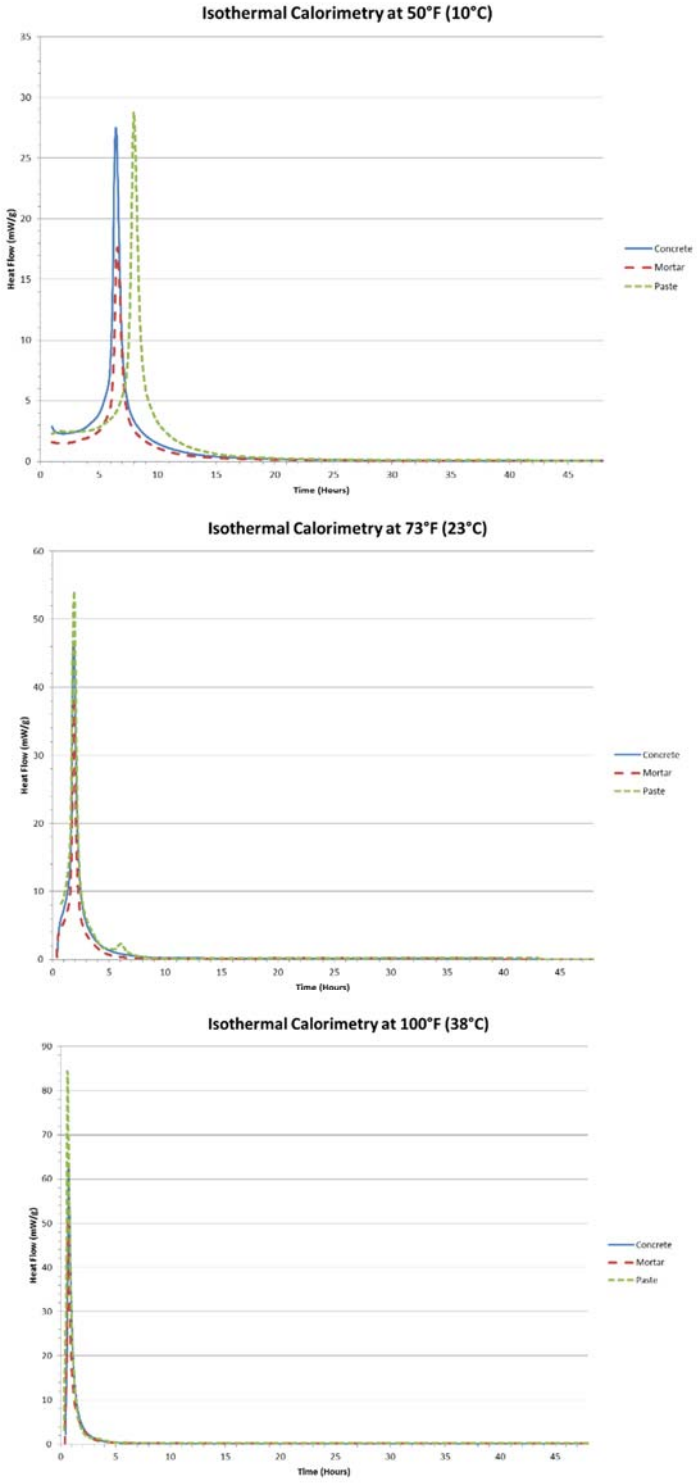

Figure 72: Isothermal Calorimetry for CSA-Latex Mixture

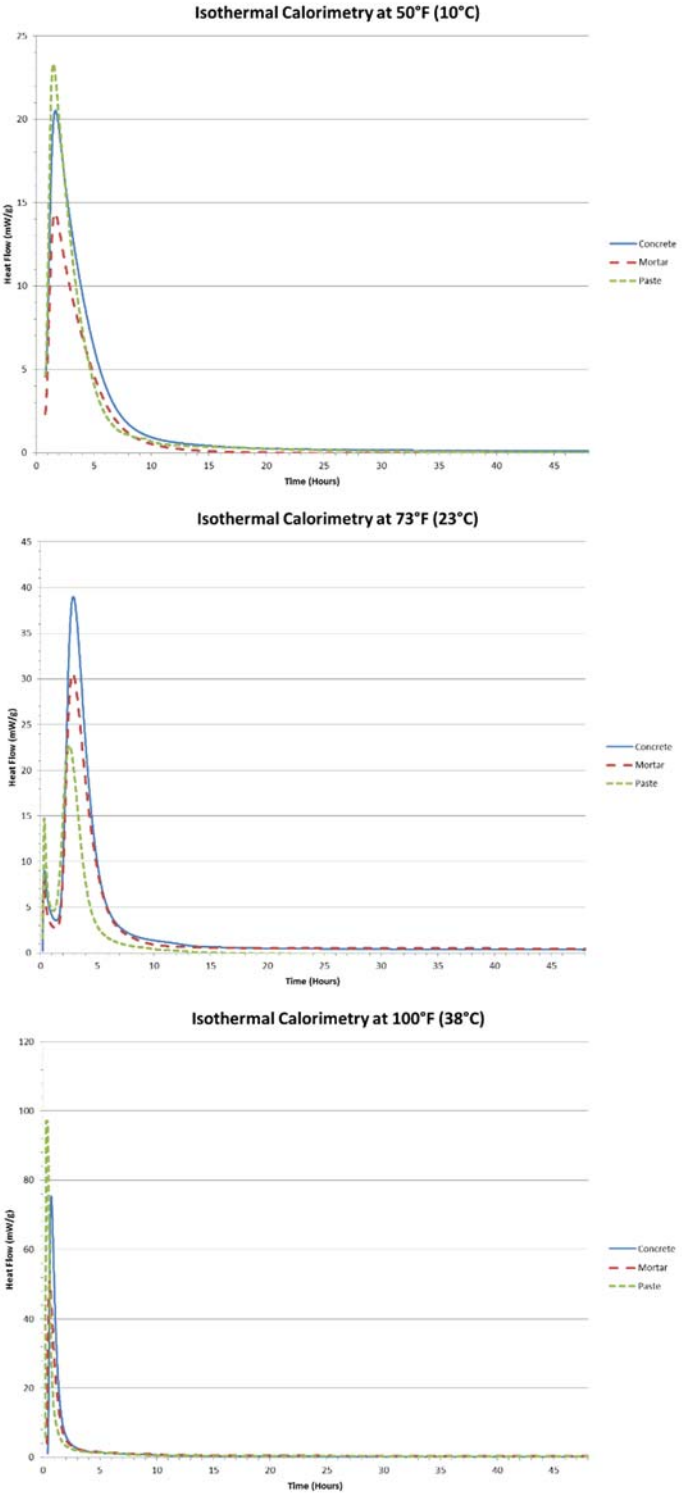

Figure 73: Isothermal Calorimetry for CAC-1 Mixture

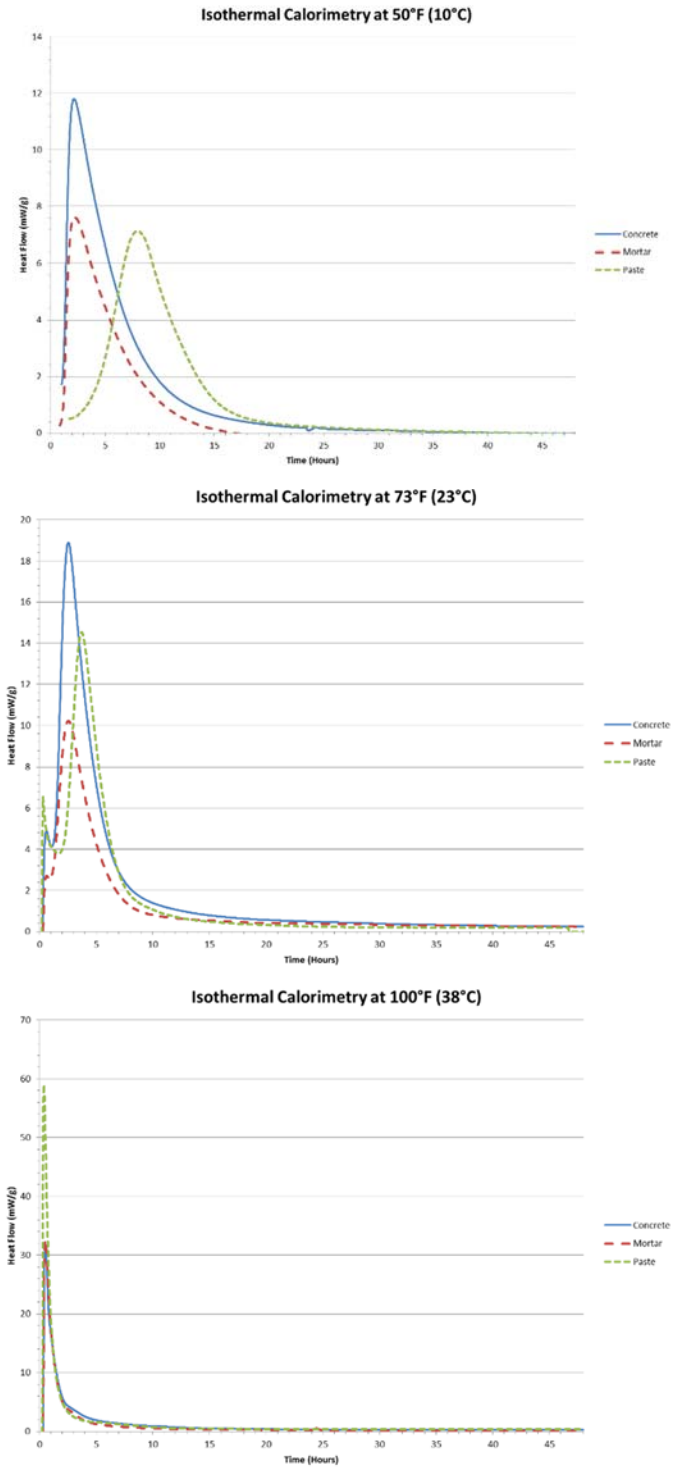

Figure 74: Isothermal Calorimetry for CAC-2 Mixture

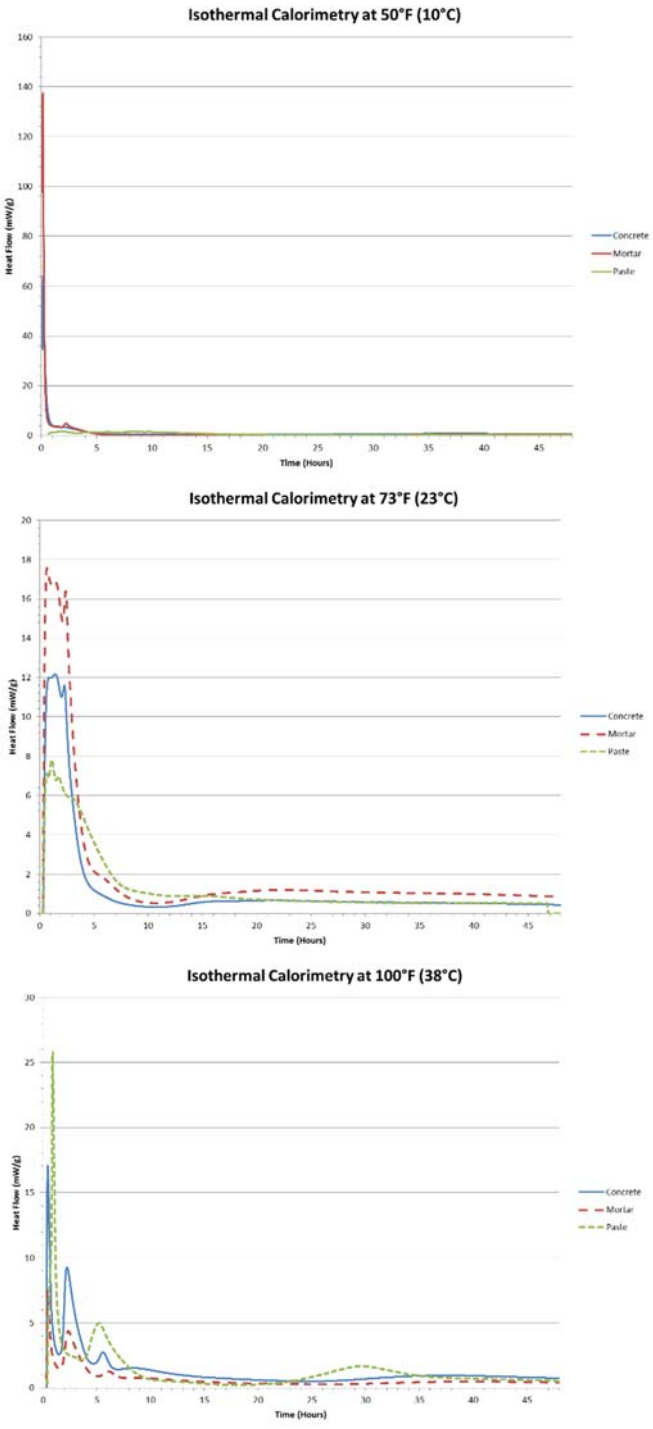

Figure 75: Isothermal Calorimetry for CAC-3 Mixture

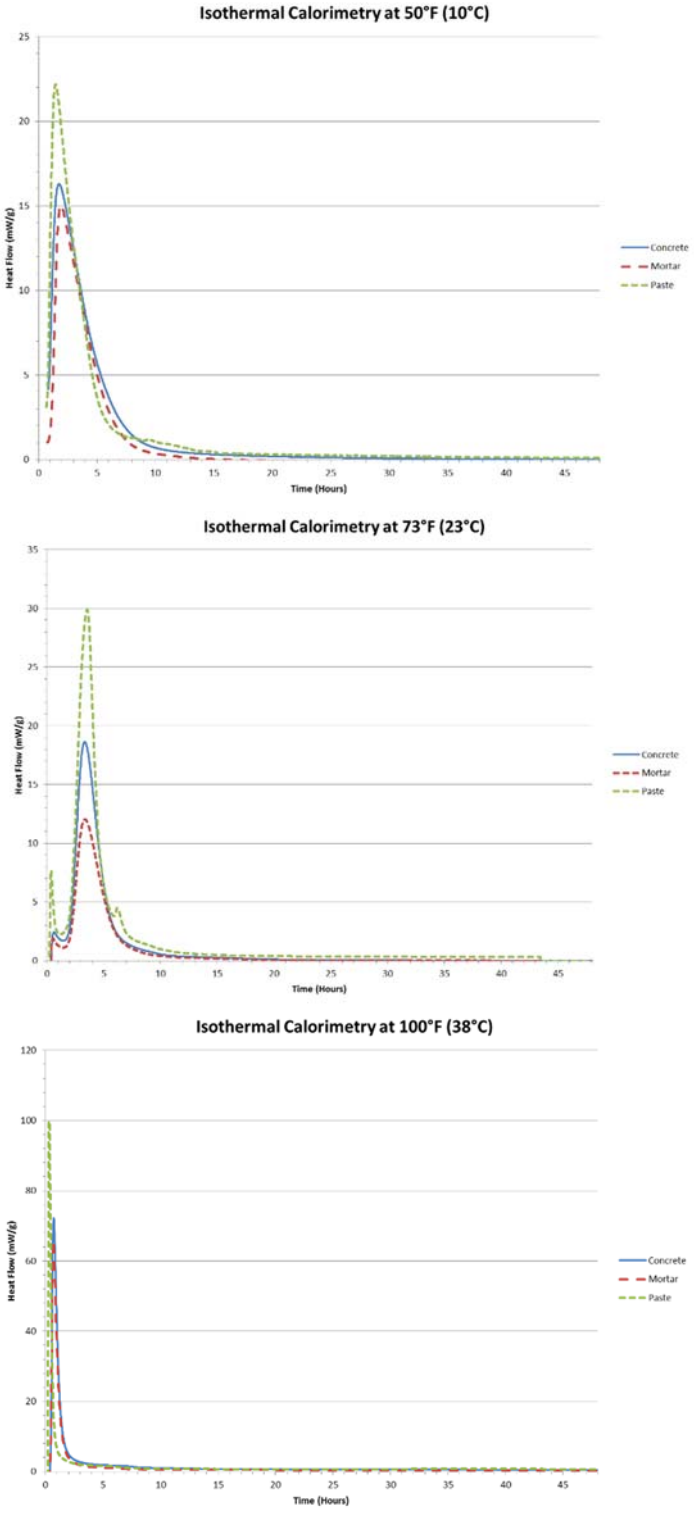

Figure 76: Isothermal Calorimetry for CAC-Latex Mixture

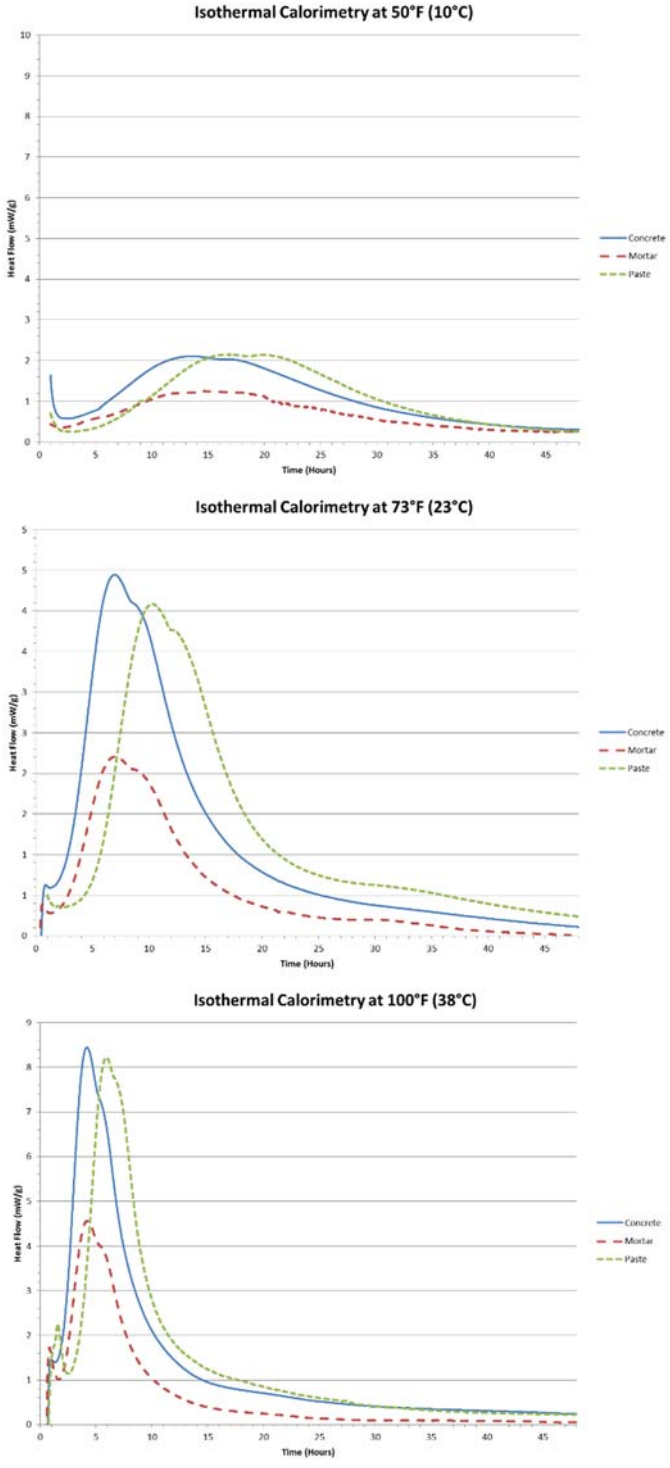

Figure 77: Isothermal Calorimetry for PC Type III Mixture

Appendix C: Field Performance

Table 23: Daily Cracking Log for Bridge Deck Repairs

	1 Day Status	2 Day Status	3 Day Status	4 Day Status	5 Day Status	6 Day Status	7 Day Status	8 Day Status	28 Day Status	6 Month Status
P-2	crack at center	2 cracks 2' from ends	Same	Same	crack 1' from center	Same	Same	Same	Same	Same
PC Type III	None	None	crack at center	Same	Same	Same	Same	Same	Same	Same
CSA-1	crack at center	Same	Same	Same	Same	Same	Same	Same	Same	Same
CAC-3	None	crack at center	Same	2 cracks 2' from ends	Same	2 cracks each 2' from center	Same	Same	Same	Same
CAC-2	crack at center; crack 2' from end; crack 1' from center	Same	crack .5' from end	Same	Same	Same	crack 1' from center	Same	Same	Same
P-AAFA	None	None	None	None	None	None	None	None	None	crack at center

Table 24: Fresh State Properties for Bridge Deck Repairs

Mixture ID	Slump (in)	Unit Weight (lb/ft^3)	Air Content (%)
P-2	10.5	146.0	3.9
PC Type III	0	154.0	2.9
CSA-1	4	145.6	3.5
CAC-3	6.5	148.0	2.5
CAC-2	10	148.8	3.7
P-AAFA	8.5	150.6	3

Figure 78: Removal of Existing Concrete using Jackhammers

Figure 79: Thermocouples at Mid-Span of each Repair Section

Figure 80: Finished Repair Section before Wet-Cure with Burlap

Figure 81: Bridge Deck Repair for P-2 Mixture

Figure 82: Bridge Deck Repair for CAC-3 Mixture

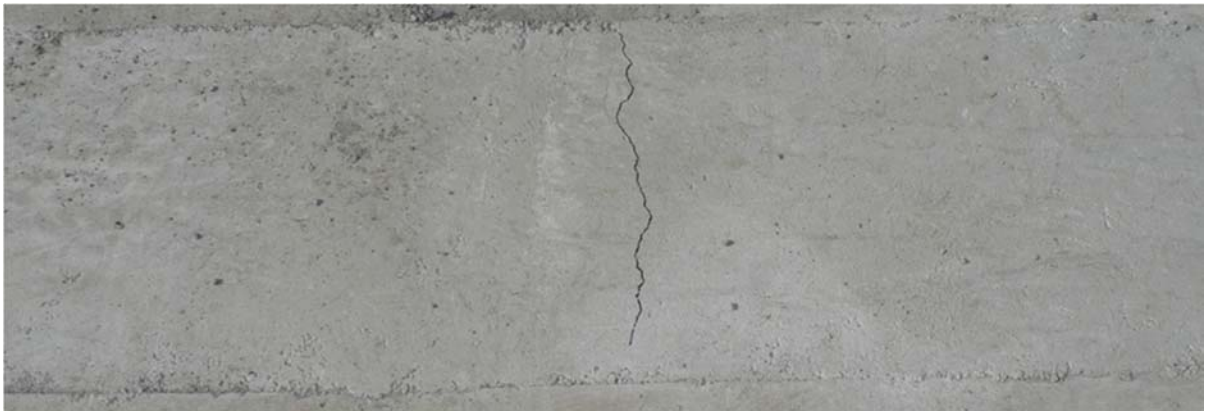

Figure 83: Bridge Deck Repair for PC Type III Mixture

Figure 84: Bridge Deck Repair for P-AAFA Mixture

Figure 85: Bridge Deck Repair for CSA-1 Mixture

Figure 86: Bridge Deck Repair for CAC-2 Mixture

Figure 87: Mixture P-1 Repair at Cotulla Site

Figure 88: P-2 Mixture Repair at Cotulla Site

Figure 89: P-AAFA Mixture Repair at Cotulla Site

Figure 90: Plastic Cracking for CSA-1 Mixture at Cotulla Site

Figure 91: Mixture CSA-2 Repair at Cotulla Site

Figure 92: Mixture CSA-3 Bond Interface at Cotulla Site

Bibliography

AASHTO (2011) Standard Method of Test for Coefficient of Thermal Expansion of Hydraulic Cement Concrete AASHTO T 336-11, American Association of State Highway and Transportation Officials.

ACI Committee 318. (2011). Building Code Requirements for Structural Concrete. Farmington Hills, Mich.: American Concrete Institute.

ASTM C1231. (2013) Standard Practice for Use of Unbonded Caps in Determination of Compressive Strength of Hardened Concrete Cylinders. Pennsylvania: American Society of Testing and Materials.

ASTM C138. (2013) Standard Test Method for Density, Yield, and Air Content of Concrete. Pennsylvania: American Society of Testing and Materials.

ASTM C143. (2012). Standard Test Method for Slump of Hydraulic-Cement Concrete. Pennsylvania: American Society of Testing and Materials.

ASTM C157. (2008). Standard Test Method for Length Change of Hardened Hydraulic-Cement Mortar and Concrete. Pennsylvania: American Society of Testing and Materials.

ASTM C231. (2010). Standard Test Method for Air Content of Freshly Mixed Concrete by the Pressure Method. Pennsylvania: American Society of Testing and Materials.

ASTM C39. (2014). Standard Test Method for Compressive Strength of Cylindrical Concrete Specimens. Pennsylvania: American Society of Testing and Materials.

ASTM C403. (2008). Standard Test Method for Time of Setting of Concrete Mixtures by Penetration Resistance. Pennsylvania: American Society of Testing and Materials.

ASTM C469. (2010). Standard Test Method for Static Modulus of Elasticity and Poisson's Ratio of Concrete in Compression. Pennsylvania: American Society of Testing and Materials.

ASTM C496. (2011). Standard Test Method for Splitting Tensile Strength of Cylindrical Concrete Specimens. Pennsylvania: American Society of Testing and Materials.

ASTM C78 (2010) Standard Test Method for Flexural Strength of Concrete (Using Simple Beam with Third-Point Loading). Pennsylvania: American Society of Testing and Materials.

ASTM C882 (2013). Standard Test Method for Bond Strength of Epoxy-Resin Systems Used With Concrete By Slant Shear. Pennsylvania: American Society of Testing and Materials.

Bentivegna, A. (2012). Multi-Scale Characterization, Implementation, and Monitoring of Calcium Aluminate Cement Based-Systems. Austin: The University of Texas at Austin.

Day, R.L., & Haque, M. N. (1993). Correlation between Strength of Small and Standard Concrete Cylinders. ACI Materials Journal

Garcia, A.M. (2014). Durability Testing of Rapid, Cement-based Repair Materials for Transportation Structures. Master's Thesis, University of Texas at Austin.

Ideker, J. (2008). Early-age Behavior of Calcium Aluminate Cement Systems. PhD Thesis Austin, Texas: The University of Texas at Austin.

Mehta, P.K. & Monteiro, J.M. (1993) Concrete: Structure, Properties, and Methods. 2nd Ed. New Jersey: Prentice Hall, Inc.

Mamlouk, M.S. & Zaniewski, J.P. (2006). Materials for Civil and Construction Engineers. 2nd Ed. New Jersey: Pearson Prentice Hall, Inc.

National Cooperative Highway Research Program. (2004). NCHRP Synthesis 333 Concrete Bridge Deck Performance. Transportation Research Board

Neville, A.M. Properties of Concrete. 3rd ed. London: Pitman Books Ltd, 1981.

Poole, J. (2007). Modeling Temperature Sensitivity and Heat Evolution of Concrete. PhD Thesis, University of Texas at Austin.

Riding, K. (2007). Early age concrete thermal stress measurement and modeling. PhD Thesis, University of Texas at Austin, Civil Engineering.

TxDOT (2011). Departmental Material Specification: Concrete Repair Materials (DMS – 4655). Texas Department of Transportation.

Whigham, J. (2005). Evaluation of Restraint Stresses and Cracking in Early-Age Concrete with the Rigid Cracking Frame. Master's Thesis, Auburn University.

Zuniga, J.R. (2013). Development of Rapid, Cement-based Repair Materials for Transportation Structures. Master's Thesis, University of Texas at Austin.